

## **PHENOLIC HYDROGEN ATOM ABSTRACTION BY CARBONYL TRIPLETS**

**A NANOSECOND LASER FLASH PHOTOLYSIS STUDY  
OF REMOTE INTRAMOLECULAR PHENOLIC HYDROGEN ATOM  
ABSTRACTION BY CARBONYL TRIPLETS**

by

MICHAEL J. ST.PIERRE, B.Sc.

A Thesis

Submitted to the School of Graduate Studies

in Partial Fulfilment of the Requirements

for the Degree

Master of Science

McMaster University

June, 1995

© Copyright by Michael St.Pierre, June 1995

MASTER OF SCIENCE (1995)

(Chemistry)

McMASTER UNIVERSITY

Hamilton, Ontario

TITLE:       A nanosecond laser flash photolysis study of remote intramolecular  
phenolic hydrogen atom abstraction by carbonyl triplets.

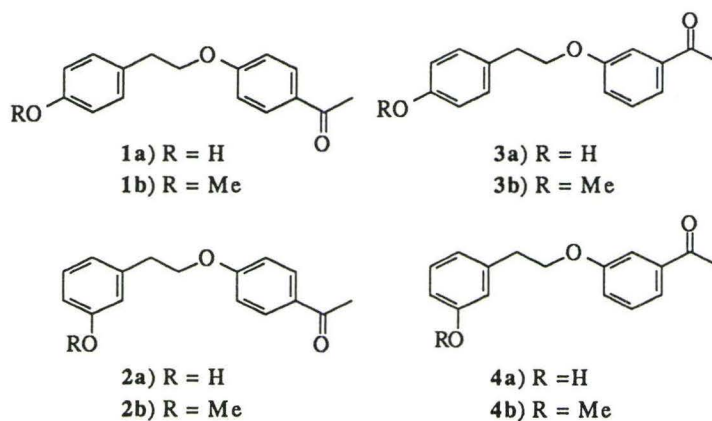
AUTHOR:     Michael J. St. Pierre, B.Sc. (McMaster University)

SUPERVISOR:     Dr. William J. Leigh

NUMBER OF PAGES:     xiv,112

## ABSTRACT

It has been shown that the hydroxy compounds **1a-4a** possess triplet states which are substantially shorter-lived than those of their methoxy analogs (**1b-4b**). In each case the efficient quenching of the excited carbonyl triplet state has been attributed to intramolecular phenolic hydrogen abstraction. Evidence for this is found in the detection of biradical species generated from triplet decay, primary hydrogen-deuterium kinetic isotope effects and thermodynamic parameters which support both atom transfer (enthalpy) and high degrees of order (entropy) in the transition state necessary for the proposed abstraction process. The difference in triplet lifetimes (16 ns to 1135 ns) is due almost exclusively to varying degrees of difficulty in obtaining a transition state geometry in which the phenoxy hydrogen is properly lined up for intramolecular hydrogen abstraction.





## ACKNOWLEDGEMENTS

I would like to thank my supervisor, Dr. William J. Leigh for sharing his insight, enthusiasm and passionate love of chemistry. His selfless knowledge and know-how truly made graduate school a learning experience.

I would also like to thank Dr. Nick Werstiuk for his time and patience in teaching me the basic points of performing calculations with MIRANDA.

To my labmates: Jo-Ann, Dr. Alberto Postigo, Dr. Jonathan Lewis, Christine, Nick, Dr. Greg Sluggett and Dr. Mark Workentin, a heart felt thanks for providing support and friendship throughout my stay.

Special thanks to Dr. Chandra Roy, Mike, Lisa, Tom, Karim, Grant and Theresa. Their companionship made life very eventful and enjoyable.

To my family, I can not say enough. The support, love and friendship throughout my life has been second to none. I am deeply indebted.

Most importantly to Cristina, whose unconditional love, patience and understanding has given me the strength and the ability to embrace life and attain happiness.

Finally I would like to offer my sincere appreciation to McMaster University and the Pulp and Paper Industry for financial assistance.

## TABLE OF CONTENTS

<b>CHAPTER I: Introduction</b>	<b>1</b>
1.1 The Photochemistry of Phenyl-Alkyl-Ketones	1
1.2 Electronic Configuration of Phenyl-Ketones	2
1.3 Substituent Effects on Reactivity of Phenyl-Alkyl-Ketones	8
1.4 Substituent Effects on the Reactivity of Hydrogen Donors	11
1.5 Orientational Requirements for Hydrogen Abstraction	13
1.6 Conformational Requirements for Hydrogen Abstraction	16
1.7 Intermolecular Hydrogen Atom Abstraction by Carbonyl Triplets	20
1.8 Intramolecular Hydrogen Atom Abstraction by Carbonyl Triplets	22
 <b>CHAPTER II: Results</b>	 <b>25</b>
2.1 General Synthesis of Linked Phenolic Ketones	25
2.2 Ultraviolet Absorption Spectra	26
2.3 Steady State Photolysis of <b>1-8</b> in solution	30

2.4	Phosphorescence Emission Spectroscopy	31
2.4.1	Phosphorescence Lifetimes	33
2.5	Nanosecond Laser Flash Photolysis	35
2.5.1	Transient Species in Solution	35
2.5.2	Transient U.V. Absorption Spectra	37
2.5.3	Quenching Plots and Transient Characterization	48
2.6	Triplet Lifetimes Determined by Nanosecond Laser Flash Photolysis	52
2.6.1	Indirect Triplet Lifetime Determination	53
2.6.2	Direct Triplet Lifetime Determination	56
2.7	Hydrogen/Deuterium Kinetic Isotope Effects	57
2.8	Triplet Characterization of Model Compounds	58
2.8.1	Bimolecular Phenolic Triplet Quenching	59
2.9	Arrhenius Parameters for Intramolecular Phenolic-Hydrogen Abstraction	60
<b>CHAPTER III: Discussion</b>		<b>65</b>
3.1	Bimolecular Phenolic Hydrogen Atom Abstraction	71
3.2	Intramolecular Phenolic Hydrogen Atom Abstraction	73
3.3	Biradical Formation	77
3.4	Comparison of Unimolecular and Bimolecular Reactions	79

3.5	Activation Parameters for Intramolecular Phenolic Quenching	81
<b>CHAPTER IV: Summary</b>		<b>85</b>
<b>CHAPTER V: Experimental</b>		<b>88</b>
5.1	General	88
5.2	Commercial Solvents and Reagents Used	90
5.3	Preparation and Spectral Data of Compounds	92
5.3.1	Preparation of 1-bromo-2-(4-hydroxyphenyl)ethane	92
5.3.2	Preparation of 1-bromo-2-(3-hydroxyphenyl)ethane	92
5.3.3	Preparation of 1-bromo-2-(4-methoxyphenyl)ethane and 1-bromo-2-(3-methoxyphenyl)ethane	93
5.3.4	Preparation of <b>1a</b>	94
5.3.5	Preparation of and Spectral Data for <b>4a</b>	95
5.4	General Method	96
5.4.1	Preparation of Hydroxy Containing Compounds	96
5.4.2	Spectral Data for <b>2a</b>	97
	Spectral Data for <b>3a</b>	98
	Spectral Data for <b>5</b>	99
	Spectral Data for <b>6</b>	99
	Spectral Data for <b>7</b>	100
	Spectral Data for <b>8</b>	100
5.5	Preparation of Methoxy Analogs - General Procedure	102

5.5.1	Spectral Data for <b>1b</b>	
	Spectral Data for <b>2b</b>	
	Spectral Data for <b>3b</b>	
5.5.2	Preparation and Spectral Data for <b>4b</b>	104
5.6	Instrumentation and Techniques	106
5.6.1	Nanosecond Laser Flash Photolysis Experiments	106
5.6.2	Steady State Photolysis	106
5.6.3	Phosphorescence Spectrum and Lifetime Measurements	107
	<b>APPENDIX</b>	109
	<b>REFERENCES</b>	110

## LIST OF FIGURES

Figure 1.	Jablonski Diagram of Electronic States	3
Figure 2.	Resonance Structures of a Phenyl-Alkyl-Ketone ( $\pi, \pi^*$ ) <sup>3</sup> state	5
Figure 3.	Triplet Energy Gap for a Phenyl-Alkyl-Ketone with $\pi, \pi^*$ Lowest Lying Triplet State	7
Figure 4.	Effect of Substituents on the Energies of Pure $n, \pi^*$ and $\pi, \pi^*$ triplet states of Phenyl-Alkyl-Ketones	9
Figure 5.	$n, \pi^*$ Triplet State of a Phenyl-Alkyl-Ketone Showing the Two Singly Occupied p-Orbitals	9
Figure 6.	Norrish Type II Photoreaction	10
Figure 7.	Geometry of 'in plane' Hydrogen Atom Abstraction	14
Figure 8.	Important Factors which Affect Hydrogen Atom Abstraction Efficiency	15
Figure 9.	Bimolecular Phenolic Hydrogen Abstraction by a ( $\pi, \pi^*$ ) <sup>3</sup> ketone	20
Figure 10.	Intramolecular Excited State Quenching Mechanism of <b>1a</b>	21
Figure 11.	Compounds of interest in the Study	23
Figure 12.	Additional Compounds for Study - Different Chromophores	24
Figure 13.	Ultraviolet Absorption Spectra	
a)	UV Spectrum of <b>1a</b>	27

b)	UV Spectrum of <b>1b</b>	27
c)	UV Spectrum of <b>2a</b>	27
d)	UV Spectrum of <b>2b</b>	27
e)	UV Spectrum of <b>3a</b>	27
f)	UV Spectrum of <b>3b</b>	27
g)	UV Spectrum of <b>4a</b>	28
h)	UV Spectrum of <b>4b</b>	28
i)	UV Spectrum of <b>5</b>	28
j)	UV Spectrum of <b>6</b>	28
k)	UV Spectrum of <b>7</b>	28
l)	UV Spectrum of <b>8</b>	28
m)	UV Spectrum of <b>15</b>	29
n)	UV Spectrum of <b>16</b>	29
o)	UV Spectrum of <b>17</b>	29
p)	UV Spectrum of <b>18</b>	29

Figure 14. Phosphorescence Spectra

a)	Phosphorescence Spectrum of <b>2a</b>	31
b)	Phosphorescence Spectrum of <b>6</b>	31
c)	Phosphorescence Spectrum of <b>4a</b>	31
d)	Phosphorescence Spectrum of <b>8</b>	31

Figure 15.		
a)	Transient Decay of <b>4a</b> in acetonitrile at 22°C	36
b)	Transient Decay of <b>1a</b> in acetonitrile at 22°C	36
Figure 16.	Transient UV Spectrum of <b>1a</b>	38
Figure 17.	Transient UV Spectrum of <b>1b</b>	38
Figure 18.	Transient UV Spectrum of <b>2a</b>	39
Figure 19.	Transient UV Spectrum of <b>2b</b>	39
Figure 20.	Transient UV Spectrum of <b>3a</b>	40
Figure 21.	Transient UV Spectrum of <b>3b</b>	40
Figure 22.	Transient UV Spectrum of <b>4a</b>	41
Figure 23.	Transient UV Spectrum of <b>4b</b>	41
Figure 24.	Transient UV Spectrum of <b>5</b>	42
Figure 25.	Transient UV Spectrum of <b>6</b>	42
Figure 26.	Transient UV Spectrum of <b>7</b>	43
Figure 27.	Transient UV Spectrum of <b>8</b>	43
Figure 28.	Transient UV Spectrum of <b>15</b>	44
Figure 29.	Transient UV Spectrum of <b>16</b>	44
Figure 30.	Transient UV Spectrum of <b>17</b>	45
Figure 31.	Transient UV Spectrum of <b>18</b>	45
Figure 32.	Transient UV Spectrum of <b>19</b>	46
Figure 33.	Time Resolved Transient UV Spectrum of <b>1a</b>	47



Figure 34.	Quenching Plot of <b>18</b> by 1,3-cyclohexadiene	50
Figure 35.		
a)	1-Methylnaphthalene Quenching of <b>5</b> in 5% aqueous (H <sub>2</sub> O/D <sub>2</sub> O) acetonitrile	55
b)	1-Methylnaphthalene Quenching of <b>7</b> in 5% aqueous (H <sub>2</sub> O/D <sub>2</sub> O) acetonitrile	55
Figure 36.	Arrhenius Plot of Compound <b>1a</b>	61
Figure 37.	Arrhenius Plot of Compound <b>2a</b>	61
Figure 38.	Arrhenius Plot of Compound <b>3a</b>	62
Figure 39.	Arrhenius Plot of Compound <b>4a</b>	62
Figure 40.	Arrhenius Plot of Compound <b>5</b>	63
Figure 41.	Arrhenius Plot of Compound <b>6</b>	63
Figure 42.	Arrhenius Plot of Compound <b>7</b>	64
Figure 43.	Arrhenius Plot of Compound <b>8</b>	64
Figure 44.	Valerophenone Derivative of <b>1a</b>	65
Figure 45.	Quenching Geometries for Compounds <b>1a</b> , <b>2a</b> , <b>3a</b> and <b>4a</b>	76
Figure 46.	Correlation Between Bi- and Unimolecular Reactions	80

## LIST OF TABLES

Table I.	Phosphorescence Data Obtained at 77K in EtOH/MeOH	34
Table II.	Rate Constants for Triplet Quenching of Compounds <b>1-8</b> by 1,3-Cyclohexadiene	51
Table III.	Stern-Volmer Constants for 1-Methylnaphthalene Quenching	55
Table IV.	Lifetimes of Carbonyl Triplets in Acetonitrile	56
Table V.	Rate Constants for Triplet Decay in 5% aqueous (H <sub>2</sub> O/D <sub>2</sub> O) acetonitrile at 22°C.	57
Table VI.	Triplet Quenching of Model Compounds by 1,3-Cyclohexadiene	58
Table VII.	Triplet Quenching of Model Compounds by Substituted Phenols	59
Table VIII.	Lifetimes of Carbonyl Triplets in Acetonitrile	74
Table IX.	Kinetic Isotope Effects in Deoxygenated Acetonitrile.	78
Table X.	Activation Parameters for Intramolecular Phenolic Quenching	83

## **LIST OF SCHEMES**

Scheme I.	Kinetic Scheme of Similar Bimolecular and Unimolecular Reactions	17
Scheme II.	Ground State $\leftrightarrow$ Excited State Kinetic Relationships	18
Scheme III.	General Synthesis of Linked Phenolic Ketones	25
Scheme IV.	General Synthesis of Methoxy Analogs	26

## **CHAPTER I**

### **INTRODUCTION**

#### **1.1**            **Photochemistry of Phenyl Alkyl Ketones**

Throughout the past fifty years the photophysics and the photochemistry of phenyl ketones has been a topic which has received a great deal of attention. Various studies of phenyl ketones have concentrated on electron or energy transfer reactions; but arguably their most interesting photochemical reaction is abstraction of a hydrogen atom from a suitable donor. This particular process has been the subject of many studies in both solution and the solid state, wherein many factors which influence reactivity have been identified. Recently, Wagner has indicated that when dealing with these reactions one must account for five fundamental questions which are essential in understanding how and why hydrogen atom abstraction by a carbonyl triplet occurs.<sup>(1)</sup> These questions are:

1. How does the electronic configuration of the reacting triplet affect the process being studied?
2. How do substituent effects influence the rates of reaction for both the phenyl ketone and the hydrogen donor?

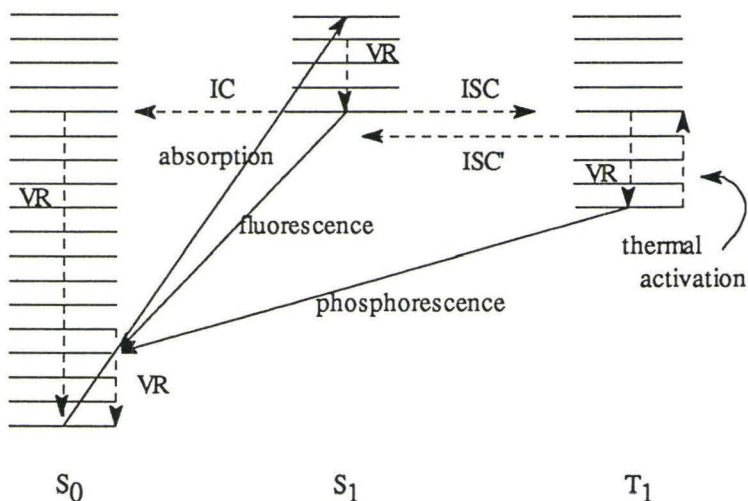
3. How are the rate constants for hydrogen abstraction dependent on the thermodynamics of the reaction?
4. What are the orientational, conformational and stereoelectronic requirements for the reaction?
5. How does charge transfer contribute to the process of hydrogen abstraction?

## **1.2 Electronic Configuration of Phenyl Ketones**

The excited state of a molecule cannot last indefinitely because of its instability relative to the ground state. The process of relaxation to the ground state may involve the release of either thermal energy or radiation. Those processes that do not involve the emission of radiation are called nonradiative transitions. The transitions that do emit radiation are of interest because they can provide valuable information regarding excited state energies and lifetimes.

The emitted radiation is called fluorescence if it involves transitions between states of like spin multiplicity. Fluorescence is most commonly observed from the  $S_1$  state to the singlet ground state ( $S_0$ ) as most organic molecules (except radicals) are closed-shell in the ground state. The emitted radiation is called phosphorescence if the radiative transition occurs between excited electronic states of opposite spin multiplicity.

**Figure 1.** Jablonski diagram of electronic states.



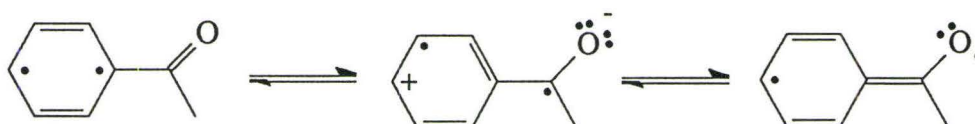
In Figure 1, all transitions that involve emission or absorption of electromagnetic radiation are shown by solid arrows. Those transitions that are nonradiative in nature are depicted by dotted arrows. Radiative transitions are ‘vertical’ transitions that involve a change in the total energy of the molecule. Nonradiative transitions are essentially ‘horizontal’ transitions which are conversions from one excited state to another of similar energy. Non-radiative conversion between states with the same multiplicity is called internal conversion (IC) while conversion between states with a different multiplicity is called intersystem crossing (ISC). ISC from  $S_1$  to  $T_1$  (the triplet state of lowest energy) leaves some excess energy which is quickly removed by the solvent as vibrational energy (VR).<sup>(2)</sup> Normally IC from upper singlet or triplet states to the lowest excited state within the same manifold is very fast and usually precedes any other type of excited state decay.

Phenyl alkyl ketones exhibit very efficient  $S_1 \rightarrow T_m$  ISC ( $\Phi \geq 0.96$ )<sup>(3)</sup>. These ketones possess two low lying singlet and triplet states  $(n, \pi^*)^{1,3}$  or  $(\pi, \pi^*)^{1,3}$ ; either of which may be obtained upon excitation of the ketone. The symbols in the parentheses refer to the molecular orbitals that are half-filled in the excited state of the molecule. Each type of excited state has significantly different reactivities with regard to hydrogen abstraction processes. The lowest excited state obtained for a given ketone depends on the relative energies of the non-bonding molecular orbital and of the pi molecular orbital. The factors which contribute to the relative energies of these molecular orbitals and ultimately to the nature of the lowest excited state obtained for a given ketone are predominantly from electronic effects by substituents on the phenyl ring. To a lesser extent, environmental effects such as solvent polarity can act to stabilize the non-bonding molecular orbital and raise the energy of the  $(n, \pi^*)^3$  state relative to the  $(\pi, \pi^*)^3$  state.

Hydrogen abstraction by carbonyl triplets has been reported by ketones in both the  $n, \pi^*$  and  $\pi, \pi^*$  triplet states.<sup>(3,6,10)</sup> However, it is widely accepted that the  $(n, \pi^*)^3$  state is generally much more reactive than the  $(\pi, \pi^*)^3$  state toward abstraction of alkyl hydrogen atoms.<sup>(4,5)</sup> The main difference between the  $(\pi, \pi^*)^3$  and the  $(n, \pi^*)^3$  excited states remains in their electronic distributions. The  $(\pi, \pi^*)^3$  state can be represented in terms of the resonance structures shown in Figure 2. The carbonyl group is electron rich in nature and can delocalize its electron density throughout the  $\pi$  system, making it seemingly more difficult to undergo reaction. The  $(n, \pi^*)^3$  state on the other hand has analogous

reactivities to alkoxy radicals which has the reactive site of the molecule in the singly occupied  $n$  orbital on oxygen (Figure 5).

**Figure 2.** Resonance structures of a phenyl alkyl ketone  $(\pi, \pi^*)^3$  state.



The carbonyl group  $(n, \pi^*)^3$  states are electron deficient by nature and their electron demand in the transition state for hydrogen transfer is stabilized by charge transfer from the developing radical site to the carbonyl oxygen.

Thus one may ask, from where do  $\pi, \pi^*$  triplets derive their reactivity? Yang in 1967 found that ketones with  $\pi, \pi^*$  lowest triplets are photoreduced in isopropyl alcohol.<sup>(6)</sup> A fair amount of work has been done on this subject and essentially there are two different explanations for the observed reactivities of these triplet ketones. The first explanation is that a certain amount of  $(n, \pi^*)^3$  character is mixed vibronically into the lowest  $(\pi, \pi^*)^3$ , thereby accounting for the reactivity of ketones with lowest  $(\pi, \pi^*)^3$  states. The second explanation, resulting from more detailed studies, suggests that reactivity comes from low concentrations of the  $(n, \pi^*)^3$  state, which is attained through thermal population from the



lower  $(\pi, \pi^*)^3$  state. This is considered to account for all reactivity when  $\Delta E (E_{n,\pi} - E_{\pi,\pi}) < 5 \text{ kcal/mole.}^{(3)}$

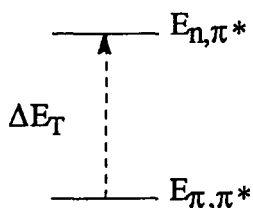
$$k_{\text{obs}} = \chi_{n,\pi} k_{n,\pi} + \chi_{\pi,\pi} k_{\pi,\pi} \quad [1]$$

$$\chi_{n,\pi} = (1 - \chi_{\pi,\pi}) = e^{-\Delta E/RT} / [1 + e^{-\Delta E/RT}] \quad [2]$$

One main reason for this view is that rate constants for triplet state  $\gamma$ -hydrogen abstraction by phenyl alkyl ketones are ca. 100 times greater than those for p-anisyl ketones, where hydrogen abstraction rate constants for both p-anisyl substituted and unsubstituted phenyl alkyl ketones are equally reduced by electron withdrawing substituents on the  $\delta$ -carbon. Such results can only be described by equation 1 above if in fact it is the  $(n, \pi^*)^3$  state which is responsible for the abstraction. Equation 1 depicts the rate constant for hydrogen abstraction ( $k_{\text{obs}}$ ) as the weighted sum ( $\chi_{\pi,\pi} + \chi_{n,\pi} = 1$ ) of the rate constants due to reaction from both the  $(n, \pi^*)^3$  state ( $k_{n,\pi}$ ) and the  $(\pi, \pi^*)^3$  state ( $k_{\pi,\pi}$ ). Equation 2 illustrates how the weighting of the excited states in equation 1 are influenced by Boltzmann factors.

The other evidence for thermal population of the upper state comes from flash kinetic experiments. Activation parameters for hydrogen abstraction by several ring-substituted phenyl ketones were measured for both intermolecular and intramolecular reactions.<sup>(7,8)</sup> Although both cases showed little variation in the entropy of activation for a given reaction, they did show an increase in the activation energies for ketones with  $\pi, \pi^*$  lowest triplet states corresponding to the energy difference between the  $\pi, \pi^*$  triplet state and its upper  $n, \pi^*$  triplet state.

**Figure 3.** Triplet energy gap for phenyl alkyl ketones with  $\pi, \pi^*$  lowest lying triplet state.



Steele<sup>(9)</sup> has pointed out that reactivity differences which arise from varying degrees of  $(n, \pi^*)^3$  state character for the reactive state would appear in the thermodynamics in terms of activation entropy, but this was not observed.

What still has not been established is the intrinsic reactivity of the  $(\pi, \pi^*)^3$  state of phenyl-ketones toward hydrogen abstraction. Hammond and Leermakers<sup>(10)</sup> in 1962 began investigating the reactivity of ketones with low  $(\pi, \pi^*)^3$  state energies and found the rate constant for hydrogen abstraction from butylstannane by 1-acetylnaphthalene  $\pi, \pi^*$  triplet to be  $1-2 \times 10^6$ . Later studies<sup>(11)</sup> showed that  $n, \pi^*$  triplets abstract hydrogen from stannane with rate constants approaching  $10^9$ , thus indicating that  $\pi, \pi^*$  triplets are  $\approx 10^3$  times less reactive than  $n, \pi^*$  triplets. This difference probably arises because of the spin localization difference in the two excited states. Hammond and Leermakers suggest that  $n, \pi^*$  triplets have their spin localized on the oxygen atom and take on a 1,2-diradical nature, thus reacting like an alkoxy radical. The  $\pi, \pi^*$  triplet state on the other hand has

the spin delocalized throughout the phenyl ring and would thus be expected to exhibit substantially reduced radical character.

### **1.3 Substituent Effect on Reactivity of Phenyl Alkyl Ketones**

Although the photoreduction of benzophenone is one of the most well known and best studied photoreactions, only a handful of studies have looked at what effect placing ring substituents on phenyl-alkyl-ketones have on the hydrogen abstraction process. Two major reasons exist for the lack of extensive studies into this issue. Firstly, we have already seen that substitution can alter the electronic configuration of the lowest lying triplet state (Figure 4). In fact, substituents on phenyl-alkyl-ketones alter the nature of the lowest excited state so drastically that Hammett plots tend to contain considerable scatter.<sup>(12)</sup> The substituents are not conjugated directly to the reactive half-filled orbital on oxygen. Because the two unpaired electrons are of the same spin multiplicity they want to be as far apart from each other as possible and therefore adopt an orthogonal orientation. In doing so (as can be seen in Figure 5), the half-occupied p-orbital on oxygen is prevented from direct conjugation, thereby allowing only small inductive effects from ring substituents.

**Figure 4.** Effect of substituents on the energies of pure  $n, \pi^*$  and  $\pi, \pi^*$  triplet states of para substituted phenyl-alkyl-ketones.

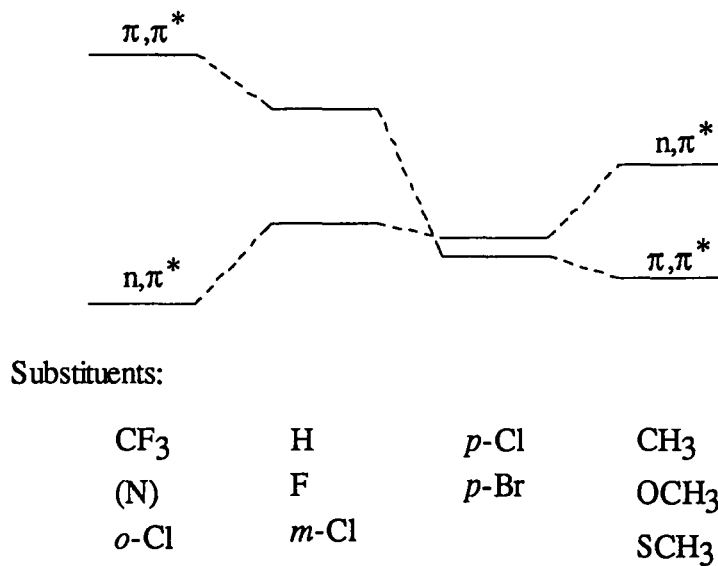
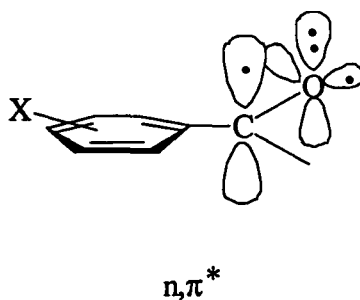


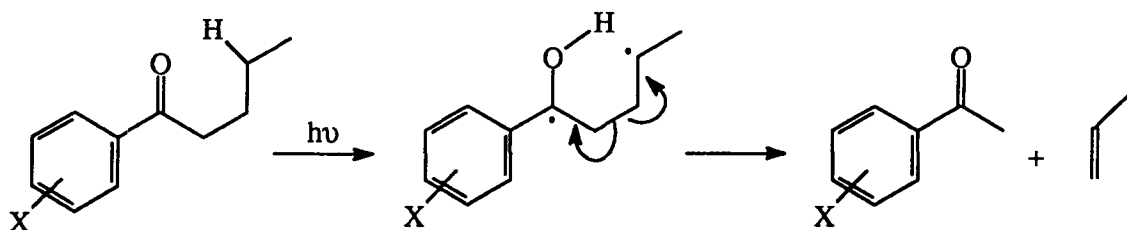
**Figure 5.**  $n, \pi^*$  triplet state of a phenyl-alkyl-ketone showing the two singly occupied p-orbitals.



This complicates the process of hydrogen atom transfer and makes isolating factors that affect reactivity quite difficult. Another problem arises in that electron-deficient ketone triplets react with even weak donors such as alkylbenzenes by charge-transfer mechanisms, which acts to obscure a value for pure hydrogen abstraction.

As a result, most of the studies performed on substituent effects on phenyl ketone reactivity deal with the Norrish II reaction. Studies of the efficiency of this intramolecular hydrogen abstraction process in substituted valerophenones were the key to sorting out what affect substituents have on aromatic ketone photochemistry. Wagner<sup>(4)</sup> used this

**Figure 6.** Norrish type II photoreaction.



reaction (Fig. 6) to show that methyl substituents on the phenyl ring lower the rate of intramolecular hydrogen abstraction by one order of magnitude relative to the unsubstituted compound. Valerophenones substituted with methoxy groups are at least two orders of magnitude less reactive than the unsubstituted case. Furthermore, meta substitution on the ring leads to a tenfold increase in the rate of nonradiative, nonproductive decay compared to the corresponding para-substituted analogs and show a

tenfold decrease in reactivity. These results led Wagner to suggest that the  $(n, \pi^*)^3$  and  $(\pi, \pi^*)^3$  states of the *meta*-substituted compounds must have a separation of at least 3 kcal/mol greater than their *para*-substituted counterparts.

Wagner also found that the same effects of excited state inversion could be accomplished by changing the solvent polarity from a hydrocarbon solvent to an alcohol solvent.<sup>(13,14)</sup> This is possible since the  $(n, \pi^*)^3$  state is less polar than the ground state; while the  $(\pi, \pi^*)^3$  state is more polar. The inversion of the triplet states can be observed by phosphorescence measurements, which correlate decreased triplet reactivity due to substitution with lower energy 0-0 band phosphorescence energies.

Although it is quite difficult to compare substituent effects because of the electronic factors, one can easily see that both *meta*- and *para*-methoxy substitution on a phenyl-alkyl-ketone results in a lowest lying  $(\pi, \pi^*)^3$  state with a similar triplet energy gap.

#### **1.4 Substituent Effects On The Reactivity of Hydrogen Donors**

There is another aspect of these bimolecular reactions that do not deal with the reacting ketone, the chromophore in these photochemical reactions, but with the hydrogen donor. As mentioned previously, ketones with lowest  $(\pi, \pi^*)^3$  states are known to be less reactive than those with lowest  $(n, \pi^*)^3$  states towards hydrogen abstraction from alkyl hydrogen-atom donors. Scaiano, however, has shown that  $\pi, \pi^*$  triplets do abstract

hydrogen very efficiently if the hydrogen donor is a phenol.<sup>(7,15)</sup> Again, because we are looking at conjugated systems, consideration must be given to the phenolic moiety of the reaction, which can also be susceptible to substituent effects. Scaiano has used both phenyl ketones and *t*-butoxy radicals to look at reactivity trends with phenolic substitution. Specifically, he used benzophenone [ $(n, \pi^*)^3$ ] and *para*-methoxypropiophenone [ $(\pi, \pi^*)^3$ ] as standards to monitor the reaction with substituted phenols. Surprisingly, he observed that rate constants for quenching of *p*-methoxypropiophenone triplets by phenols are consistently higher than those for benzophenone in benzene solution. The difference between the two sets of rate constants is smaller in solvents such as 9:1 acetonitrile:water. These results are in significant contrast with data reported for hydrogen atom abstraction from hydrocarbons or alcohols, as previously presented. This would seem to indicate that the mechanism for hydrogen atom abstraction of carbonyl triplets from phenols is different from that involving hydrocarbons. Since the triplet energy of phenol is 81.7 kcal/mole,<sup>(16)</sup> it appears unlikely that phenol would quench the carbonyl triplets ( $\Delta E_T \equiv 72$  kcal/mole<sup>(17)</sup>) efficiently by an energy transfer mechanism. This is supported by the very slow rate of quenching by anisole ( $E_T = 80.8$  kcal/mole<sup>(16)</sup>). The Hammett plot for *p*-methoxypropiophenone in benzene shows virtually no dependence of the rates of reaction with the  $\sigma$  value of the substituent on the phenol ( $\rho \approx 0.02$ ). Scaiano suggested that the reason for this is that the rate constants are almost diffusion-controlled, which renders the process relatively insensitive to substituent effects. In wet acetonitrile, the reactions are slower, and show a greater selectivity. The difference in solvent polarity indicates the

importance of hydrogen bonding for the phenols containing substituents with large sigma values. Kinetic isotope effects on the reaction were also measured in acetonitrile-D<sub>2</sub>O solution. Phenolic proton exchange with D<sub>2</sub>O occurs such that rates obtained in this solvent can be attributed exclusively to deuterium atom abstraction. The hydrogen/deuterium isotope effects are much higher for the methoxypropiophenone reactions ( $k_H/k_D \sim 3.9$ ) than for the benzophenone reactions ( $k_H/k_D \sim 1.2$ ). The rather large isotope effects in the methoxypropiophenone case indicate that hydrogen abstraction is in fact the rate determining step for quenching of the carbonyl triplet by phenols. Benzophenone seems to be quenched by a more complex mechanism where hydrogen atom transfer is not as well-developed in the transition state as in the valerophenone case.

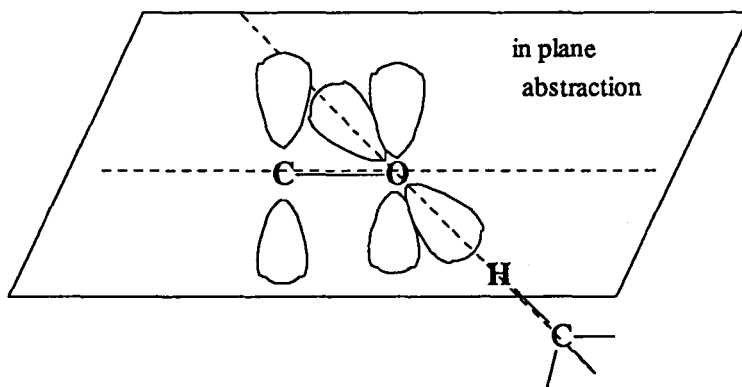
### **1.5                    Orientational Requirements For Hydrogen Abstraction**

Over twenty years ago, Turro suggested that the hydrogen atom being abstracted in the photochemical reaction of  $n, \pi^*$  triplets ketones would be expected to lie on the axis of the singly-occupied carbonyl n-orbital.<sup>(18)</sup> This was the first time that orientational requirements had been considered to be important. The appeal became apparent because of the 'alkoxy-like'  $(n, \pi^*)^3$  reactivity of these molecules, which would likely centre upon the n-orbital of the oxygen. A study of the orientational requirements of the abstraction process<sup>(19)</sup> led to the conclusion that for large ketones where the  $(\pi, \pi^*)^3$  state is below



that of the  $n, \pi^*$  triplet, in-plane reaction of the  $(\pi, \pi^*)^3$  state (Figure 7) takes place owing to the crossing over of the 'zero order' reaction profiles of the  $(n, \pi^*)^3$  and  $(\pi, \pi^*)^3$  states.

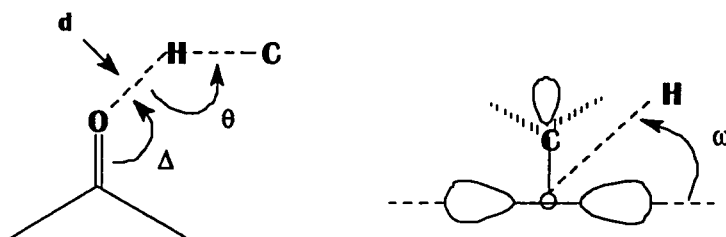
**Figure 7.** Geometry of 'in-plane' hydrogen atom abstraction.



Many examples have been reported in which abstraction of a hydrogen atom which lies outside of the nodal plane of the carbonyl  $\pi$ -system occurs.<sup>(20)</sup> It was thought that perhaps there is a cosine-squared dependence between the out-of-plane angle and the rate of hydrogen abstraction. Scheffer and coworkers have examined the geometric parameters which are important for hydrogen atom transfer to take place, using compounds which undergo hydrogen atom transfer in their crystalline states.<sup>(20,21)</sup> X-ray crystallography was used to depict the ground state parameters which are the most important in determining the rate of the  $(n, \pi^*)^3$  hydrogen atom abstraction process (Figure 8). Over two dozen examples have been analysed, and the data extracted from the

crystallographic data showed that the O-H distances ranged from 2.3 to 2.7 Å. The optimum distance (d) was found to be 2.7 Å (Fig. 8), which corresponds to the sum of the van der Waals radii of the two elements. In Figure 8,  $\Delta$  and  $\theta$  are defined as the ‘in plane’ angles while  $\omega$  depicts the ‘out-of-plane’ angle.

**Figure 8.** Important factors which affect hydrogen atom abstraction efficiency.



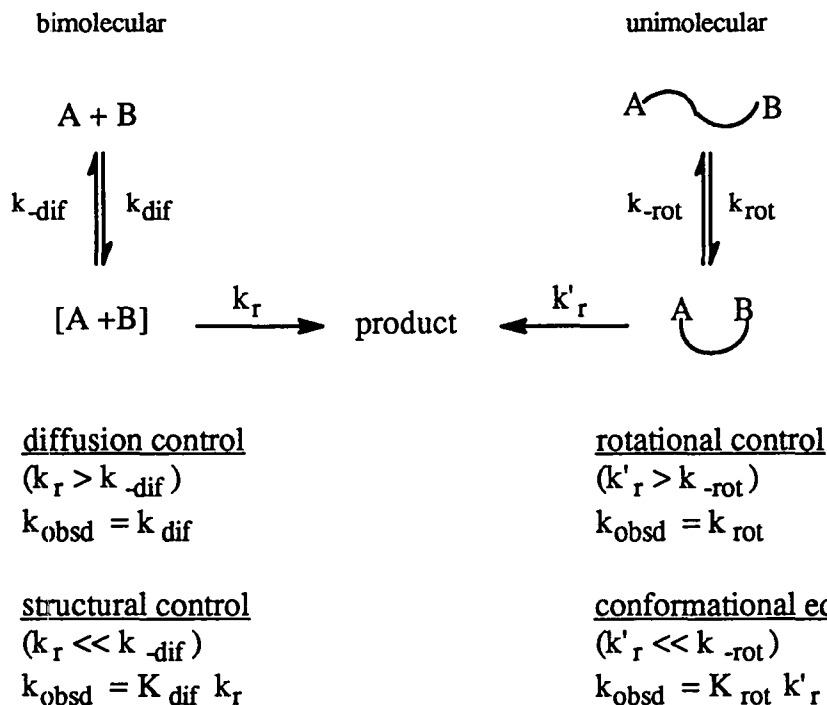
$$\Delta = 90 - 120^\circ \quad \theta = 180^\circ \quad \omega = 0^\circ \quad d \leq 2.7 \text{ Ang}$$

Scheffer indicated that whenever a hydrogen is approximately 2.7 Å away from the carbonyl oxygen in the ground state, minimal molecular motions are required in the excited state for removal of the hydrogen atom. It is interesting to note that while all the angles seem to have an optimal range or fixed value,  $\omega$  (the dihedral angle of C-C=O--H) can depart significantly from 0° and still result in efficient reaction. This has been observed in a number of systems.

## **1.6 Conformational Requirements**

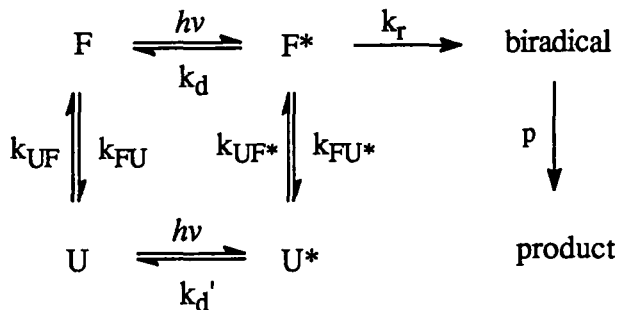
Intramolecular excited state reactions often proceed at rates which are limited by those of conformational changes. Excited state behaviour in systems that are conformationally constrained can thus provide information on the orientational requirements that are necessary for reaction or interaction of two functional groups.

Most intramolecular reactions have an intermolecular counterpart with which useful comparisons can be made. Wagner<sup>(22)</sup> and others<sup>(23)</sup> have studied the relationships between corresponding inter- and intramolecular reactions in the excited state and in the ground state. Scheme I describes the distinct kinetic implications that the uni- and bimolecular reactions possess. Both bimolecular and unimolecular schemes deal with reaction between moieties A and B, which is either slower or faster than their movement apart. In the bimolecular case, it is possible to have diffusion controlled reactions. The unimolecular equivalent is the rotation-controlled reaction as governed by  $k_{rot}$ . This type of situation is therefore limited to highly energetic molecules, such as those obtained upon absorption of light. Wagner also points out that the observed rate constants from 'slow' reaction indicate a structure dependence on the rate constant  $k_r$  which is modified by the preequilibrium constant. The major difference between the unimolecular and the bimolecular reactions is due to the fact that the conformational equilibrium ( $K_{rot}$ ) is much more sensitive to the structure of the reacting molecule than is the bimolecular equilibrium constant ( $K_{dif}$ ) as shown in Scheme I.

**Scheme I.** Kinetic scheme of similar bimolecular and unimolecular reactions.

To deal with excited state reactions we must also look at the relationship between the ground state and the excited state. Scheme II shows this relationship, where F and U represent the favorable and unfavorable conformations for an intramolecular reaction to proceed. Three separate cases arise depending on how the rates of excited state conformational change compete with the rates of various chemical and physical excited state decay processes.

**Scheme II.** Ground state <-> excited state kinetic relationships.



In the case of slow excited state reactions, conformational equilibrium is established prior to reaction. Equation 3 shows that the observed reaction rate constants include contributions from excited state conformational equilibrium constants. Wagner<sup>(22)</sup> stresses that in this case there is only one kinetically distinct excited state, even though two different conformations may undergo two different reactions (Equation 3: see Appendix for definition of symbols).

Conformational Equilibrium:  $k_{FU^*}, k_{UF^*} \gg k_r, k_d$

$$k_{\text{obsd}} = k_r k_{UF^*} / (k_{FU^*} + k_{UF^*}) = \chi_{F^*} k_r \quad [3]$$

$$\Phi = k_r \chi_{F^*} / (k_r \chi_{F^*} + k_d \chi_{F^*} + k_d' \chi_{U^*}) \quad [4]$$

With fast excited state reactions and/or slow conformational change, the quantum yield of reaction is limited by the ground state population of favorable conformations (F). In this case there exists at least two distinct excited states, where only one of them (F\*)

can lead to the desired reaction. This case is said to possess ‘ground state control’ and can only be applied to reactions which are photochemically excited.

Ground State Control:  $k_{FU^*}, k_{UF^*} \ll k_r, k_d$

$$k_{\text{obsd}}(F) = k_r \quad [5]$$

$$\Phi = k_r \chi_F P / (k_r + k_d) \quad [6]$$

The third case is where conformational change and decay are competitive; here conformationally-controlled reactions can occur. There are again two distinct excited states. Reaction in this case can occur from either excited state but determines the lifetime of only one conformer (F). The rate of conformational change is lifetime-determining for the other (U).

Rotational Control:  $k_{UF^*} \sim k_d : k_{FU^*} \ll k_r$

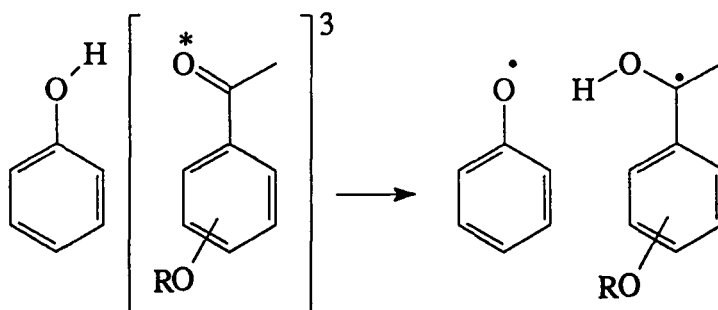
$$k_{\text{obsd}}(F) = k_r \quad k_{\text{obsd}}(U) = k_{UF^*} \quad [7]$$

$$\Phi = [ k_r \chi_F P / (k_r + k_d) ] + [ k_{UF^*} \chi_{U^*} P / (k_{UF^*} + k_d') ] \quad [8]$$

### 1.7 Intermolecular Hydrogen Atom Abstraction

For many years it was thought that alkoxy-substituted phenylalkyl ketones were unreactive towards hydrogen atom abstraction. Results published in 1981, however, indicated that these compounds do in fact undergo quite efficient hydrogen atom abstraction if the hydrogen donor is a phenol (Fig. 9).<sup>(15)</sup> Scaiano suggested that the abstraction process is accompanied by charge transfer in the transition state. To what extent hydrogen atom abstraction or charge transfer participates in the quenching of the excited state is difficult to ascertain.

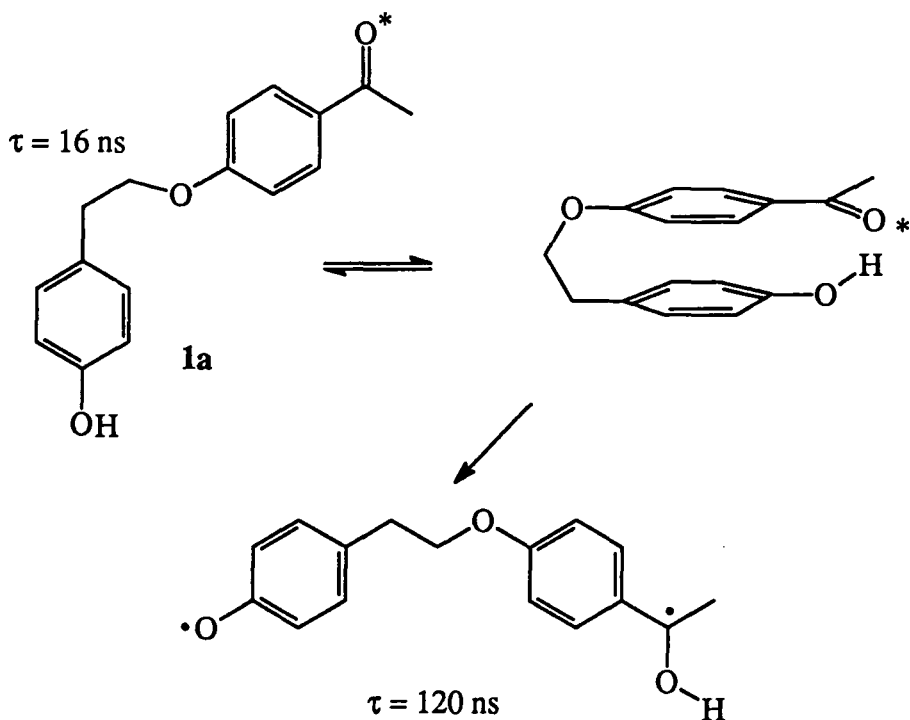
**Figure 9.** Bimolecular phenolic hydrogen atom abstraction by a  $(\pi, \pi^*)^3$  ketone.



Subsequent work was done on compound **1a** which incorporates the same ideas of the above process, but promotes quenching of the excited state through an intramolecular mechanism.<sup>(24)</sup> It was shown that upon irradiation, compound **1a** gives a carbonyl triplet with a lifetime of only 16 ns in acetonitrile solution. The triplet is thought to be short-lived because of very fast intramolecular abstraction of the phenolic hydrogen atom (Fig.

10). Evidence for this is the detection of a longer-lived transient ( $\tau = 120$  ns) whose spectrum appears to be the superposition of phenoxy and ketyl radical components. The triplet lifetime of the methoxy analog (**1b**) is much longer ( $2.6 \mu\text{s}$ ), which is what would be expected if the hydrogen abstraction reaction has been inhibited. Along with this, a hydrogen/deuterium kinetic isotope effect of 1.8 on the triplet lifetimes of **1a** was reported, indicating that hydrogen atom abstraction is the rate determining step in quenching the triplet. The rates of the molecular motions necessary to achieve the proper conformation for hydrogen transfer must have a negligible effect on the lifetime of the triplet in fluid solution.

**Figure 10.** Intramolecular excited state quenching mechanism of **1a**.



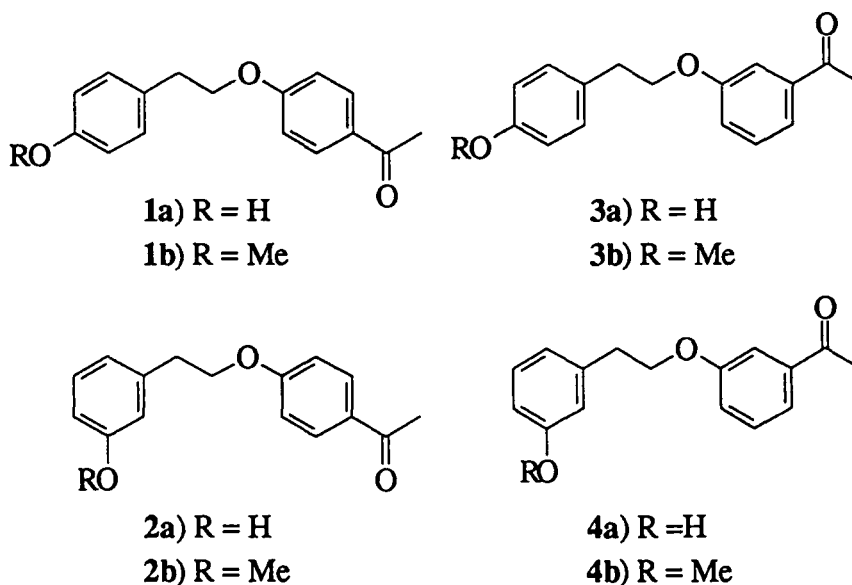


Further studies have shown that dissolution of **1a** in liquid crystals or cyclodextrins results in an increase in the lifetime of the triplet to about 1  $\mu\text{s}$ .<sup>(25)</sup> Liquid crystals and cyclodextrins are ordered media which inhibit solute molecular motions and can prevent the two ends of the molecule from 'seeing' each other during the lifetime of the excited state. These experiments confirm that for the hydrogen abstraction process to occur, the ends of the molecule must come within fairly close proximity, and attain a favorable orbital overlap between the phenolic hydrogen and the carbonyl triplet. Such a conformation as depicted in Figure 10 implies a 'sandwich' like conformation which would most likely be a high energy conformer because of the orbital overlap of the pi systems. These results proved quite interesting and provide the main stimulus for the following study.

### **1.8 Intramolecular Phenolic Hydrogen Abstraction by Carbonyl Triplets**

Considering the conformation from which hydrogen atom abstraction is believed to occur in compound **1a**, varying the relative positions of the hydroxy and acetyl substituents of the phenyl rings would be expected to affect the lifetime of the carbonyl triplet. The molecules shown below were chosen for study because of the relative positions of their substituents and their electronic configuration which produces  $\pi,\pi^*$  lowest lying triplets in the excited state.

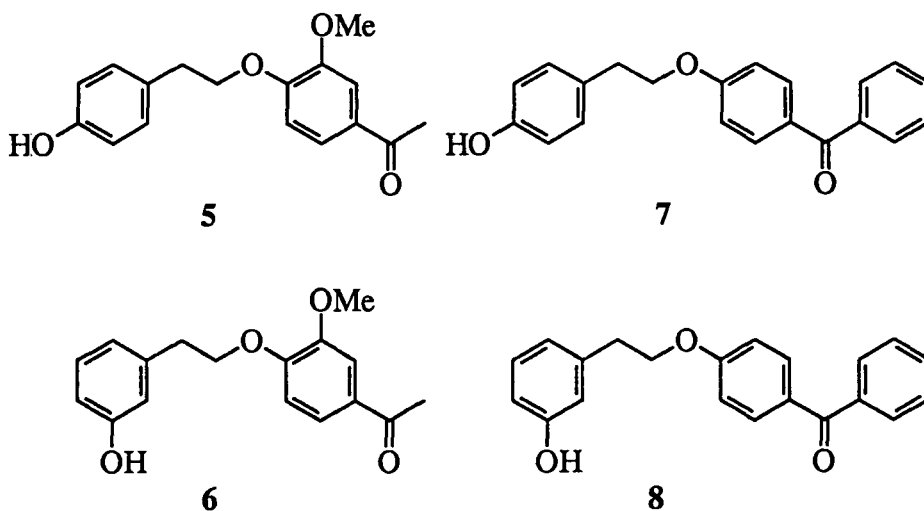
**Figure 11.** Compounds of interest in the study.



It is evident from first inspection that compounds **1a** - **4a** require very different geometries in order for the excited state to be quenched by hydrogen abstraction. It is the purpose of this work to determine the effects of such geometric factors on the kinetics and thermodynamics of the intramolecular phenolic hydrogen abstraction process in this system.

In addition to these, additional compounds were studied in order to provide insight into other factors which might affect the rate of intramolecular hydrogen abstraction in these systems. Compounds **5**, **6** provide larger triplet energy gaps ( $\Delta E_T$ ) without much additional steric interference compared to molecules [1-4].

**Figure 12.** Additional compounds for study - different chromophores.



Molecules 7 and 8 simply provide another comparable system; however, the lowest triplet state is  $n,\pi^*$  in character. This now gives a reacting chromophore to compare excited state reactivity as well as geometric differences.

The factors that need to be addressed when comparing the photochemistry of these systems are the same as those discussed in the previous pages. Consideration must be given not just to the molecule, but also to the electronic configuration of the excited state and the energy separation of the  $(n, \pi^*)^3$  and  $(\pi, \pi^*)^3$  triplet states in each molecule. Furthermore, the substitution on both the ketone and the phenolic moieties play a crucial role as far as affecting reactivity of the system as a whole. Finally, the most important factor should be the conformational possibilities; some molecules need to develop much more strain and orbital overlap in the transition state for phenolic hydrogen abstraction than others.

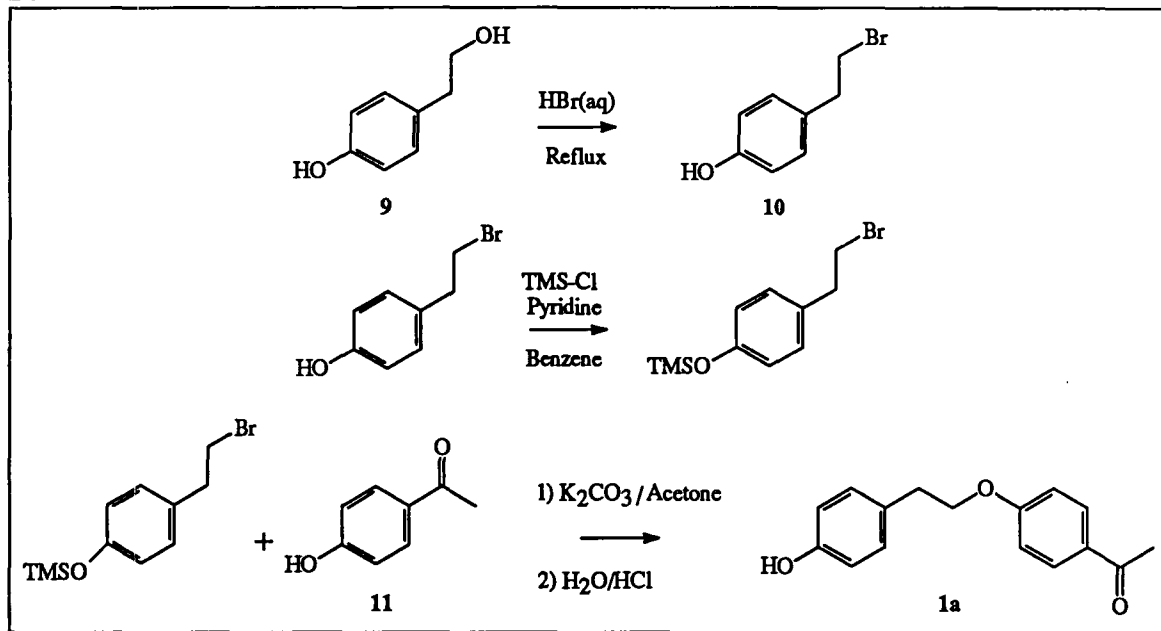
## CHAPTER II

### RESULTS

#### 2.1 General Synthesis of Linked Phenolic Ketones

The synthesis of the hydroxy-containing molecules [1-8] in this study all followed the general route shown for **1a** in Scheme III. A major side-product of the last step in the sequence is the respective styrene, the yield of which appeared to be dependent (inversely)

**Scheme III**



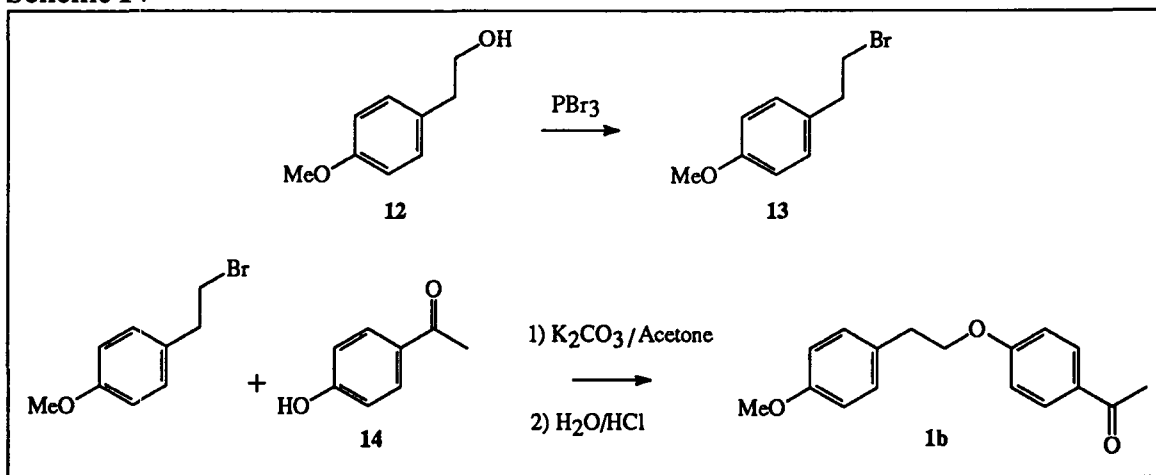
on how rigorously pyridine was removed from the system after protection of **10** as the trimethylsilyl ether. The desired product was obtained in yields of 25 - 40% (the rest

consisting of the corresponding styrene) as determined by  $^1\text{H}$  N.M.R spectroscopy.

Isolation and purification of the product was achieved by careful chromatography followed by several recrystallizations from ethanol/water.

The syntheses of the corresponding methoxy analogs were carried out in similar fashion (see Scheme IV). Yields of 50 - 80 % were achievable in this manner, with the amount of styrene formed being an inverse function of the strength of the nucleophile used in the coupling reaction. Purification and isolation was again performed by careful chromatography on silica gel. In a few cases, these compounds were synthesized by methylation of the corresponding phenolic compound with iodomethane.

**Scheme IV**

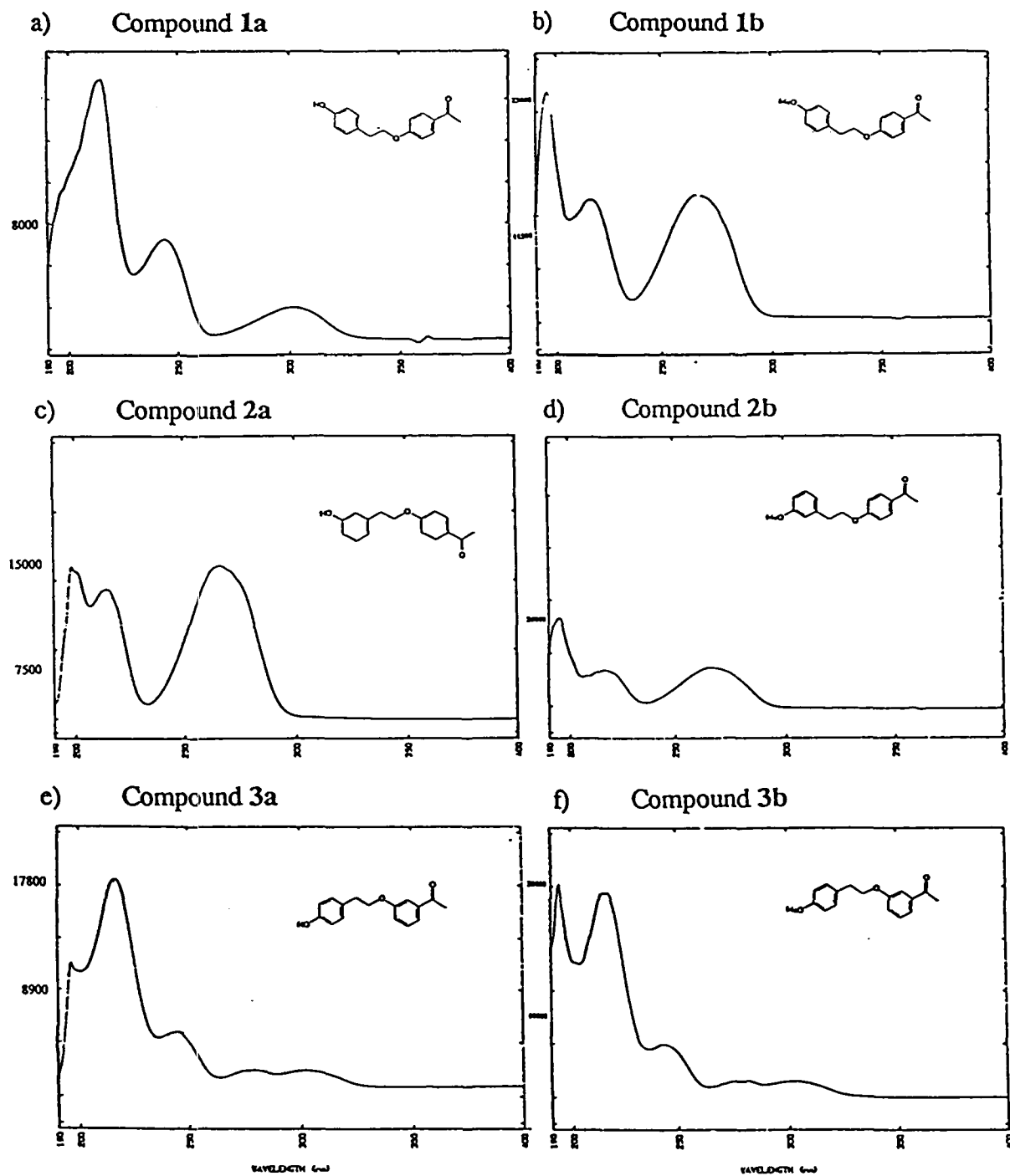


## 2.2 Ultraviolet Absorption Spectra

Ultraviolet absorption spectra of 1-8 were recorded in acetonitrile solution, and are shown in Fig 13a - 13l as plots of extinction coefficient vs. wavelength. For comparison, spectra of model compounds 15-19 are also shown Fig. 13m - 13p.

## ULTRAVIOLET ABSORPTION SPECTRA

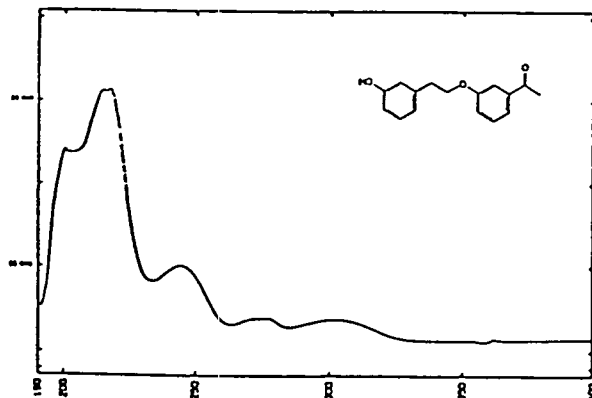
**Figure 13.** Ultraviolet absorption spectra taken in acetonitrile solution at 23°C.



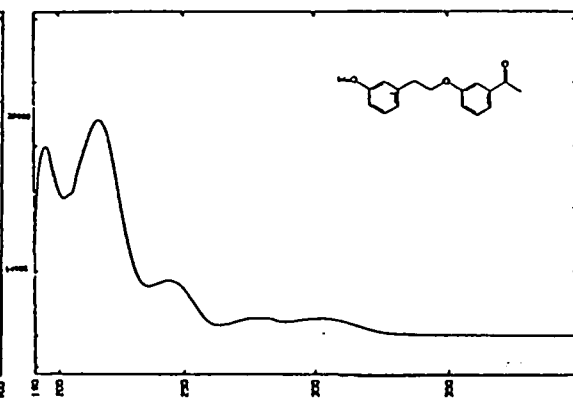
### ULTRAVIOLET ABSORPTION SPECTRA

**Figure 13.** Ultraviolet absorption spectra taken in acetonitrile solution at 23°C.

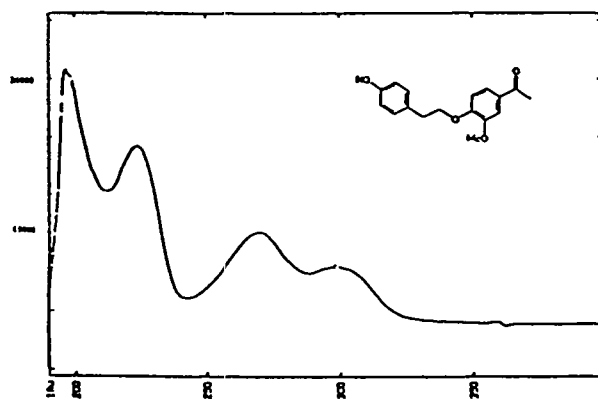
**g) Compound 4a**



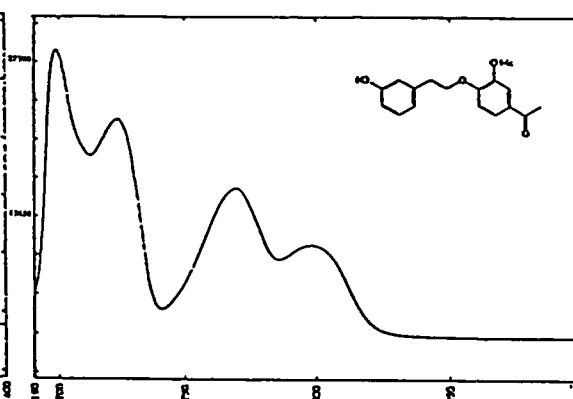
**h) Compound 4b**



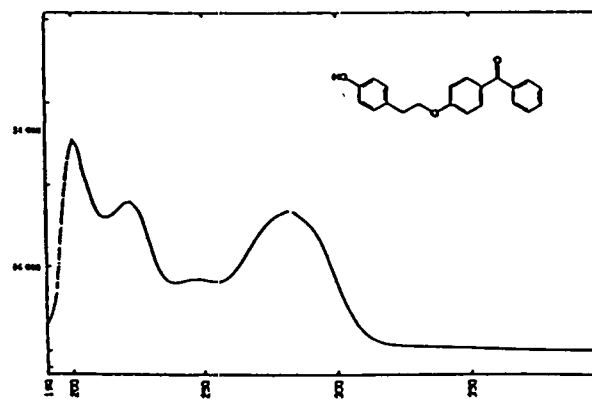
**i) Compound 5**



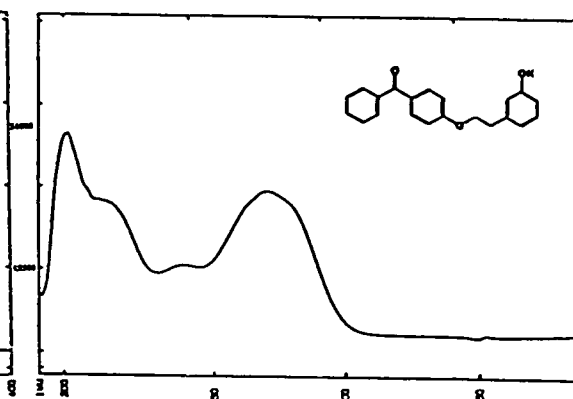
**j) Compound 6**



**k) Compound 7**



**l) Compound 8**



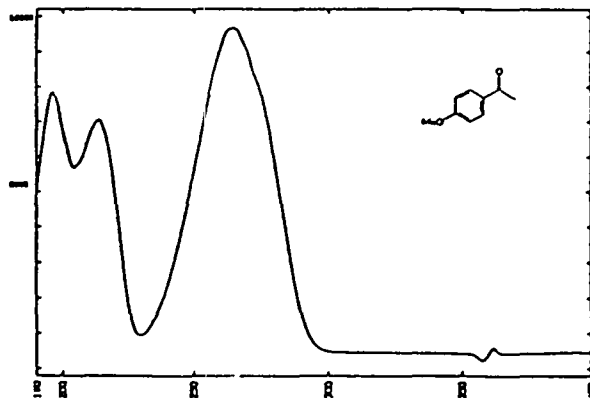
WAVELENGTH (nm)

WAVELENGTH (nm)

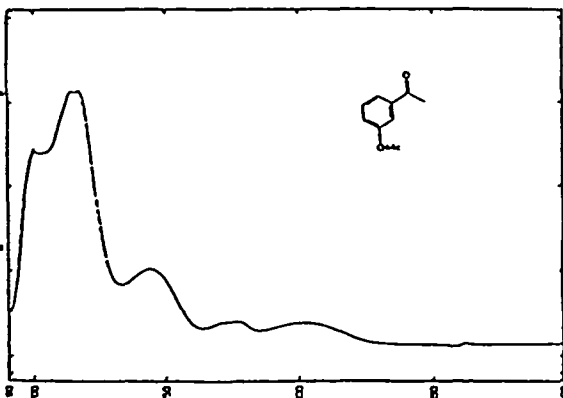
### ULTRAVIOLET ABSORPTION SPECTRA

**Figure 13.** Ultraviolet absorption spectra taken in acetonitrile solution at 23°C.

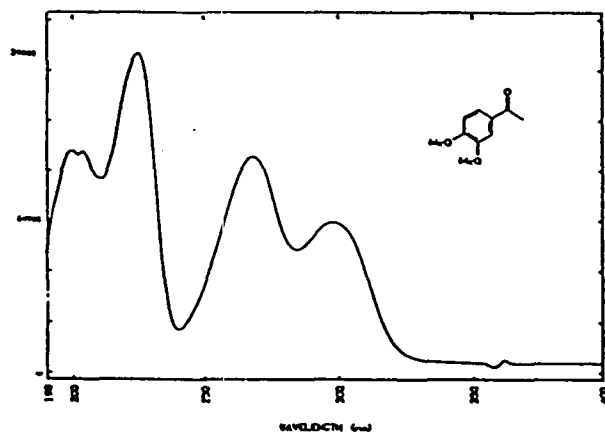
m) Compound 15



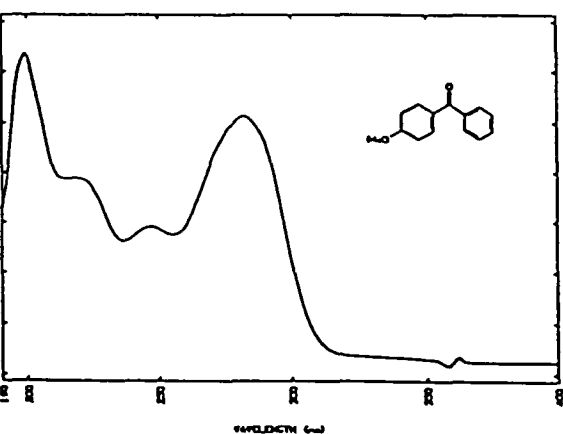
n) Compound 16



o) Compound 17



p) Compound 19





### 2.3 Phosphorescence Emission Spectroscopy

Phosphorescence emission spectra of 1-8 were recorded in a 4:1 ethanol/methanol glass at 77K, using pulsed excitation (1Hz repetition rate) and gated detection (0.02 - 0.2 seconds after the excitation pulse). This procedure isolates the relatively long-lived phosphorescence emission spectrum from the prompt emission due to light scattering and fluorescence. Representative spectra are shown in Figure 14. The triplet energy ( $E_T$ ) of each compound was calculated according to equation 9, where  $\lambda_{o-o}$  corresponds to the onset of the highest energy emission band in the phosphorescence spectrum (the O-O band).

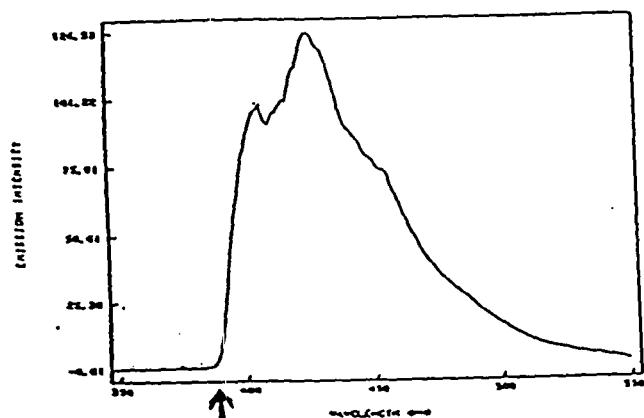
$$E = h c / \lambda_{o-o} \quad [9]$$

The  $\lambda_{o-o}$  wavelength was determined for each compound except 4a as the lowest wavelength at which emission is detectable. The arrows in the spectra in Figure 14 demonstrate how the  $\lambda_{o-o}$  wavelengths were determined for each compound in this study. The spectrum of 4a (representative of all the meta-alkoxy substituted chromophores) contains a weak emission band on the high energy side of the phosphorescence band, and is typical of meta-alkoxy acetophenones.<sup>(3)</sup> The  $\lambda_{o-o}$  value for these compounds have been estimated according to Wagner's procedure.

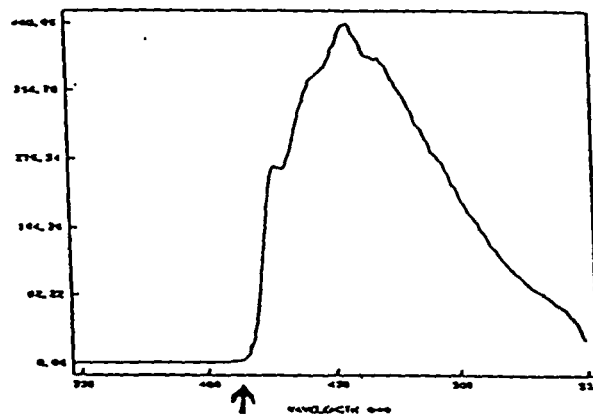
## PHOSPHORESCENCE SPECTRA

Figure 14. Phosphorescence spectra taken in a EtOH/MeOH 4:1 glass at 77K.

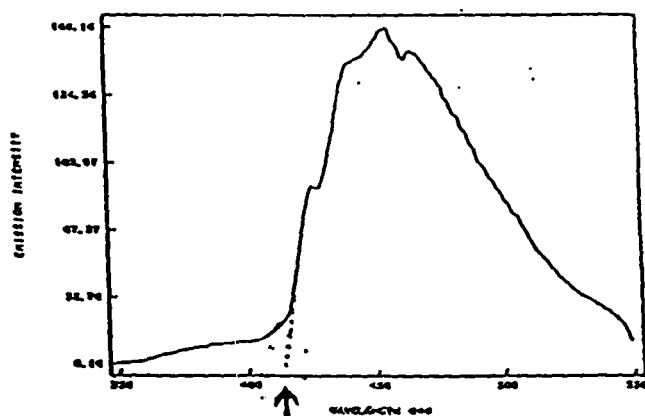
a) Compound 2a



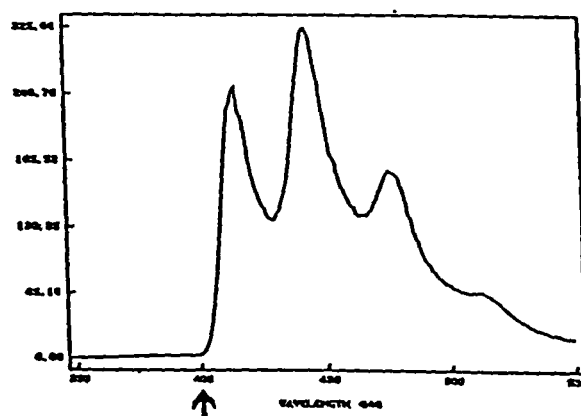
b) Compound 6



c) Compound 4a



d) Compound 8



### **2.3.2 Phosphorescence Lifetimes**

Phosphorescence lifetimes ( $\tau_p$ ) were determined by monitoring the emission intensity as a function of time after the excitation pulse. Phosphorescence lifetimes were determined by least squares analysis of the decay profiles according to equation 10, where  $k_p$  is the measured rate of phosphorescence decay,  $k_p^\circ$  is the intrinsic rate of phosphorescence decay in the absence of any quencher,  $k_{nr}$  is the rate of non-radiative decay, and  $\Sigma k_q[Q]$  is the bimolecular impurity quenching term.

$$k_p = k_p^\circ + k_{nr} + \Sigma k_q[Q] \quad [10]$$

$$\text{if} \quad 1/\tau_p = k_p$$

$$\text{and at 77K} \quad \Sigma k_q[Q] \cong 0$$

$$\text{then} \quad \tau_p \cong 1/\{k_p^\circ + k_{nr}\}$$

Table I lists the  $\lambda_{o-o}$ ,  $E_T$  and  $\tau_p$  values for compounds 1-8 determined from these experiments.

**Table I** - Results obtained are at 77K in EtOH/MeOH 4:1.

<b>Compound<sup>a</sup></b>	<b><math>\lambda_{O-O \text{ band}}</math> (nm)</b>	<b><math>E_T</math> (kcal/mole)</b>	<b><math>\tau_p</math> (ms)<sup>b</sup></b>
<b>1a</b> (p-p/OH)	389	73.5	256
<b>1b</b> (p-p/MeO)	386	74.1	240
<b>2a</b> (p-m/OH)	387	73.9	261
<b>2b</b> (p-m/MeO)	386	74.1	256
<b>3a</b> (m-p/OH)	410	~69.7	86.5
<b>3b</b> (m-p/MeO)	410	~69.7	127
<b>4a</b> (m-m/OH)	410	~69.7	97.4
<b>4b</b> (m-m/MeO)	410	~69.7	121
<b>5</b> (a-p/OH)	414	69.0	340
<b>6</b> (a-m/OH)	414	69.0	393
<b>7</b> (b-p/OH)	400	71.5	9.4
<b>8</b> (b-m/OH)	400	71.5	8.0

a      "(p-m/OH)" indicates linked compound with para-acetyl and meta phenol, for example.

b      Error in lifetimes is considered to be ca. 10%.

## **2.4**                    **Steady State Photolysis of 1-8 in Solution**

Nitrogen-purged samples of 0.0025 M solutions of **1-8** in acetonitrile were irradiated with six 300 nm lamps in a Rayonet reactor fitted with a merry-go-round . The progress of the photolyses were monitored by gas chromatography (GC) at 30 minute intervals up to 2.5 hours. Photolysis in this fashion caused the solutions to turn slightly yellow and cloudy. GC analysis revealed that destruction of starting material was accompanied by the formation of 1-5 products of long retention time (relative to starting material), but no identifiable products of retention time shorter than that of the starting material were formed in yields greater than 0.5%.

By comparing the extent of starting material disappearance as a function of time to that obtained for **1a**, the quantum yield for photolysis of each ketone ( $\phi_{dis}$ ) can be estimated from the reported value of ( $\phi_{dis}^{1a} = 0.006$ ). The  $\phi_{dis}$  values ranged between 0 and 0.01 for the series of ketones in this study.

## **2.5 Nanosecond Laser Flash Photolysis**

### **2.5.1 Transient Species in Solution**

Flash photolysis experiments were carried out with an excitation wavelength of either 248 nm (F<sub>2</sub>/Kr/He, ca. 16ns), 308 nm (HCl/Xe/H<sub>2</sub>/He, 15 ns, ca. 40mJ) or 337 nm (N<sub>2</sub>/He, 6 ns, ca. 4mJ) supplied by an excimer laser. The laser acts to excite the sample whose absorbance at a single wavelength is monitored as a function of time using a fast time-resolved ultraviolet absorption spectrometer. A representative transient decay trace of an alkoxy-substituted acetophenone (**4a**) is shown in Figure 15a. The trace is a plot of the change in optical density at the monitoring wavelength (a function of the concentration of the transient) versus time. The amount of time that it takes to decay to 1/e of the original concentration of transient species is the reported lifetime of the transient, as shown in equation 11 -14. The decay is usually of first order and can be readily analysed by least squares procedures.

$$A_t = A_o e^{-kt} \quad [11]$$

$$\ln A_t = \ln A_o - kt \quad [12]$$

$$\ln A_t/A_o = -kt \quad [13]$$

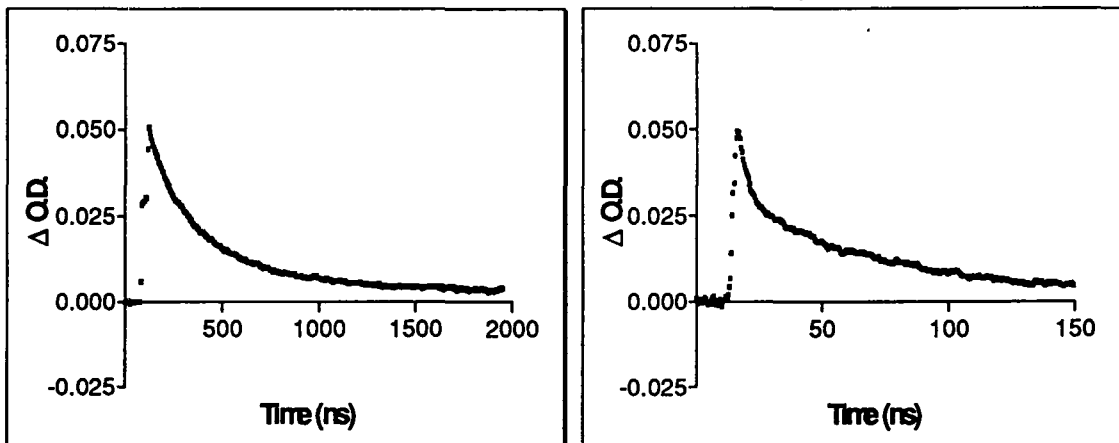
$$\text{if } A_t = (1/e) A_o \quad 1 = k\tau \quad \text{or} \quad \tau = 1/k \quad [14]$$

This kinetic scheme shows the mathematical definition of the transient lifetime in a first order reaction.<sup>(31)</sup>

Problems do arise, however, when the decays are either not first order or include a photoproduct which absorbs light. The latter case has been noted by Scaiano and coworkers<sup>(24)</sup> and occurs in this study when the triplet being monitored is short-lived and the photoproduct produced is relatively long-lived. Figure 15b shows a representative trace where the first part of the decay is due mostly to triplet depletion and the latter part of the decay is due to secondary decay of a photoproduct. Because the photoproduct forms as the triplet decays, the decay becomes more complicated as there are varying mixtures of two components at each point.

**Figure 15.**

- a) Transient decay of **4a** in acetonitrile at 22°C monitored at 375 nm.      b) Transient decay of **1a** in acetonitrile at 22°C monitored at 375 nm.



### **2.5.2 Transient UV Absorption Spectra**

Transient absorption spectra (Figure 16-32, 33; curves a and b) were measured on the laser system as previously mentioned. Spectra are recorded by plotting the top O.D. value obtained from a series of decay traces (Fig. 15) taken at different monitoring wavelengths, against the wavelength at which the decay was measured. The wavelength range used for this study was typically from 300 to 600 nm as indicated in the figures. The transient UV spectra of ketones **1-8** as well as the model compounds **15-19** were recorded at 23°C in deoxygenated acetonitrile solution.

In each figure, an inset of a decay trace is placed so as to show the quality of the decay trace and the interference (if any) of photoproducts. The decay traces are plots of change in optical density versus time in nanoseconds.



### TRANSIENT UV SPECTRA

**Figure 16.** Transient spectrum obtained 0-20 ns after laser excitation of **1a** in acetonitrile at 23°C. Insert depicts the decay of the transient absorption of **1a** monitored at 375 nm under the same conditions.

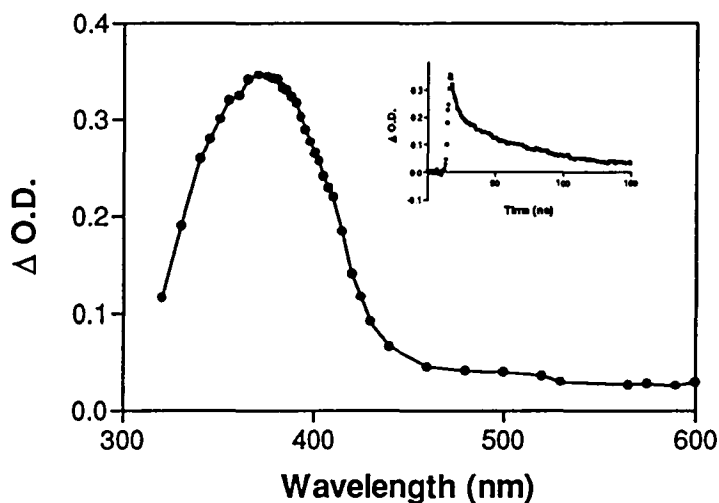
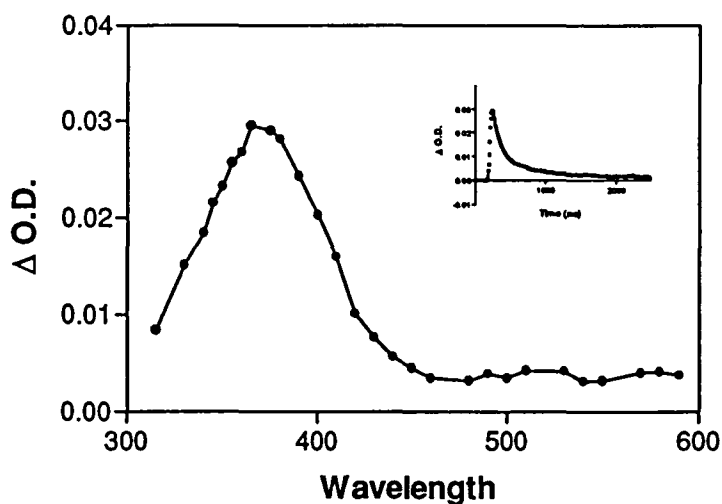


**Figure 17.** Transient spectrum obtained 0-50 ns after laser excitation of **1b** in acetonitrile at 23°C. Insert depicts the decay of the transient absorption of **1b** monitored at 375 nm under the same conditions.



### TRANSIENT UV SPECTRA

**Figure 18.** Transient spectrum obtained 0-20 ns after laser excitation of **2a** in acetonitrile at 23°C. Insert depicts the decay of the transient absorption of **2a** monitored at 375 nm under the same conditions.

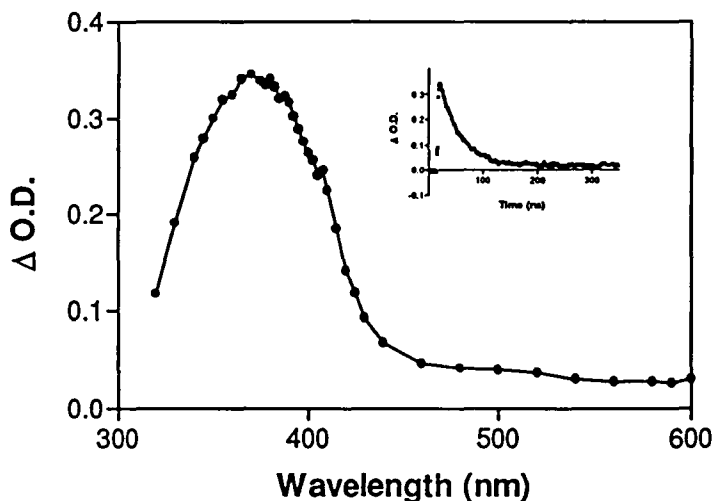
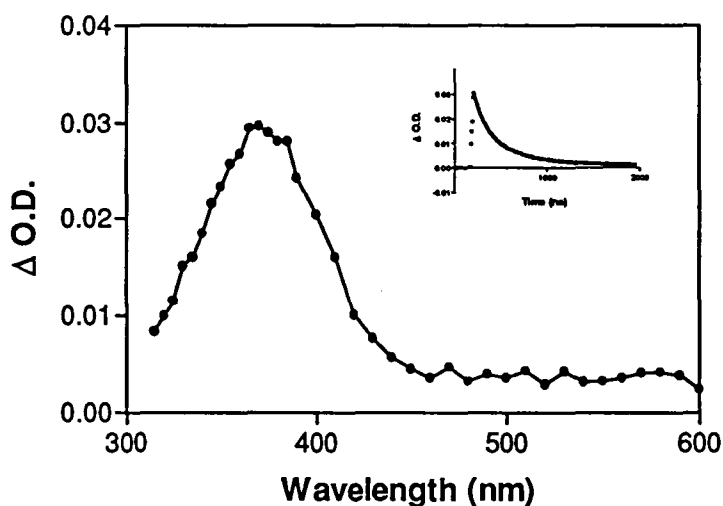


**Figure 19.** Transient spectrum obtained 0-60 ns after laser excitation of **2b** in acetonitrile at 23°C. Insert depicts the decay of the transient absorption of **2b** monitored at 375 nm under the same conditions.



### TRANSIENT UV SPECTRA

**Figure 20.** Transient spectrum obtained 0-50 ns after laser excitation of 3a in acetonitrile at 23°C. Insert depicts the decay of the transient absorption of 3a monitored at 375 nm under the same conditions.

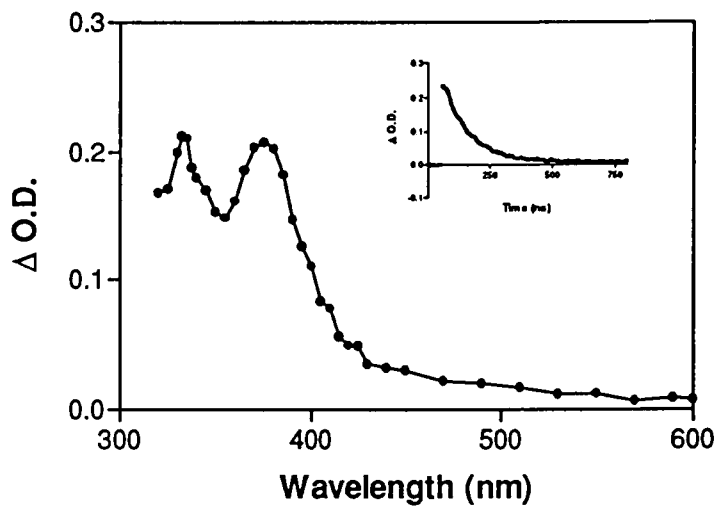
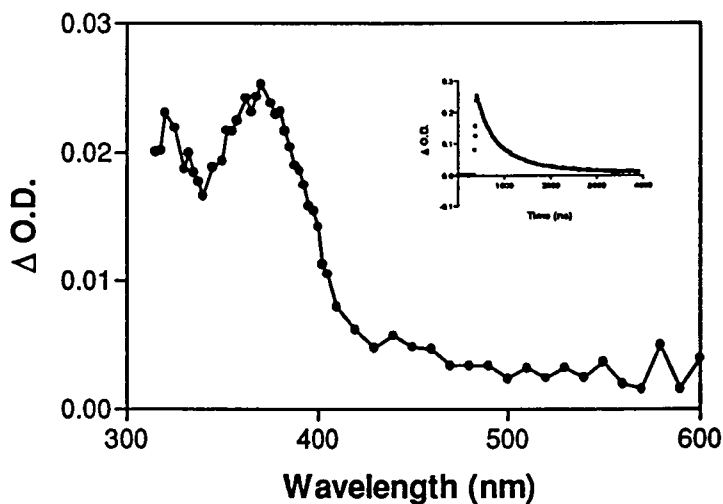


**Figure 21.** Transient spectrum obtained 0-60 ns after laser excitation of 3b in acetonitrile at 23°C. Insert depicts the decay of the transient absorption of 3b monitored at 375 nm under the same conditions.



### TRANSIENT UV SPECTRA

**Figure 22.** Transient spectrum obtained 0-50 ns after laser excitation of **4a** in acetonitrile at 23°C. Insert depicts the decay of the transient absorption of **4a** monitored at 375 nm under the same conditions.

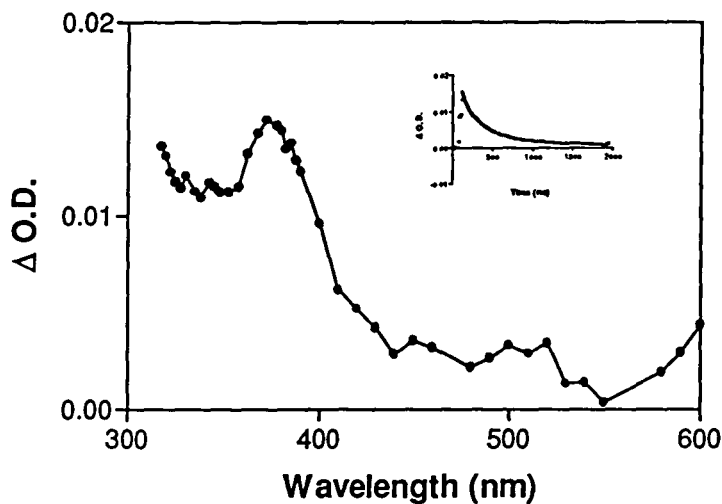
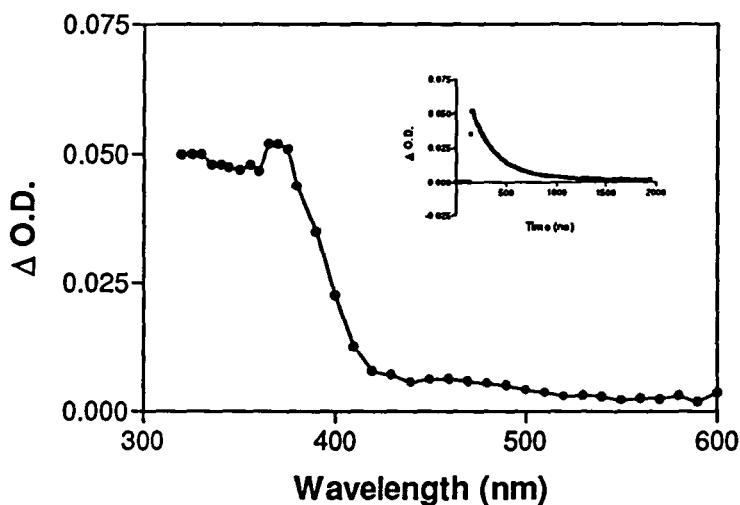


**Figure 23.** Transient spectrum obtained 0-60 ns after laser excitation of **4b** in acetonitrile at 23°C. Insert depicts the decay of the transient absorption of **4b** monitored at 375 nm under the same conditions.



### TRANSIENT UV SPECTRA

**Figure 24.** Transient spectra obtained (a) 0-20 ns and (b) 60-110 ns after laser excitation of **5** in acetonitrile at 23°C. Insert depicts the decay of the transient absorption of **5** monitored at 375 nm under the same conditions.

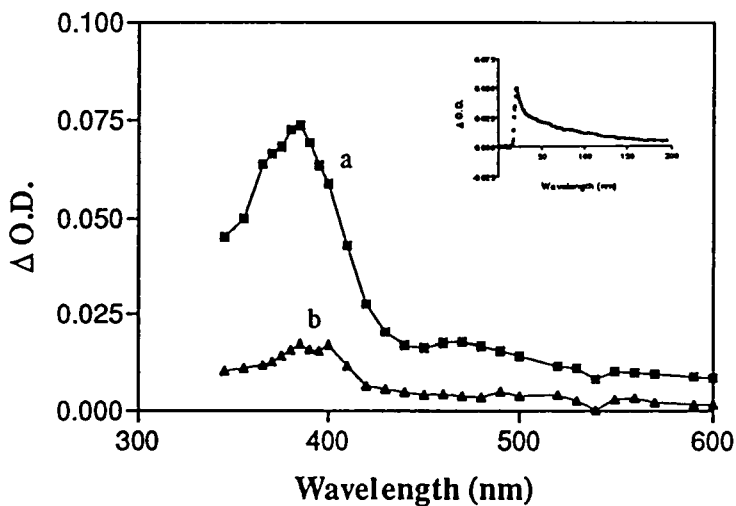
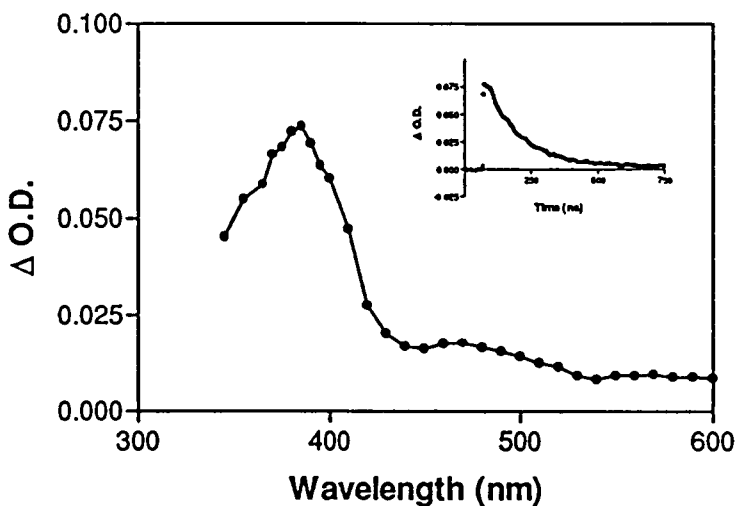


**Figure 25.** Transient spectrum obtained 0-50 ns after laser excitation of **6** in acetonitrile at 23°C. Insert depicts the decay of the transient absorption of **6** monitored at 375 nm under the same conditions.



### TRANSIENT UV SPECTRA

**Figure 26.** Transient spectra obtained (a) 0-20 ns and (b) 50-100 ns after laser excitation of 7 in acetonitrile at 23°C. Insert depicts the decay of the transient absorption of 7 monitored at 525 nm under the same conditions.

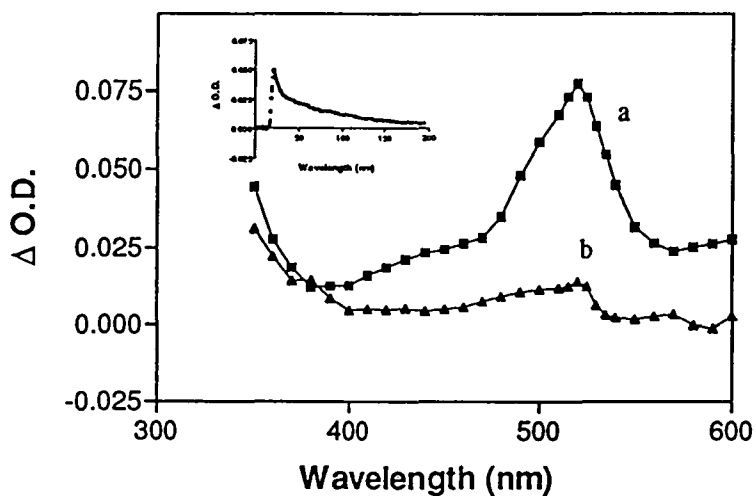
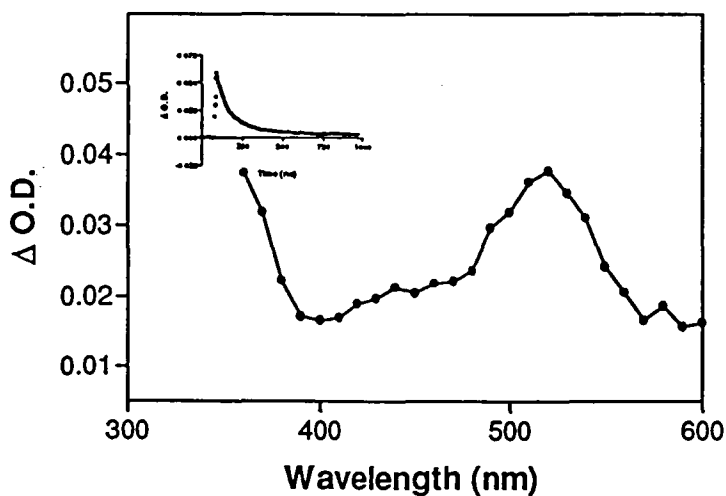


**Figure 26.** Transient spectra obtained 0-50 ns after laser excitation of 8 in acetonitrile at 23°C. Insert depicts the decay of the transient absorption of 8 monitored at 525 nm under the same conditions.



### TRANSIENT UV SPECTRA

**Figure 28.** Transient spectrum obtained 0-60 ns after laser excitation of **15** (p-Methoxy acetophenone) in acetonitrile at 23°C. Insert depicts the decay of the transient absorption of **15** monitored at 375 nm under the same conditions.

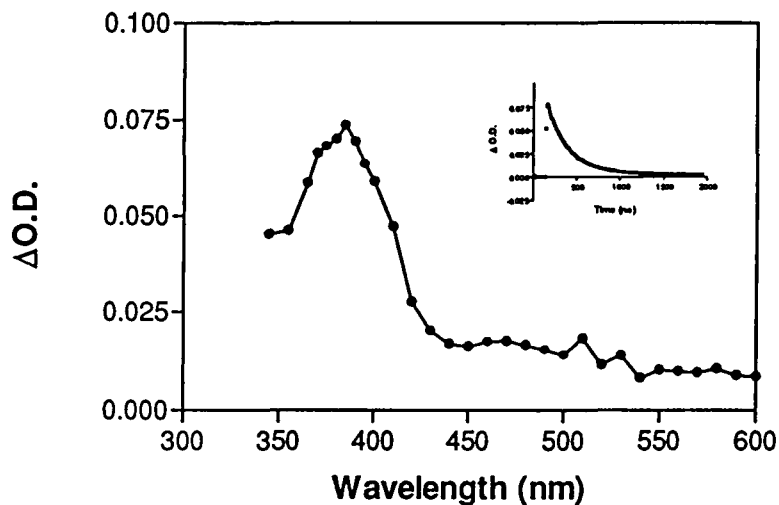
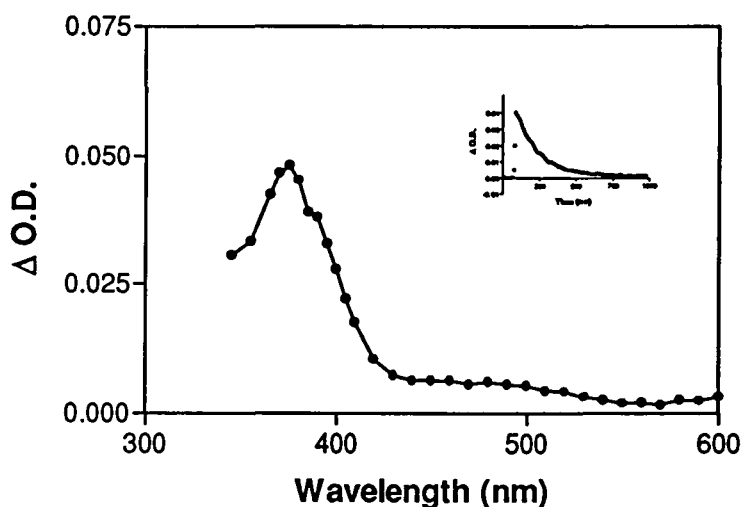


**Figure 29.** Transient spectrum obtained 0-60 ns after laser excitation of **16** (m-Methoxy acetophenone) in acetonitrile at 23°C. Insert depicts the decay of the transient absorption of **16** monitored at 375 nm under the same conditions.



### TRANSIENT UV SPECTRA

**Figure 30.** Transient spectrum obtained 0-60ns after laser excitation of **17** (acetoveratrone) in acetonitrile at 23°C. Insert depicts the decay of the transient absorption of **17** monitored at 375 nm under the same conditions.

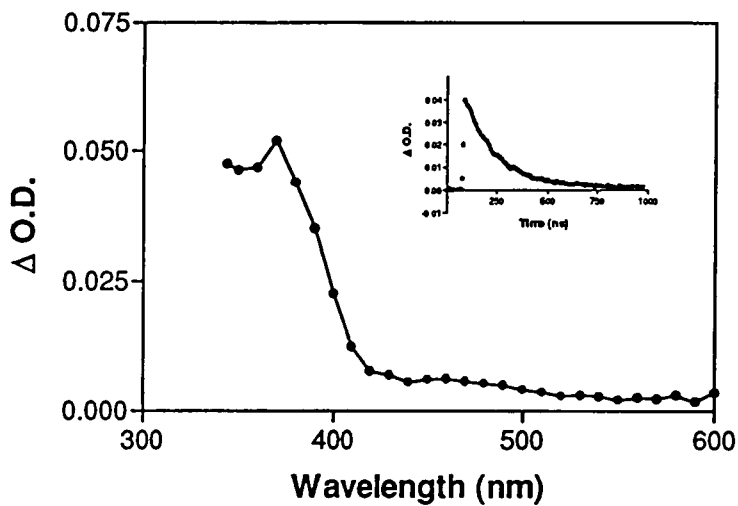
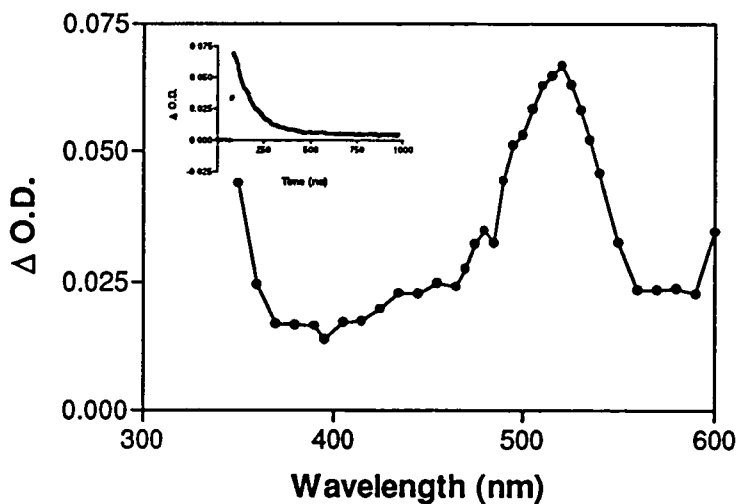


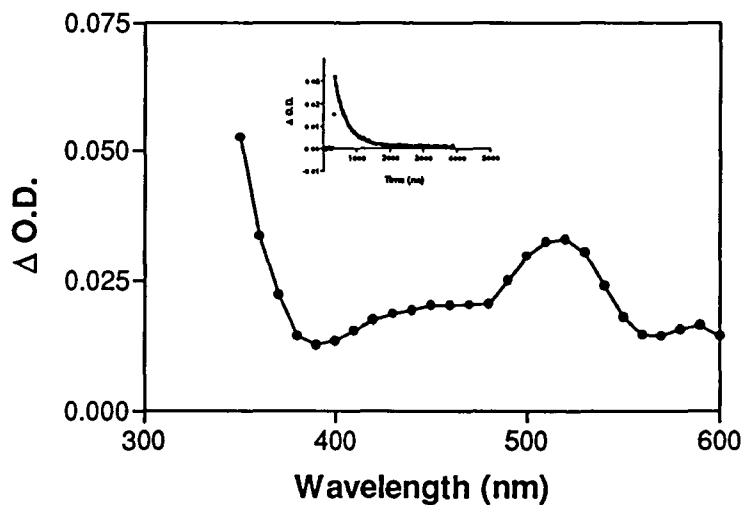
**Figure 31.** Transient spectrum obtained 0-60 ns after laser excitation of **18** (benzophenone) in acetonitrile at 23°C. Insert depicts the decay of the transient absorption of **18** monitored at 525 nm under the same conditions.





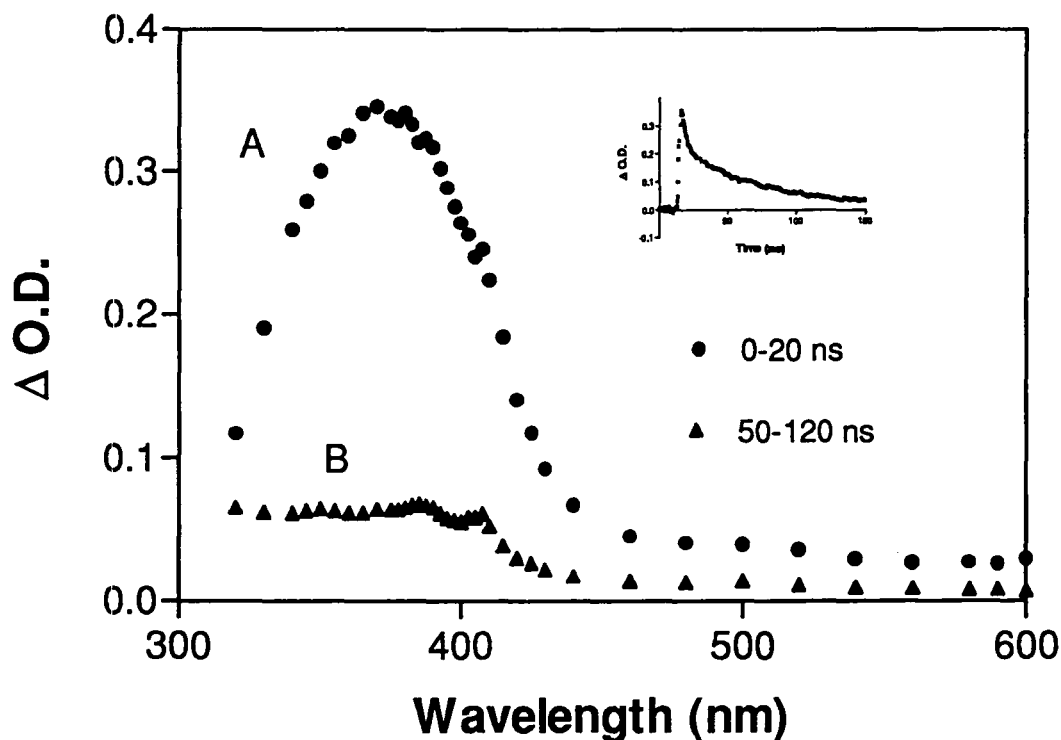
### TRANSIENT UV SPECTRA

**Figure 32.** Transient spectrum obtained 0-60 ns after laser excitation of **19** (4-Methoxy benzophenone) in acetonitrile at 23°C. Insert depicts the decay of the transient absorption of **19** monitored at 525 nm under the same conditions.



The spectra in Figures 16-32 are time resolved spectra. All these figures as well as Fig. 33a display spectra that are taken immediately after the excitation pulse, and show the absorption characteristics of the transients directly produced from the laser pulse. Figure 33b, on the other hand, is taken after a time of 100 ns after the laser pulse and shows absorptions not characteristic of the original transient (carbonyl triplet) but as a distinct absorption pattern.

**Figure 33.** Time resolved Transient UV spectra of **1a** in acetonitrile solution at 22°C. Curve A is the spectrum obtained 0-20 ns after the laser pulse. Curve B is obtained 50-120 ns after the laser pulse. The inset is a transient decay of **1a** under the same conditions monitored at 375 nm.



### 2.5.3 Quenching Plots and Transient Characterization

Another tool that is used in order to identify transient species in solution is energy transfer quenching. Quenching of an excited state is essentially any deactivation process which results from interaction of the excited molecules with the components of a system. As a specific example, consider the quenching of emission of an excited state  $D^*$  by the addition of a second molecule A. The following mechanism then applies<sup>(27)</sup>:

<i>Process</i>		<i>Rate</i>	
Absorption	$D_o + h\nu \rightarrow D^*$	$I_a$ (einsteins/L's)	[15]
Emission	$D^* \rightarrow D_o + h\nu$	$k_1 [D^*]$	[16]
Quenching	$D^* + A_o \rightarrow A^* + D_o$	$k_2 [D^*][A]$	[17]
Deactivation	$D^* \rightarrow D_o + \text{heat}$	$k_3 [D^*]$	[18]

The rate constants  $k_1$ ,  $k_2$  and  $k_3$  in equations 16-18 are those for the emission from  $D^*$ , energy transfer from  $D^*$  to A, and thermal deactivation of  $D^*$ , respectively. When the energy of the excited state of  $A^*$  is lower than that of  $D^*$  quenching occurs at a rate approaching that of diffusion.

The longer a molecule remains in the excited state the greater the probability that it will transfer energy to a suitable acceptor, given a constant rate of energy transfer. Because triplets have relatively long lifetimes, they are more likely to participate in energy transfer than the short-lived singlet counterparts. Measurements of the decay rate of the

excited donor ( $D^*$ ) as a function of the concentration of A allows determination of the rate constant for quenching of  $D^*$  by A.

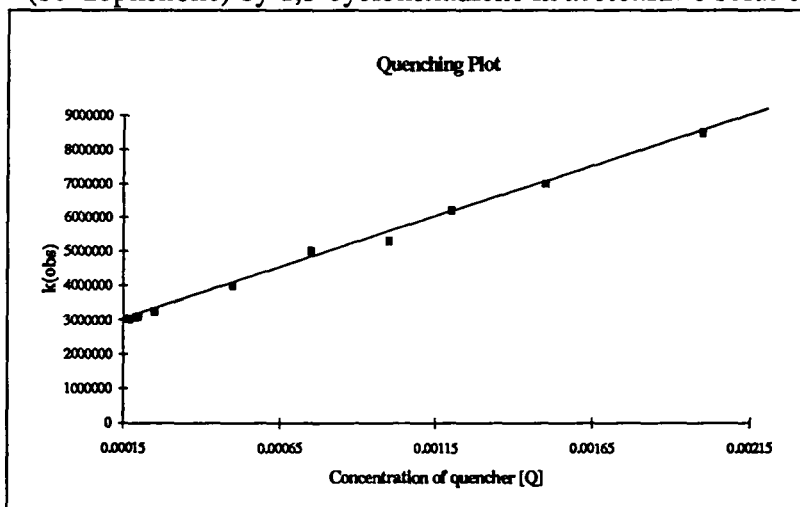
Aromatic ketones possess triplet energies that range from 40 - 80 kcal/mole above the energy of their ground states.<sup>(16,17)</sup> Thus, what is needed is an acceptor with a triplet energy below those measured for the ketones in Table I of this chapter. 1,3-cyclohexadiene provides a perfect candidate for this purpose as it has a triplet energy of 52.4 kcal/mole<sup>(16)</sup>, which is 20 kcal/mole lower (on average) than those of the phenylalkyl ketones in this study.

The Stern -Volmer equation is used for these experiments; it relates the observed transient decay rate ( $k_{obs}$ ) to the rate of quenching of the transient ( $k_q$ ) by the quencher Q.

$$1/\tau_{obs} = k_{obs} = k_o + k_q [Q] \quad [19]$$

In Figure 34, the lifetime of the transient changes as a function of 1,3-Cyclohexadiene concentration indicating that the transient is being quenched by the diene. The fact that the transient is quenched allows assignment of the transient (in this case) to a triplet species.<sup>(28)</sup> The slope of the line in Figure 34 gives the rate constant for bimolecular energy transfer. The magnitude of this rate constant is also characteristic of the quenching process. Energy transfer requires direct contact between the two molecules, so that the reaction should proceed at the diffusion-controlled rate if it is more than ~3 kcal/mol exothermic.<sup>(27)</sup> The fact that quenching occurs at close to the diffusion-controlled rate in all cases strongly suggests that the triplet assignment is correct.

**Figure 34.** Quenching plot:  $k_{\text{obs}}$  vs. quencher concentration for quenching of 18 (benzophenone) by 1,3-cyclohexadiene in acetonitrile solution at 25°C.



The laser wavelengths used for these experiments were 308 or 337 nm. The choice of the excitation wavelength is important as the desired effect is to preferentially excite the ketone. Thus, an excitation wavelength must be chosen such that everything at that wavelength is transparent except the ketone. This is accomplished for both these wavelengths but is not the case for 248 nm laser excitation. The rate constants for these experiments were obtained in rigorously deoxygenated acetonitrile solution at 25°C and are shown below.

**Table II** - Triplet quenching by 1,3-cyclohexadiene in deoxygenated acetonitrile at 25°C.

Compound	$\lambda_{\text{max}}$ (nm) <sup>a</sup>	$k_q$ (M <sup>-1</sup> s <sup>-1</sup> )
<b>1a</b> (p-p/OH)	380	c
<b>1b</b> (p-p/MeO)	380	$6.7 \pm 0.3 \times 10^9$
<b>2a</b> (p-m/OH)	380	$1.1 \pm 0.1 \times 10^{10}$
<b>2b</b> (p-m/MeO)	380	$1.1 \pm 0.4 \times 10^{10}$
<b>3a</b> (m-p/OH)	375	$1.2 \pm 0.2 \times 10^{10}$
<b>3b</b> (m-p/MeO)	375	$8.4 \pm 0.2 \times 10^9$
<b>4a</b> (m-m/OH)	375	$1.0 \pm 0.2 \times 10^{10}$
<b>4b</b> (m-m/MeO)	375	$1.0 \pm 0.2 \times 10^{10}$
<b>5</b> (a-p/OH)	375	$\sim 9.2 \times 10^9$ <sup>b</sup>
<b>6</b> (a-m/OH)	375	$9.0 \pm 0.1 \times 10^9$
<b>7</b> (b-p/OH)	525	$\sim 1.0 \times 10^{10}$ <sup>b</sup>
<b>8</b> (b-m/OH)	525	$1.0 \pm 0.3 \times 10^{10}$

a  $\lambda_{\text{max}}$  of the transient absorption spectrum of the species monitored.

b Transient quenched by diene; reported rate constants are estimates from 2 point quenching plots.

c Quenched by 1,3-Octadiene at 22°C. <sup>(24)</sup>

These rate constants are typical values for diffusion-controlled bimolecular triplet

quenching by dienes in acetonitrile.<sup>(16)</sup> These  $\lambda_{\text{max}}$  and  $k_q$  values are known for similar

chromophores and are characteristic of triplet species in solution.<sup>(16,17)</sup>

## **2.6 Triplet Lifetimes Determined by Nanosecond Laser Flash Photolysis**

To determine lifetimes of the triplet states of compounds **1a - 8**, rigorously deoxygenated samples of approximately  $5 \times 10^{-4}$  M in acetonitrile were irradiated at 248 nm with the laser system described previously.<sup>(26)</sup> This laser wavelength was utilised so that the concentration of substrate could be as low as possible (the absorption of all compounds is dramatically stronger at 248 nm than at either 308 or 337 nm). The solutions must be dilute, since bimolecular self-quenching can occur and would interfere in the determination of the intramolecular quenching rate constants that are of primary interest. To be sure, the Stern-Volmer equation can be utilized to demonstrate that the observed rate constant for triplet decay is a combination of both intramolecular and bimolecular reaction.

$$k_{\text{obs}} = k_d^{\circ} + k_{\text{sq}}[\text{Ketone}] \quad [20]$$

Hence, the bimolecular portion  $k_{\text{sq}}[\text{Ketone}]$  must be made negligible such that the  $k_{\text{obs}}$  measured is equal to  $k_d^{\circ}$ , the intrinsic lifetime of the triplet in solution at 22°C. It becomes apparent that when concentrations are approximately  $5 \times 10^{-4}$  M and the bimolecular rate constant for phenolic quenching are on the order of  $10^9 \text{ M}^{-1}\text{s}^{-1}$  (Table VII), the  $k_{\text{sq}}[\text{Ketone}]$  portion of the equation becomes less than 10% of the  $k_{\text{obs}}$  measured by direct methods. It is for this reason that samples were diluted until the lifetimes measured for a given compound remained constant.

### 2.6.1 Indirect Triplet Lifetime Determination

The original paper<sup>(24)</sup> which studied compound **1a** indicated that a direct measurement of the triplet lifetime was not possible due to the interference created by the presence of a photoproduct which was also absorbing light at the same wavelength. Figure 15b shows this problem, which occurs in some of these systems when the triplet lifetime is particularly short. To circumvent this problem of interference between the triplet and its corresponding photoproduct, an indirect method was used to obtain a value for the triplet lifetime. This method involves 1-methylnaphthalene energy transfer quenching and is the method used to determine the triplet lifetimes of compound **1a**, **5** and **7**, as well as the deuterium kinetic isotope effects on triplet lifetime.

The triplet of methylnaphthalene can easily be observed because of its strong absorption spectrum with  $\lambda_{\text{max}}$  at 425 nm. The experiments do not provide direct information but can be used mathematically to provide a value of  $k_q\tau_K$ , where  $k_q$  is the rate constant for quenching of the excited ketone by 1-methylnaphthalene and  $\tau_K$  is the lifetime of the excited ketone.<sup>(29)</sup> The derivation is shown below (see Appendix for definitions):

$$\begin{aligned}\Phi_{\text{MN}^*}^3 &= \phi_{\text{isc}} \times \phi_{\text{MN}^*}^3 \\ &= \phi_{\text{isc}} (k_q[\text{MN}]) / (1/\tau_K + k_q[\text{MN}]) \\ (\Phi_{\text{MN}^*}^3)^{-1} &= \phi_{\text{isc}}^{-1} \{ 1 + (1/k_q\tau_K[\text{MN}]) \}\end{aligned}$$

where  $\Phi_{\text{MN}^*}^3 = [\text{MN}^*] / I_a = \text{TOP OD}_{\text{MN}^*} / (I_a)(l)(\epsilon_{\text{MN}^*})$

and  $\text{TOP OD}_{\text{MN}^*} = \text{initial absorbance due to MN}^*$



If  $I_a$  (the laser intensity) is constant over the duration of the experiment ( $\sim 1$  hour) then..

$$\Phi_{MN^*3} = \alpha_{MN^*} (\text{TOP OD}_{MN^*3}) \quad \alpha_{MN^*} = 1 / (I_a)(I)(\epsilon_{MN^*3})$$

and

$$(\text{TOP OD}_{MN^*3})^{-1} = \alpha_{MN^*} \phi_{isc}^{-1} \{ 1 + (1/k_q \tau_K [MN]) \}$$

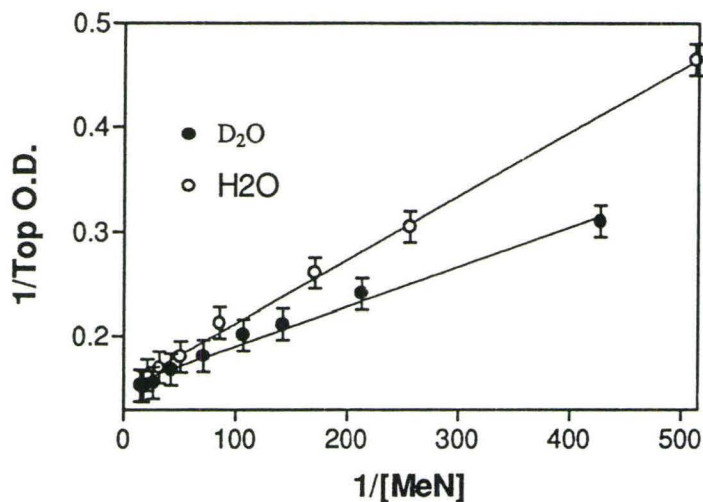
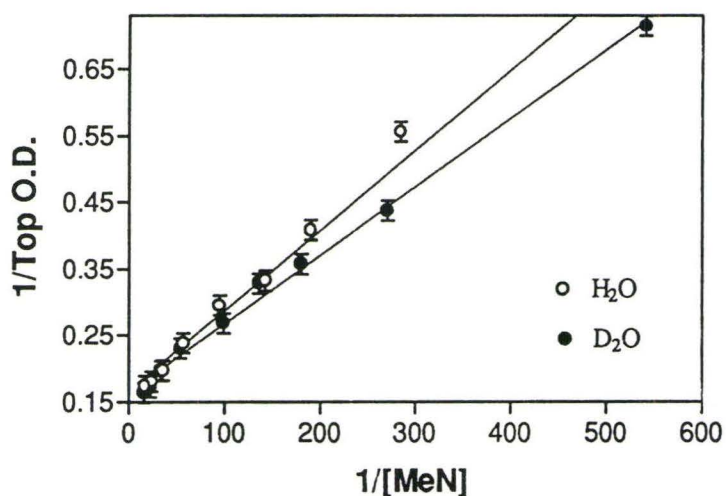
Plot  $(\text{TOP OD}_{MN^*3})^{-1}$  vs  $[MN]^{-1}$

$$\text{intercept} = \alpha_{MN^*} \phi_{isc}^{-1} \quad \text{slope} = \alpha_{MN^*} \phi_{isc}^{-1} / k_q \tau_K$$

$$\text{int/slope} = k_q \tau_K \quad [21]$$

By assuming a value of  $k_q = 8 \times 10^9 \text{ M}^{-1} \text{ s}^{-1}$  in acetonitrile<sup>(16,24)</sup> for 1-methylnaphthalene,  $\tau_K$  is easily obtained. For the isotope effects a value of  $k_q$  is not necessary as a ratio of two values of  $k_q \tau_K$  is taken which eliminates the  $k_q$  value altogether.

Quenching of **1a**, **5** and **7** by 1-methylnaphthalene was investigated in acetonitrile, 0.005 M  $\text{H}_2\text{O}$  in acetonitrile, and 0.005 M  $\text{D}_2\text{O}$  in acetonitrile solutions. Examples of the quenching plots for compound **5** and **7** are shown in Figure 34 and the rate constants for the various 1-methylnaphthalene quenching experiments are given in Table III.

**Figure 35a.** 1-Methylnaphthalene quenching of **5** in 5% aq.(H<sub>2</sub>O/D<sub>2</sub>O) acetonitrile(23°C).**Figure 35b.** 1-Methylnaphthalene quenching of **7** in 5% aq.(H<sub>2</sub>O/D<sub>2</sub>O) acetonitrile(23°C).**Table III.** 1-Methylnaphthalene Stern-Volmer constants in deoxygenated acetonitrile at 23°C.

Compound	$k_q\tau_K$ (M <sup>-1</sup> ) <sup>a</sup>	$k_q\tau_K$ (5 mmol H <sub>2</sub> O) <sup>a</sup>	$k_q\tau_K$ (5 mmol D <sub>2</sub> O) <sup>a</sup>
<b>1a</b>	121	110	149
<b>5</b>	459	244	398
<b>7</b>	166	136	159

<sup>a</sup> associated error is ~10%.

### 2.6.2 Direct Lifetime Determination

The majority of the ketones studied, that is to say all except **1a**, **5** and **7** from the previous section, had lifetimes long enough such that decay traces followed first order kinetics and the lifetimes could be measured directly from the decay traces. Table IV shows the lifetimes of all the compounds studied as well as the wavelength at which such determinations were made. The values denoted by  $\xi$  indicate values which were determined by 1-methylnaphthalene quenching as presented in section 2.6.1.

**Table IV** - Lifetimes of carbonyl triplets in acetonitrile at 22°C.

Compound	$\lambda_{\max}$ (nm)	$\tau_K$ (ns) <sup>Ⓢ</sup>
<b>1a</b> (p-p/OH)	380	13 <sup>ξ</sup>
<b>1b</b> (p-p/MeO)	380	2400
<b>2a</b> (p-m/OH)	375	320
<b>2b</b> (p-m/MeO)	375	1800
<b>3a</b> (m-p/OH)	375	670
<b>3b</b> (m-p/MeO)	375	4800
<b>4a</b> (m-m/OH)	375	1135 <sup>Ⓢ</sup>
<b>4b</b> (m-m/MeO)	375	3500
<b>5</b> (a-p/OH)	375	55 <sup>ξ</sup>
<b>6</b> (a-m/OH)	375	860
<b>7</b> (b-p/OH)	525	20 <sup>ξ</sup>
<b>8</b> (b-m/OH)	525	350

Ⓢ By plotting self-quenching curves at various temperatures and extrapolating to infinite dilution.

ξ 1-methylnaphthalene quenching was utilized.  $k_q = 8.3 \times 10^9 \text{ M}^{-1} \text{ s}^{-1}$ .

Ⓢ 10% associated error.

## 2.7 Hydrogen/Deuterium Kinetic Isotope Effects

The hydroxy containing compounds (**1a** through **8**) have carbonyl triplets which are substantially shorter-lived than the methoxy analogs or model compounds. This suggests that these hydroxy compounds possess a mechanism for excited state quenching that the methoxy analogs do not have. It would seem evident that such a mechanism involves hydrogen abstraction of the phenolic proton by the acetyl group.

The indirect method for obtaining a kinetic isotope effect has already been described in section 2.6.1 and is performed by energy transfer to 1-methylnaphthalene. The remainder of the isotope effects can be determined directly from the rate constants for triplet decay in deoxygenated acetonitrile solution at 23°C containing either D<sub>2</sub>O or H<sub>2</sub>O. The rate constants that have been determined are given in Table V.

**Table V.** Rate constants for triplet decay in deoxygenated 5% aqueous (as H<sub>2</sub>O or D<sub>2</sub>O) acetonitrile at 22°C.

Compound	k <sub>H2O</sub> (s <sup>-1</sup> )	k <sub>D2O</sub> (s <sup>-1</sup> )
<b>1a</b> (p-p/OH)	*	*
<b>2a</b> (p-m/OH)	3.8 ± 0.4 × 10 <sup>6</sup>	1.7 ± 0.3 × 10 <sup>6</sup>
<b>3a</b> (m-p/OH)	5.3 ± 0.5 × 10 <sup>6</sup>	2.0 ± 0.2 × 10 <sup>6</sup>
<b>4a</b> (m-m/OH)	1.6 ± 0.2 × 10 <sup>6</sup>	7.8 ± 0.5 × 10 <sup>5</sup>
<b>5</b> (a-p/OH)	*	*
<b>6</b> (a-m/OH)	9.7 ± 0.5 × 10 <sup>5</sup>	5.1 ± 0.3 × 10 <sup>5</sup>
<b>7</b> (b-p/OH)	*	*
<b>8</b> (b-m/OH)	4.2 ± 0.4 × 10 <sup>6</sup>	2.4 ± 0.2 × 10 <sup>6</sup>

\* k<sub>q</sub>τ<sub>k</sub> values by 1-methylnaphthalene quenching in H<sub>2</sub>O(D<sub>2</sub>O) /acetonitrile given in Table III.

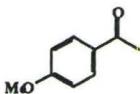
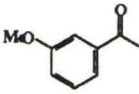
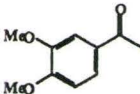
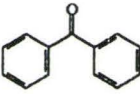
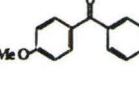
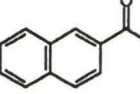
## 2.8 Triplet Characterization of Model Compounds

Before rate constants are measured, we must again characterize the triplet state in all cases for the model compounds by both  $\lambda_{\text{max}}$  values and diene quenching experiments. The rates constants in Table VI shown below were obtained by performing the same type of diene quenching experiments as has already been described in this chapter. The quenching rate constants were determined in deoxygenated acetonitrile solution at 25°C, utilizing a laser wavelength of 337 nm to avoid excitation of the diene.

**Table VI.** Triplet quenching by 1,3-cyclohexadiene in deoxygenated acetonitrile at 25°C.

Compound	Type	$\lambda_{\text{max}}$ (nm)	$k_q$ ( $\text{M}^{-1}\text{s}^{-1}$ )
15	$(\pi, \pi^*)^3$	375	$9.5 \pm 0.4 \times 10^9$
16	$(\pi, \pi^*)^3$	375	$9.8 \pm 0.4 \times 10^9$
17	$(\pi, \pi^*)^3$	375	$8.0 \pm 0.2 \times 10^9$
18	$(n, \pi^*)^3$	525	$1.1 \pm 0.1 \times 10^{10}$
19	$(n, \pi^*)^3$	525	$1.0 \pm 0.1 \times 10^{10}$
20	$(\pi, \pi^*)^3$	425	$9.8 \pm 0.3 \times 10^9$

					
15	16	17	18	19	20

### 2.8.2 Bimolecular Phenolic Triplet Quenching

The rate constants for phenolic quenching of carbonyl triplets have been determined by Stern-Volmer kinetics, which monitors the change in triplet lifetime as a function of phenol concentration. The phenols used in this study are those of *p*-methyl phenol (*p*-cresol) and *m*-methylphenol (*m*-cresol), as they are the two phenols which most closely match the phenolic portion of the compounds 1-8 in this study.

**Table VII - Triplet quenching by substituted phenols in deoxygenated acetonitrile at 23°C.**

Compound	$\lambda_{\max}$ (nm)	$k_{p\text{-cresol}}^{\xi}$	$k_{m\text{-cresol}}^{\xi}$
15	375	$1.24 \pm 0.02 \times 10^9$	$7.1 \pm 0.1 \times 10^8$
16	375	$1.4 \pm 0.1 \times 10^9$	$1.1 \pm 0.1 \times 10^9$
17	375	$8.0 \pm 0.2 \times 10^8$	$5.1 \pm 0.1 \times 10^8$
18	525	$3.4 \pm 0.1 \times 10^8$	$2.0 \pm 0.1 \times 10^8$
19	525	$1.2 \pm 0.1 \times 10^9$	$9.6 \pm 0.3 \times 10^8$
20	425	$\sim 3.4 \times 10^6$	$< 10^6$

$\xi$  Units of rate constants are  $M^{-1}s^{-1}$ .



## **2.9 Arrhenius Parameters for Intramolecular Phenolic-Hydrogen**

### **Abstraction**

To obtain the Arrhenius parameters for triplet decay of the phenolic ketones [**1a - 8**], lifetimes of a given triplet were measured as a function of temperature by methods similar to the other laser experiments already discussed. The samples were allowed to equilibrate for ten minutes prior to recording an experiment. Excitation pulses of 248 nm were utilized so as to keep the concentration of ketone as low as possible ( $\sim 2 \times 10^{-4} \text{M}$ ).

Arrhenius plots of kinetic data for the compounds **1a - 8** are shown in Figure 36 - 43. The slope of the best fit line, the intercept and the correlation coefficient are also given for each individual plot.

Thermodynamic Data

**Figure 36.** Arrhenius plot of compound **1a** ( $4.5 \times 10^{-4}\text{M}$ ) in  $\text{N}_2$  purged acetonitrile.

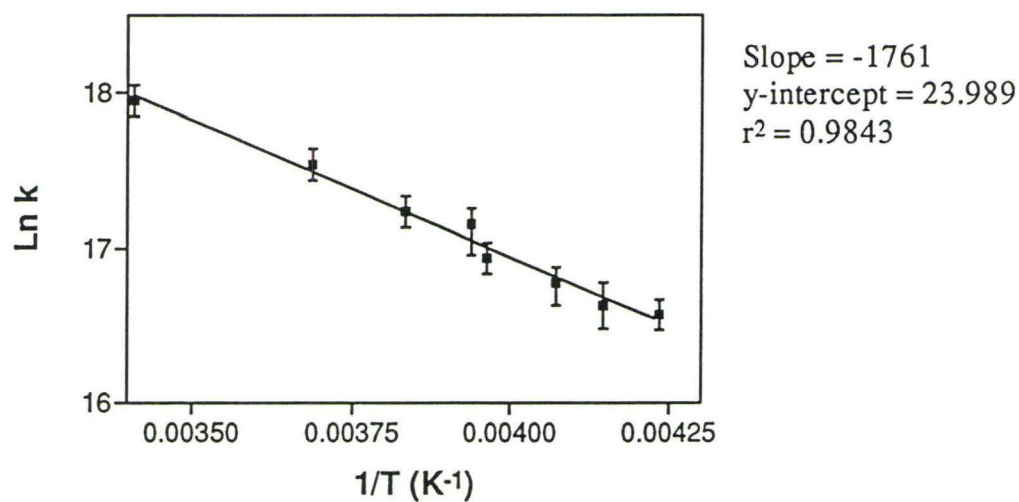
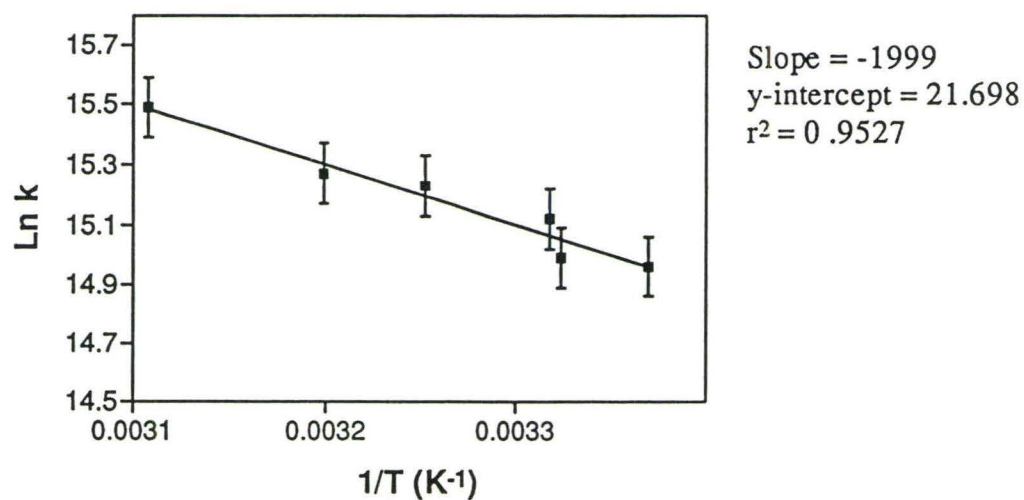


**Figure 37.** Arrhenius plot of compound **2a** ( $4.7 \times 10^{-4}\text{M}$ ) in  $\text{N}_2$  purged acetonitrile.





Thermodynamic Data

**Figure 38.** Arrhenius plot of compound 3a ( $5.0 \times 10^{-4}\text{M}$ ) in  $\text{N}_2$  purged acetonitrile.

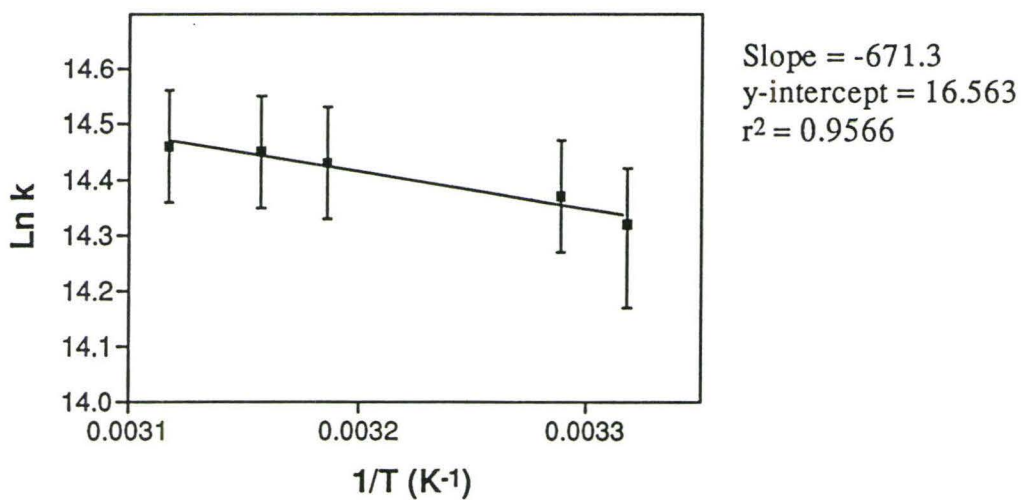
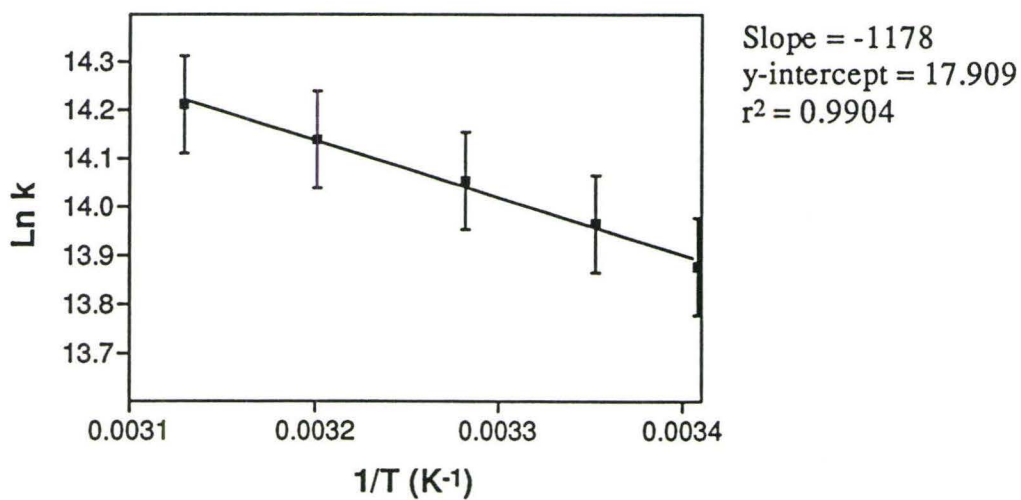


**Figure 39.** Arrhenius plot of compound 4a ( $5.3 \times 10^{-4}\text{M}$ ) in  $\text{N}_2$  purged acetonitrile.



Thermodynamic Data

**Figure 40.** Arrhenius plot of compound **5** ( $4.5 \times 10^{-4}\text{M}$ ) in  $\text{N}_2$  purged acetonitrile.

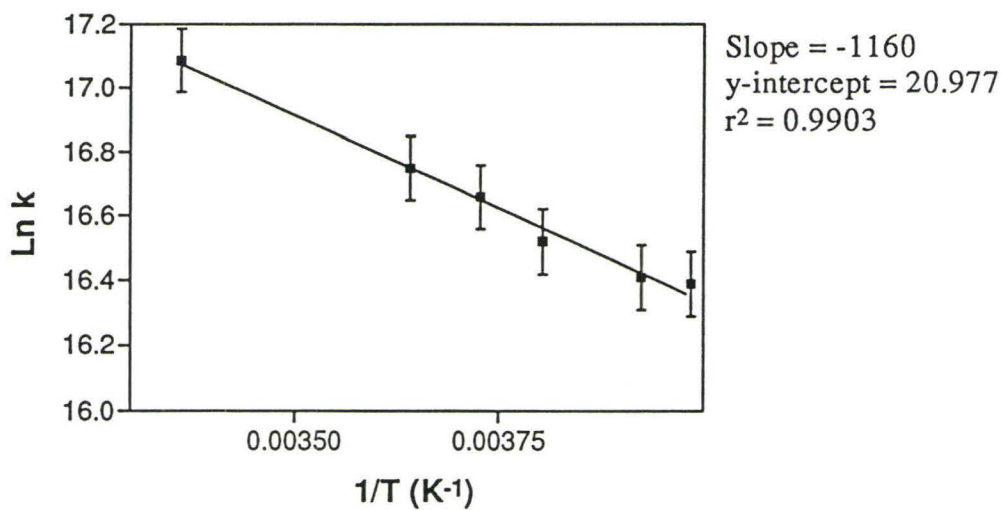
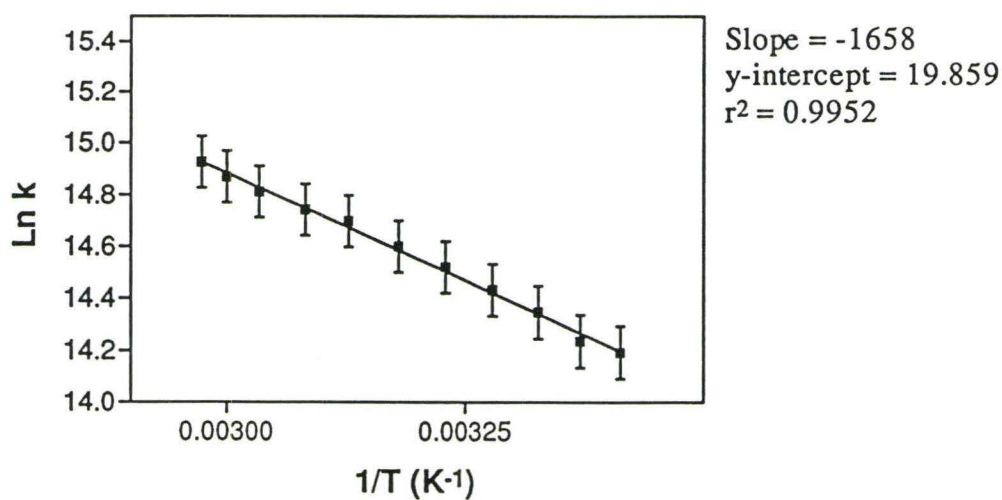


**Figure 41.** Arrhenius plot of compound **6** ( $4.5 \times 10^{-4}\text{M}$ ) in  $\text{N}_2$  purged acetonitrile.



Thermodynamic Data

**Figure 42.** Arrhenius plot of compound **7** ( $4.5 \times 10^{-4}\text{M}$ ) in  $\text{N}_2$  purged acetonitrile.

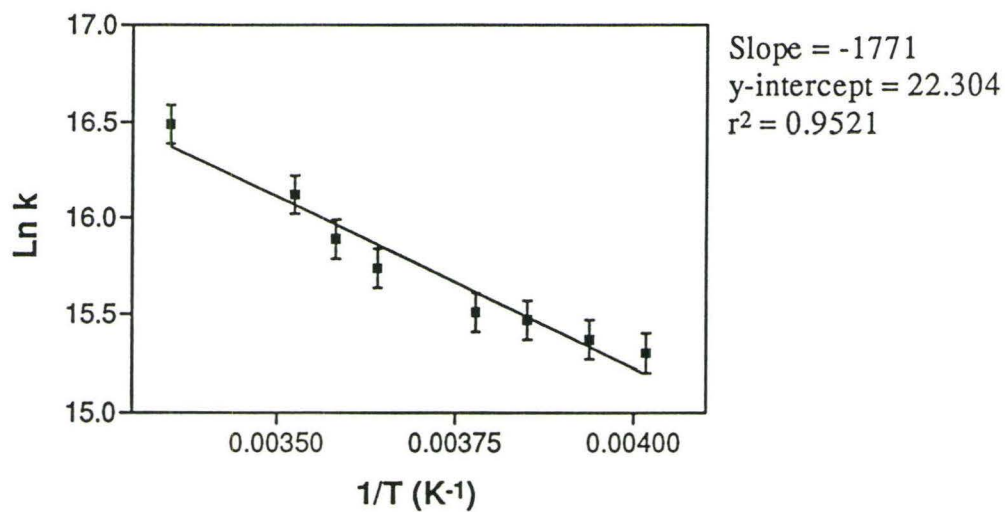
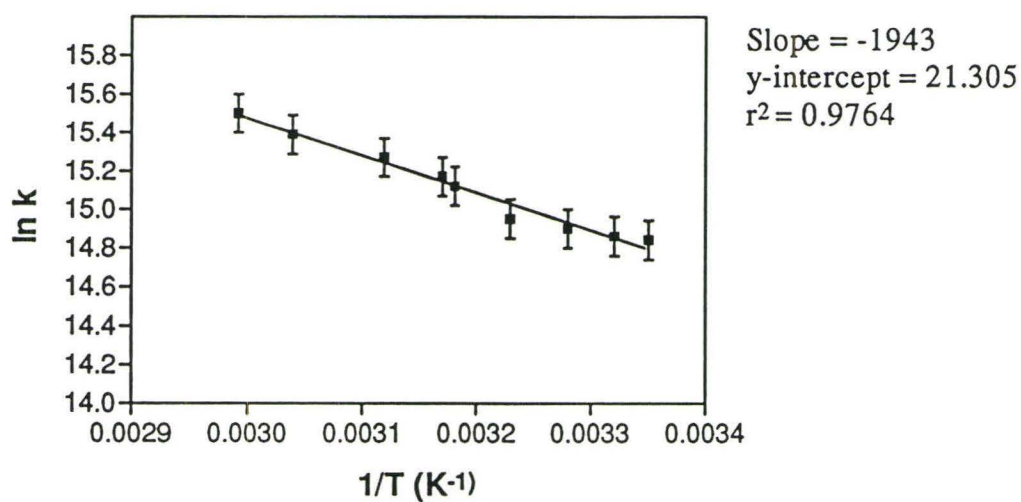


**Figure 43.** Arrhenius plot of compound **8** ( $4.5 \times 10^{-4}\text{M}$ ) in  $\text{N}_2$  purged acetonitrile.

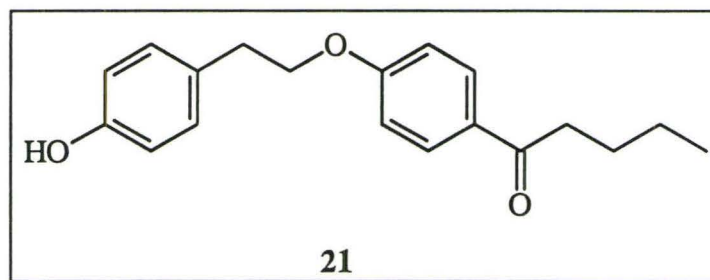


### CHAPTER III

#### DISCUSSION

Scaiano, Leigh and coworkers have previously reported the photochemistry of compound **1a** (p-p/OH) and **1b** (p-p/MeO) in isotropic<sup>(24)</sup> and liquid crystalline solvents<sup>(25)</sup> and in cyclodextrin inclusion complexes.<sup>(32)</sup> In order to corroborate their conclusions they studied compound **21** (Figure 44), which shows very inefficient photodecomposition in acetonitrile solution at ambient temperature ( $\Phi_{\text{dis}} = 0.009$ ). The lack of Norrish Type II photoreactivity of this molecule has been attributed to efficient intramolecular quenching of the carbonyl triplet state via abstraction of the remote phenolic hydrogen atom. Further evidence for this is that the quantum yield for disappearance of starting material for the methoxy analog **21** is within normal ranges for substituted valerophenone photoreactivity

**Figure 44.** Valerophenone Derivative of **1a**.



( $\Phi_{\text{dis}} = 0.13$ ).<sup>(4)</sup> Thus, the molecular motions necessary to achieve a favorable geometry for intramolecular abstraction of the phenolic hydrogen and the abstraction itself are both fast enough such that Norrish II reactivity is essentially completely suppressed. In fluid solution, rate constants for conformational motion are expected to be on the order of  $2\text{-}10 \times 10^8 \text{ s}^{-1}$ <sup>(33)</sup>; which is ca. 2 orders of magnitude faster than the rate of  $\gamma$ -hydrogen abstraction in triplet 4-methoxyvalerophenone.<sup>(4)</sup>

The work on compound **1a** (p-p/OH) has revealed that upon photolysis at 300 nm, a triplet state of the molecule is obtained. The lifetime of the ketone as determined by 1-methylnaphthalene quenching in the present work is 13 ns in deoxygenated acetonitrile solution at 22°C. This is in satisfactory agreement with the value of 16 ns reported previously.<sup>(24)</sup> The methoxy analog **1b** also generates the carbonyl triplet, but has a lifetime of 2.6  $\mu\text{s}$ . Furthermore, when **1a** is dissolved in ordered media such as liquid crystals or cyclodextrins<sup>(25)</sup>, media which inhibit molecular motions, the triplet lifetime is increased dramatically to approximately 1  $\mu\text{s}$ . Thus it was concluded that the hydroxy compound **1a**, as compound **20**, has an efficient quenching mechanism which is not available in the methoxy analog (**1b**), where molecular motions and the presence of the phenoxy group are necessary for efficient quenching. Further evidence for this is obtained from the deuterium kinetic isotope effect on the triplet lifetime ( $k_{\text{H}}/k_{\text{D}} = 1.8$ ), which confirms that hydrogen atom transfer is the rate determining step for triplet decay in **1a**.

This is reasonable in the light of Scaiano's work which shows that  $(\pi, \pi^*)^3$  triplet ketones are quenched quite rapidly by phenols.<sup>(7)</sup> However the sandwich-like conformer



(Figure 10) which is thought to be responsible for the quenching of the carbonyl triplet in **1a**, is a high energy conformer which will be similarly easy to obtain in all the compounds in the study. The difference between ketones and ultimately their triplet lifetime is the number of conformers in which the phenoxy group is in a correct position for hydrogen-abstraction and the ease of their formation.

The experiments performed in this study began with the intention of establishing the excited state electronic configuration of each molecule as well as their spectroscopic differences and similarities.

The phosphorescence measurements performed allow identification of the electronic configurations of the lowest excited triplet state of the compounds in this study. Compounds **1a** through **6** all possess substituted acetophenone chromophores and show typical  $(\pi, \pi^*)^3$  phosphorescence spectra and phosphorescence lifetimes on the order of 100 to 400 ms (Table I). The triplet energies and lifetimes obtained for these compounds are consistent with data reported for the parent chromophores.<sup>(16)</sup> Compound **1a** (p-p/OH) possesses a triplet energy of 73.5 kcal/mole and a phosphorescence lifetime of 256 ms, which are similar to those of 4-methoxyacetophenone ( $E_T = 71.5$  kcal/mole ;  $\tau_P = 260$  ms).<sup>(16)</sup> The spectrum in Fig. 14a is representative of all the para-alkoxy-substituted phenyl-alkyl-ketones in this study; the triplet energy is estimated as the onset of the 0-0 band emission at 389 nm shown by the arrow in the figure.

Compounds **3a** (m-p/OH), **3b** (m-p/MeO), **4a** (m-m/OH) and **4b** (m-m/MeO) show similar phosphorescence spectra to that of 3-methoxyacetophenone ( $E_T = 72.4$

kcal/mole).<sup>(16)</sup> The phosphorescence lifetimes are a factor of 2 - 3 shorter than those of the compounds which have para substitution on the acetyl ring. Wagner has observed similar trends in meta-substituted valerophenones, which possess rates of radiationless decay at least ten times faster than for the analogous para-substituted ketone due to  $\Delta E_T$  gap differences.<sup>(4)</sup> The triplet states of the dialkoxy-substituted chromophores **5** and **6** are also long-lived (340 and 393 ms, respectively) and possess comparable triplet energies to the other  $\pi$ ,  $\pi^*$  triplets previously discussed.

Figure 14d shows the spectrum of compound **8** (b-m/OH), which again is representative of the chromophore in this molecule. The phosphorescence spectrum contains better-resolved fine structure than the spectra in a,b or c, and the phosphorescence lifetimes of both **7** and **8** are at least an order of magnitude smaller than for the other compounds studied. In fact, both the definition in the spectrum and the short phosphorescence lifetime ( $\tau_p$ ) are characteristic of  $(n, \pi^*)^3$  triplet emission and is one method for classifying the electronic configuration of these triplets as such.<sup>(27)</sup>

The steady state photolysis experiments show that all of the compounds in the study are relatively nonreactive. Irradiation of the compounds in deoxygenated acetonitrile solution at 22°C gave no indication of shorter retention time photoproducts. The quantum yield of starting material disappearance found for **1a** (p-p/OH) was reported to be  $\Phi_{dis} = 0.006$ .<sup>(24)</sup> Thus, a comparison of **1a** with the other ketones in this study allows estimates of the quantum yields for disappearance of compounds **1-8** in the 0.002 - 0.010 range. What this implies is that photodecomposition is not easily accomplished, and

that all compounds have some manner in which non-destructive excited state quenching occurs.

Ultraviolet spectra are given for the compounds in this study as well as the model compounds for comparison (Fig 13a-l). For the most part, all the compounds show absorption spectra which are very similar to those of the corresponding model compounds. Ground state association of the phenolic and the phenyl acetyl portions of these molecules, if it takes place, alters the nature of the chromophore only in one case. Compound **1a** as shown in Figure 13a has essentially the same absorption pattern as the methoxy analog **1b** shown in Figure 13b. The main difference is that the absorptions are broader and are shifted to lower energy. One possible explanation for this would be ground state association of the two ends of the molecule.

Excitation of these compounds for most of the experiments are performed at 248 nm; at this wavelength all compounds in this study show strong absorption such that monitoring photochemical behaviour at low ketone concentration is possible.

The compounds in this study possess similar ultraviolet absorption spectra, steady state photoreactivity and phosphorescence properties to those of compounds **1a** (p-p/OH) and **1b** (p-p/MeO) which have previously been studied.<sup>(24)</sup>

Nanosecond laser flash photolysis of any of these compounds in acetonitrile solution yields intense, short-lived transients at either 375 nm (alkoxyacetophenone) or 525 nm (alkoxybenzophenone). Figures 15a and 15b show transient decay traces recorded at 375 nm, which appear as either one-component (Fig. 15a) or two-component



(Fig. 15b) decays. The transient in Figure 15a and the shorter-lived transient in Fig. 15b are both quenchable by dienes (Table II), and dominate the transient absorption spectra taken immediately after the laser pulse (Fig. 33 curve a). The transients produced immediately after the excitation pulse can in all cases [1a-8] be assigned as due to the triplet states of the respective compounds, based on the diene quenching experiments and the transient absorption spectra (Figures 16-27). In all cases, the data are similar to those obtained for the parent chromophore (Table VI and Figures 28-32).

The transient absorption spectrum of compound 2a (p-m/OH), as shown in Figure 33, is representative of all the hydroxy-containing compounds in this study. The spectrum (A) is recorded 0-50 ns after the laser pulse, while (B) is the spectrum taken after the initial transient has disappeared (200-250 ns in this case). Curve B is clearly different from curve A and suggests a transformation is occurring. The triplet decay traces reveal the presence of a second component only when the compound itself possesses a short triplet lifetime ( $\tau < \sim 150$  ns). The lifetimes of the triplets are more difficult to determine in these cases, as the decays are not clean first-order; they were thus determined by 1-methylnaphthalene quenching. The advantage of this technique is that not only can energy transfer be monitored (verifying that the species being quenched by 1-methylnaphthalene is a triplet), but also indirect lifetime measurements can be performed. For these experiments the optical density of 1-methylnaphthalene (MeN) triplets is monitored at  $\lambda_{\text{max}} = 425$  nm. The data is plotted in a double reciprocal form according to equation 22,

where  $A_{425}$  is the transient optical density at 425 nm due to the MeN triplet, before significant decay takes place,  $k_q\tau_K$  is the Stern-Volmer parameter, and  $\alpha$  is a constant.

$$1/A_{425} = \alpha + \alpha/(k_q\tau_K[\text{MeN}]) \quad [22]$$

Plot  $1/A_{425}$  vs  $[\text{MN}]^{-1}$

$$\text{intercept} = \alpha_{\text{MN}^*} \phi_{\text{isc}}^{-1} \quad \text{slope} = \alpha_{\text{MN}^*} \phi_{\text{isc}}^{-1} / k_q\tau_K$$

$$\text{int/slope} = k_q\tau_K$$

$k_q\tau_K$  values are obtained from the intercept to slope ratio and by assuming a value for  $k_q$  of  $8.3 \times 10^9 \text{ M}^{-1}\text{s}^{-1}$ ,<sup>(24)</sup> the lifetime ( $\tau$ ) of the transient is obtained.

### **3.1 Bimolecular Phenolic Hydrogen Abstraction**

Every intramolecular reaction studied for compounds **1-8** has an analogous bimolecular reaction between a ketone and a phenol of similar reactivity. These rates for bimolecular quenching of the excited ketone by the corresponding phenol must be obtained so that any variation in rates due to substituent effects may be ascertained. Table VI shows the triplet characterization data of the model compounds used to provide the bimolecular rate constants. Table VII lists the rate constants for the respective ketones with either *p*-cresol or *m*-cresol. The rate constants for *m*-cresol show to be slower (less

than 2 times) then *p*-cresol for all the ketones studied; indicating a positive  $\rho$  value consistent with Scaiano's previously published results.<sup>(7)</sup> Rate constants also vary with substitution on the ketone where the *meta*-methoxy acetophenone **16** gives the fastest quenching rate, followed by the *para*-methoxy **15** and the 3,4-disubstituted analog **17** which is only about twice slower than **16**. Thus, it can be determined that the bimolecular rate constants for quenching are only marginally dependent on electronic effects induced by differences in the point of attachment of the hydroxy or carbonyl group.

Acetonaphthone (**20**) also shows reduced reactivity toward excited state phenolic hydrogen atom abstraction which may be due to either its much lower triplet energy ( $E_T$ ) or to its lowest  $\pi, \pi^*$  triplet state.

The molecules **18** (benzophenone) and **19** (4-methoxybenzophenone) both possess lowest  $n, \pi^*$  triplets and therefore are expected to have a slower rate of reaction than the  $\pi, \pi^*$  triplets. This study has shown that although **18** and **19** are  $n, \pi^*$  triplets they possess comparable rates of reaction for hydrogen abstraction to those of the  $\pi, \pi^*$  triplets, namely **15** and **16**. Scaiano<sup>(7)</sup> as previously mentioned, has already seen such circumstances and subscribes to the notion that the benzophenone quenching mechanism is more complex than a simple hydrogen atom transfer.

### **3.2 Intramolecular Phenolic Hydrogen Atom Abstraction**

The triplet lifetimes of the compounds **1-8** are given in Table IV. The data given in this table indicate dramatic differences in triplet lifetime with respect to varying the substitution patterns in the molecules.

The gross comparisons that can be made from the data are for compounds **1a/2a**, **5/6** and **7/8** which all differ in the location of the hydroxy group; in the para position for some, or in the meta position for others. In all cases triplet lifetimes indicate that hydrogen atom abstraction is approximately 10 times faster when the hydroxy group is in the para position. Bimolecular rates for analogous reactions also indicate greater para-hydroxy reactivity for all ketones but only 1-1.8 times faster. Thus, the differences in the rate of hydrogen abstraction between corresponding meta- and para- phenolic ketones cannot be due predominantly to electronic effects. Furthermore, the rates of intramolecular hydrogen abstraction are seemingly independent of the triplet configuration (as **7** and **8** are  $n,\pi^*$  triplets). Thus in these compounds at least, differences in triplet lifetime must be due to geometric factors.

**Table VIII.** Lifetimes of carbonyl triplets in acetonitrile at 22°C.

Compound	$\lambda_{\text{max}}$ (nm)	$\tau$ (ns) <sup><i>g</i></sup>
<b>1a</b> (p-p/OH)	380	15
<b>1b</b> (p-p/MeO)	380	2600
<b>2a</b> (p-m/OH)	375	320
<b>2b</b> (p-m/MeO)	375	1800
<b>3a</b> (m-p/OH)	375	670
<b>3b</b> (m-p/MeO)	375	4800
<b>4a</b> (m-m/OH)	375	1135 <sup><i>g</i></sup>
<b>4b</b> (m-m/MeO)	375	3500
<b>5</b> (a-p/OH)	375	55 <sup><i>ξ</i></sup>
<b>6</b> (a-m/OH)	375	860
<b>7</b> (b-p/OH)	525	20 <sup><i>ξ</i></sup>
<b>8</b> (b-m/OH)	525	350

⊗ By plotting self-quenching curves at various temperatures and extrapolating to infinite dilution.

ξ 1-methylnaphthalene quenching was utilized.  $k_q = 8.3 \times 10^9 \text{ M}^{-1} \text{ s}^{-1}$ .

*g* 10% associated error.

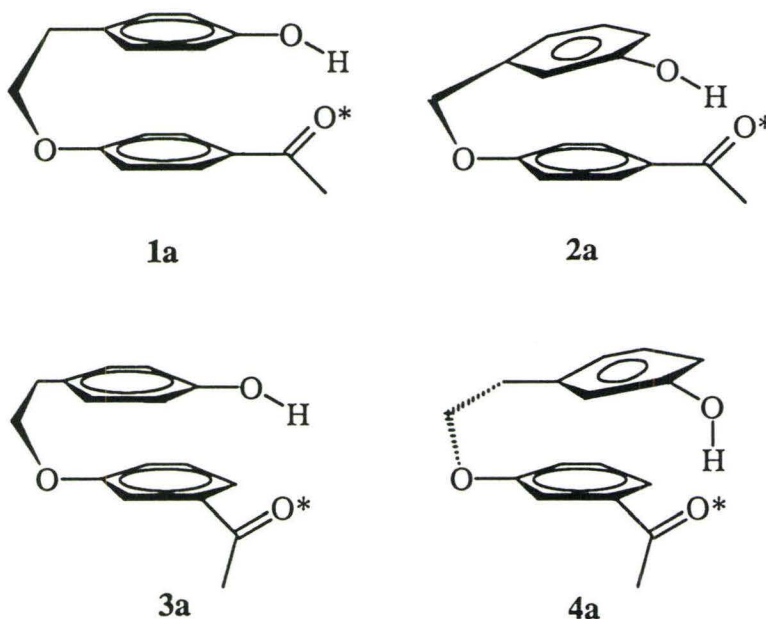
Comparisons for compounds **1a/3a** and **2a/4a** can also be made. In these cases the hydroxy groups for the two compounds are in the same location. When the hydroxy is in the para position (**1a/3a**) the lifetime variation can be monitored as a function of the acetyl group being either in the para position (**1a**) or in the meta position (**3a**). The para-acetyl case shows to be ca. 40 times faster than the meta-acetyl case. This difference cannot be accounted for through electronic effects or triplet energy gap differences. Clearly, geometric factors are key in determining the lifetime of a given ketone. For the pair **2a/4a**



the hydroxy group remains in the meta position for both. When the acetyl group is in the para position (**2a**), hydrogen abstraction occurs ca. 4 times faster than when the acetyl group is the meta position (**4a**). The triplet lifetimes are now longer and interpretation becomes somewhat more complicated as the difference in triplet lifetimes may be due to either geometric factors or differences in the nature of the ketone triplet.

Geometric factors are important and clearly contribute to the triplet lifetime in each of the compounds in the study. Calculations were performed using AMPAC on initial geometries calculated with PCModel. Structure minimization of each compound in a correct geometry for hydrogen atom abstraction was sought. The problem herein is that each molecule possesses several correct geometries from which hydrogen atom abstraction can occur. The minimized structure obtained from the calculations is a function of the input geometry which leads to several heats of formation for each compound. A general geometry could however be obtained from these calculations as invariably certain aspects of each molecule's quenching geometry remained essentially constant. Figure 45 depicts the the geometries for compounds **1a**, **2a**, **3a** and **4a**.

**Figure 45.** Quenching Geometries for Compounds **1a**, **2a**, **3a** and **4a**.



Compound **1a** seems to have the easiest task (lowest change in heat of formation from the nearest stable gauche conformer) to reach a geometry where the hydrogen atom is lined up with the n-orbital of the excited ketone. Compound **2a** has a higher energy geometry than is found for **1a**, the proximity of the two phenyl rings has to be quite close in order to line up the hydrogen atom for abstraction. The fact that the rings come close together is reflected in the angle of the phenoxy ring away from the lower portion of the molecule. **3a** and **4a** are again increasingly more difficult to achieve based on heats of formation. In **3a** the rings are no longer stacked and statistical probability may be decreased compared to **1a**. **4a** has the problems associated with both **2a** and **3a** where the functional group location lowers the number of possible geometries which satisfy

quenching behaviour and also the rings must again come within fairly close proximity which is reflected in the angle of the phenoxy ring away from the lower portion of the molecule.

### **3.3 Biradical Formation**

The spectrum of the longer lived transient Figure 15b and 33 curve b, decays monoexponentially in each case and the decay kinetics are not affected by the addition of diene, albeit the initial yield is markedly reduced. This behaviour is not consistent with triplet behaviour but instead with a transient whose precursor is a triplet species. These transients are assigned as the biradical equivalents of the 1,13-biradical produced for compound **1a**<sup>(24)</sup> as shown below.

The triplet and the biradical generated in each case are both quenched by oxygen. The quenching characteristics are consistent with triplet formation preceeding biradical production.

If this is the case then hydrogen-deuterium kinetic isotope effects should be detected for all the hydroxy containing ketones in this study as the biradicals must be formed by a self-quenching mechanism of the carbonyl triplet via intramolecular hydrogen abstraction. The values for the isotope effects in Table IX are the ratio of the rate constants obtained from Tables III and V.



Thus for all the hydroxy compounds **1a** - **6** a primary hydrogen-deuterium isotope effect is apparent. The values are consistent with what might be expected considering the proposed quenching mechanism and the value of 1.8 given for compound **1a**.<sup>(24)</sup> It is important however to note that the hydrogen-deuterium isotope effects are consistently greater for the meta-substituted analog in each pair of compounds **1a/2a**, **3a/4a**, **5/6** and **7/8**. Thus it would seem that the slower the reaction, the larger the kinetic isotope effect seen for these pairings of molecules. Similarly, if **1a** and **3a** are compared, again we see the slower reacting molecule (**3a**) having a larger kinetic isotope effect than **1a**.

**Table IX.** Kinetic isotope effects in deoxygenated acetonitrile at 22°C.

Compound	$k_H/k_D^a$
<b>1a</b> (p-p/OH)	1.4 <sup>p</sup>
<b>2a</b> (p-m/OH)	2.2
<b>3a</b> (m-p/OH)	1.8
<b>4a</b> (m-m/OH)	2.1
<b>5</b> (a-p/OH)	1.7 <sup>p</sup>
<b>6</b> (a-m/OH)	1.9
<b>7</b> (b-p/OH)	1.2 <sup>p</sup>
<b>8</b> (b-m/OH)	2.6
<sup>p</sup> a	From 1-MeN quenching; Table III. Associated error is ~10%.

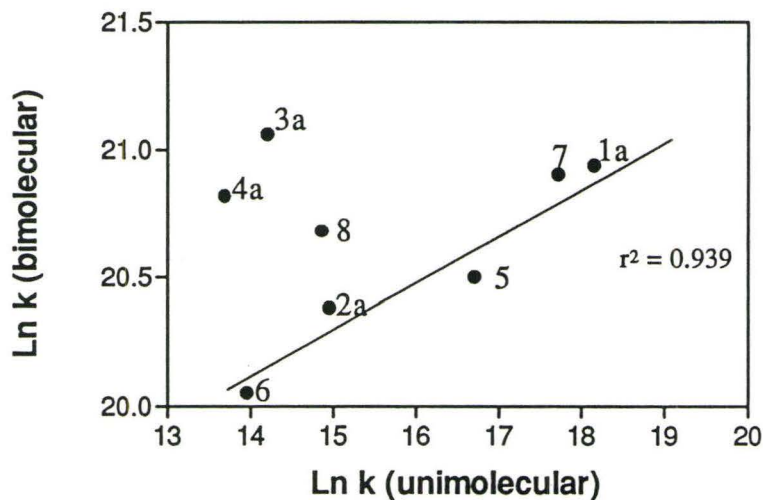
Assuming the reactions are exothermic, slower reactions have been reported to give larger kinetic isotope effects.<sup>(33)</sup> Compounds **2a** and **4a** have similar isotope effects which might indicate the location of the transition states along their respective reaction coordinate are comparable.

A very small isotope effect is found for compound **7**. This is consistent with bimolecular reactions where phenolic quenching of benzophenone triplets gave comparable isotope effects.<sup>(7)</sup> The reason put forth is simply that the quenching mechanism is more complicated than a simple hydrogen atom transfer.

### **3.4 Comparison of Unimolecular and Bimolecular Reactions**

In order to gain a better understanding of the relationship between unimolecular and bimolecular reactions a comparison of rate constants must be performed. The idea is to see if the intramolecular reactions and the bimolecular reactions are governed by similar factors. To compare these two sets of reactions Figure 46 shows a plot of the logarithm of the rate constant for intramolecular self-quenching (compounds **1a-8**) versus the logarithm of the rate constant for intermolecular reaction of the corresponding substituted phenylketone and phenol.

**Figure 46.** Correlation between bi- and unimolecular reactions.



Winnik in his review<sup>(23)</sup> compares both unimolecular and bimolecular kinetic schemes and has to make the assumption that in order for the kinetics to be the same or at least comparable, the encounter complex and indeed the transition state must be the same in both cases. Intuitively the uni- and bimolecular reactions for these systems should have pronounced differences in geometric requirements for reaction. However, it is clear that for the molecules studied here, the bimolecular and unimolecular cases show a strong correlation ( $r^2 = 0.939$ ) for five of the eight compounds (Fig. 46). According to Winnik the reactions in these five cases have transition states which are the same for both the bi- and unimolecular reactions. Conversely, it would seem that molecules **3a**, **4a** and **8** have molecular structures which do not allow the transition state geometries (for quenching of the ketone triplet) of the intramolecular and bimolecular reactions to be comparable. Perhaps the difference remains in the fact that geometrically, compounds **3a** and **4a** are the

only two compounds which have the acetyl group attached in the meta position. This makes the transition state for reaction more difficult to obtain unimolecularly than bimolecularly. Compound 8 may also have trouble in obtaining the correct geometry for quenching because of the bulky benzophenone-like chromophore and a hydroxy group in the meta position. These two factors combine to make quenching more difficult in the intramolecular reactions.

### **3.5                    Activation Parameters for Intramolecular Phenolic Quenching**

To support the proposed mechanism of intramolecular phenolic hydrogen abstraction, thermodynamic data may be considered to relate the energy of the transition states to the conformational motions of quenching. Useful information can usually be obtained by comparing the Gibbs free energy ( $\Delta G^\ddagger$ ) for the reacting systems with the proviso that the entropy of activation of each system is similar. Under such conditions  $\Delta G^\ddagger$  can be related to the structural changes of the system in order to rationalize the results in terms of the stabilization or destabilization of the transition state.

$$E = h\nu$$

$$E \approx kT \quad \quad k \text{ is Boltzmann constant}$$

$$\nu = kT / h$$

$$\begin{aligned} \text{rate of reaction} &= \nu [AB]^\ddagger \\ &= \kappa \nu k^\ddagger [A][B] \end{aligned}$$

$$-\Delta G = RT \ln K^\ddagger, \quad K^\ddagger = e^{-\Delta G/RT}$$

$$\text{so rate of reaction} = (kT/h) e^{-\Delta G/RT} [A][B]$$

$$\Delta G^\ddagger = \Delta H^\ddagger - T\Delta S^\ddagger$$

$$\text{Therefore rate} = (kT/h) e^{-\Delta H^\ddagger/RT} e^{\Delta S^\ddagger/R} [A][B]$$

$$\text{Since the rate of a bimolecular reaction is } \text{rate} = k_2 [A][B]$$

$$\text{then } k_2 = (kT/h) e^{\Delta S^\ddagger/R} e^{-\Delta H^\ddagger/RT} \quad [23]$$

The enthalpy of the reaction is reflected in the energy of activation in the above equation.

The entropic term  $\Delta S^\ddagger$  is absorbed into the preexponential term and refers to the vibrational, rotational and translational freedom of all species involved in the transition state. The entropic term gives a clear indication of the order that is necessary to obtain the sandwich-like conformer and a transition state that is prone to hydrogen abstraction. Thus, because the expected transition state has considerable order, a large negative entropic term is expected.

Hence to obtain the data, the triplet lifetime of each ketone was determined as a function of temperature and the data plotted using equation 23. The plots are given in Figures 36-43 and the data converted to thermodynamic terms in Table X.



**Table X.** Activation parameters for intramolecular phenolic quenching at 298K.

Compound	$\Delta H^\ddagger$ (kcal/mole)	$\Delta S^\ddagger$ (cal·mole <sup>-1</sup> s <sup>-1</sup> )
1a (p-p/OH)	2.9 ± 0.2	-21 ± 2
2a (p-m/OH)	3.4 ± 0.8	-26 ± 4
3a (m-p/OH)	0.7 ± 0.3	-36 ± 2
4a (m-m/OH)	1.7 ± 0.3	-33 ± 2
5 (a-p/OH)	1.7 ± 0.2	-27 ± 2
6 (a-m/OH)	2.7 ± 0.2	-29 ± 2
7 (b-p/OH)	2.7 ± 0.5	-25 ± 4
8 (b-m/OH)	3.3 ± 0.4	-28 ± 2

The  $\Delta H^\ddagger$  term is quite small in all cases but does show however a trend where the compounds with *para*-hydroxy substituents have a slightly smaller enthalpy of activation then do the *meta*-hydroxy compounds. This may reflect the acidity of the phenols or perhaps suggest that there is charge transfer accompanying hydrogen abstraction which is easier in the *meta*-hydroxy cases then in the *para*-hydroxy cases. The low value for activation enthalpy is also indicative of a transition state where there is both bond breaking and bond forming occurring in a concerted manner.<sup>(34)</sup>

Compounds **3a** and **4a** show smaller  $\Delta H^\ddagger$  values which may indicate lower reduction potentials for ketones which are *meta*-alkoxy-substituted-ketones than for their *para*-substituted counterparts (**1a** and **2a** respectively).<sup>(35)</sup>

It is safe however to say that in all cases the free energy is dominated by the entropic term ( $\Delta S^\ddagger$ ) which indicates the degree of order in the transition state. As is expected, the values measured are all negative with large magnitudes giving support for the 'sandwich' conformer expected to be responsible for the hydrogen atom transfer. The lower values of entropy for the *meta*-acetyl compounds **3a** and **4a** may reflect a statistical factor which is introduced where the location of the ketone becomes more difficult for the phenoxy group to react with. In these cases the orientation and the correct 'face' or surface of the ring in relation to the rest of the molecule will be important.

Thus, the thermodynamic data supports the proposed self-quenching mechanism for the compounds in the study. The entropic terms suggesting a high degree of order in the transition state as well as the enthalpic term indicating both bond cleavage and formation occurring concertedly.

## CHAPTER IV

### SUMMARY AND CONCLUSIONS

It has been shown that all the hydroxy compounds **1a-4a** possess triplet states which are substantially shorter-lived than those of their methoxy analogs (**1b-4b**). In each case the efficient quenching of the excited carbonyl triplet state has been attributed to intramolecular phenolic hydrogen abstraction. Evidence for this is found in the detection of biradical species generated from triplet decay, primary hydrogen-deuterium kinetic isotope effects and thermodynamic parameters which support both atom transfer (enthalpy) and high degrees of order (entropy) in the transition state necessary for the proposed abstraction process.

The triplet lifetimes of the linked phenolic ketones (**1a-4a**) differ dramatically with respect to changing the regiochemistry of the substituents. Compounds **5** and **6** were studied in order to examine what effect increasing the triplet energy gap ( $\Delta E_T$ ) of certain ketones would have on the triplet lifetimes. What is found is that the triplet lifetime of **5** (a-p/OH) is longer than that of **1a** (p-p/OH), and the triplet of **6** (a-m/OH) is longer lived than that of **2a** (p-m/OH). Since the extra methoxy substituent of **5** and **6** should not interfere sterically with the quenching process, the differences in triplet lifetimes between these pairs can be attributed to the  $\Delta E_T$ .



Thus evidence for the reactivity of the upper  $(n, \pi^*)^3$  by thermal population may be argued. The methoxy substituent effectively increases the triplet energy gap and thus makes thermal population of the upper excited state more difficult and results in longer triplet lifetimes. Wagner has shown that the  $\Delta E_T$  of the para-methoxyacetophenone and meta-methoxyacetophenone are both 3 kcal/mole.<sup>(3)</sup> If this is the case, then the differences in lifetimes between the compounds of different chromophores, namely **1a** (p-p/OH) and **3a** (m-p/OH) as well as **2a** (p-m/OH) and **4a** (m-m/OH) can be considered to be solely due to differences in geometric factors.

It is somewhat more difficult to compare compounds such as **1a** (p-p/OH) against **2a** (p-m/OH) as the acidities of the phenolic portions of the molecules are different. Hence substituent effects can play a role in the abstraction process. The bimolecular reaction of 4-methoxyacetophenone with *p*-cresol is 1.7 times faster than the reaction of the same ketone with *m*-cresol. This difference, if manifested in the compounds **1a** (13 ns) and **2a** (320 ns) does not account for a significant amount of the difference in triplet lifetime which show an approx. 25 fold increase in triplet lifetime. This difference in bimolecular reactions can not totally account for the differences in triplet reactivity for compounds **3a** and **4a** either which possess the 3-alkoxyacetophenone chromophores.

It can be concluded that dramatic effects on the triplet lifetime of molecules **1a** -**4a** are evident with respect to changing the substitution of the acetyl and hydroxy groups. The differences are due almost exclusively to varying degrees of difficulty in obtaining a transition state geometry in which the phenoxy hydrogen is properly lined up for

intramolecular hydrogen abstraction. Since conformational motions are fast with respect to the lifetimes of the triplets, it can be assumed that in each case the ketones are in total excited state equilibrium. Hence, the longer lived the ketone triplet, the lower is the percentage of conformer present responsible for hydrogen abstraction.

## CHAPTER IV

### EXPERIMENTAL

#### 4.1            General

$^1\text{H}$  NMR spectra were recorded on Varian EM390 (90 MHz), Bruker AC200 (200 MHz) or Bruker AC300 (300 MHz) spectrometers in deuteriochloroform solution, and are reported in parts per million downfield from tetramethylsilane.  $^{13}\text{C}$  NMR spectra were recorded on a Bruker AC200 (50.3 MHz) or a Bruker AC300 (75.5 MHz) spectrometer and are reported in parts per million downfield from tetramethylsilane. Ultraviolet absorption spectra were recorded on a Hewlett-Packard HP8451 UV spectrometer or a Perkin-Elmer Lambda 9 spectrometer equipped with a Model 3600 Data Station. Mass spectra and exact masses were recorded on a VG Analytical ZABE mass spectrometer; the latter employed a mass of 12.000000 for carbon. Infrared spectra were recorded on a Biorad FTS-40 FTIR spectrometer and are reported in wavenumbers ( $\text{cm}^{-1}$ ) calibrated using the  $1601.8\text{ cm}^{-1}$  polystyrene absorption. Melting points were determined on an

Olympus BH-2 polarizing microscope fitted with a Mettler hot stage controlled by a Mettler FP80 Central Processor, and are not corrected.

Gas chromatographic analyses employed a Hewlett-Packard 5890 gas chromatograph equipped with a flame ionization detector, a Hewlett-Packard 3396A recording integrator, and either a 5m or 15m x 0.53mm DB-1 column from Chromatographic Specialties. Chromatographic separations were carried out on a Harrison Research chromatotron using a 2 or 4 mm thick plate consisting of (EM Science) Silica Gel 60, PF 254 containing Gypsum.

## 4.2 Commercial Solvents and Reagents Used

Methanol (Baker; reagent), cyclohexane (Baker; Photrex), diethyl ether (Fisher; dry reagent), ethyl acetate (Caledon; reagent), ethanol (absolute and 95%) and water (Baker; HPLC grade) were all used as received from the suppliers. Dichloromethane (Caledon; reagent) was distilled from calcium hydride, dimethylformamide (Baker; reagent) was distilled from potassium hydroxide and barium oxide, and benzene (BDH; reagent) was purified by extraction with concentrated sulfuric acid followed by distillation from sodium. Acetonitrile (BDH; HPLC grade) was predried over potassium hydroxide and then refluxed and distilled under nitrogen from calcium hydride. Acetone (BDH; reagent) was distilled from potassium permanganate and then from potassium carbonate, and stored over anhydrous potassium carbonate. Pyridine (BDH; reagent) was distilled from barium oxide.

Benzophenone, 4-methoxybenzophenone, 4-methoxyacetophenone, 3-methoxyacetophenone, acetoveratrone (recrystallized 3x from ethyl acetate/petroleum ether), 1,3-cyclohexadiene, 1-methylnaphthalene, xanthone (all from Aldrich Chemical Co.), p-cresol, m-cresol, phenol (Caledon) were recrystallized from ethanol/water or were distilled as needed. 4-Hydroxyacetophenone, 3-hydroxyacetophenone, 4'-hydroxybenzophenone, 4-hydroxy-3-methoxyacetophenone, 2-(4-hydroxyphenyl)-1-ethanol, 2-(3-hydroxyphenyl)-1-ethanol, 2-(4-methoxyphenyl)-1-ethanol, 2-(3-methoxyphenyl)-1-ethanol, phosphorus tribromide, chlorotrimethylsilane, *tert*-butyl dimethylchlorosilane (Caledon), 48% HBr (all from Aldrich Chemical Co. unless

otherwise specified) were used as received from the suppliers. Deuterium oxide (MSD isotopes), deuteriochloroform (Matheson), and dimethylsulfoxide- $d_6$  (Stohler Isotope Chemicals) were also used as received from the suppliers.

**4.3****Preparation and Spectral Data of Compounds****4.3.1 Preparation of 1-bromo-2-(4-hydroxyphenyl)ethane**

In a 50 mL round-bottom flask, 2-[4-hydroxyphenyl]ethanol (10g, 81.3 mmol) was refluxed for 4 hours in 48% aqueous HBr (30 mL). The brown, oily solution was quenched with ice (30g), and extracted with diethyl ether (3 x 30 mL). The combined ether extracts were washed successively with H<sub>2</sub>O (1 x 30 mL) and saturated sodium bicarbonate (1 x 30 mL), dried over sodium sulphate, filtered, and stripped of solvent on the rotary evaporator. The solid obtained was recrystallized twice from ethanol/water (10:1) to give the desired product in an isolated yield of 80% (13g, 65 mmol, m.p. 87.0-87.8°C).<sup>(19)</sup>

**4.3.2 Preparation of 1-bromo-2-(3-hydroxyphenyl)ethane**

2-(3-hydroxyphenyl)ethanol (10 g, 81.3 mmol) was refluxed with 48% aqueous HBr (30 mL) for 4 hours. Work up was accomplished the same way as for 2-(4-hydroxyphenethyl) bromide above. The resulting oil was distilled in a short path distillation apparatus with a Vigreux column giving a colourless oil consistent with the desired product in a 90% yield (14.7g, 73.2 mmol, b.p. 113°C, 2 mbar).



#### **4.3.3 Preparation of 1-Bromo-2-(4-methoxyphenyl)ethane and 1-Bromo-2-(3-methoxyphenyl)ethane**

2-(4-Methoxyphenyl)ethanol or 2-(3-methoxyphenyl)ethanol (2 g, 13.2 mmol) in diethyl ether (5 mL) were placed in a flask under dry nitrogen. To this a solution of phosphorus tribromide in ether (1.2 mL, 12.8 mmol, and 8 mL ether) was added dropwise by syringe so as to keep the ether just refluxing. After the addition was complete the reaction mixture was allowed to stir for five more hours. The contents of the flask were then quenched with ice (20g) and then extracted with ether (3 x 30 mL). The organic layers were then washed with water (1 x 30 mL), saturated sodium bicarbonate (1 x 30 mL) and again with water (1 x 30 mL). The ethereal extracts were dried over sodium sulphate and concentrated under reduced pressure. This produced a clear oil in both cases that could be used in further steps without purification. 1-Bromo-2-(4-methoxyphenyl)ethane was obtained in a 70% yield (1.99g, 9.24mmol) and 1-bromo-2-(3-methoxyphenyl)ethane was obtained in a 60% yield (1.69g, 7.92mmol).



#### **4.3.4 Preparation of 4-[2-(4-hydroxyphenyl)ethoxy]acetophenone (1a):**

4-[2-(4-Hydroxyphenyl)ethoxy]acetophenone was prepared according to the published method,<sup>24</sup> and exhibited <sup>1</sup>H NMR, <sup>13</sup>C NMR, IR, and mass spectral characteristics which were similar to those previously published.

The compound was prepared by mixing 1-bromo-2-(4-hydroxyphenyl)ethane (0.53g, 2.66 mmol) with dry pyridine (2 mL). While keeping the flask under dry nitrogen chlorotrimethylsilane (1.2 ml, 9.4 mmol) was added dropwise via a syringe and the solution was allowed to stir for 18 hours. The mixture was cooled, ether (20 mL) was added, and the resulting suspension was filtered. Pyridine was then removed by gentle warming under high vacuum (3 mbar) for 6 hrs. The resulting oil was refluxed with potassium carbonate (0.245g, 1.8 mmol) and 4-hydroxyacetophenone (0.25g, 1.8 mmol) in dry acetone (30 mL) for 18 hours. The solution was acidified with dilute hydrochloric acid, washed with water (2 x 20 mL), dried over anhydrous sodium sulphate and filtered. Solvent evaporation yielded a viscous yellow oil which would not crystallize and showed impurities as monitored by gas chromatography. Chromatographic separation was achieved using a chromatotron with an eluant consisting of ethyl acetate /hexanes (20/80 v/v). Fractions collected were analyzed by gas chromatography. The fractions consisting of >80% of desired product crystallized and the solid was isolated and recrystallized from ethanol/water. The colorless needles gave an isolated yield of 25 % (115 mg, 0.44 mmol, m.p. 106.7-107.8°C)<sup>24</sup>.

#### 4.3.5 Preparation of (4a) 3-[2-(3-hydroxyphenyl)ethoxy]acetophenone

1-Bromo-2-(3-hydroxyphenyl)ethane (5 g, 25 mmol), imidazole (4.3 g, 65 mmol, 2.5 equivalents) and *tert*-butyldimethylchlorosilane (4.3 g, 30 mmol, 1.2 equivalents) were added to dimethyl formamide (10 mL). The reaction mixture was allowed to stir at 35 °C overnight. Water (20 mL) was added to the mixture followed by extraction with ether (2 x 20 mL). The ethereal layers were combined, washed with water and dried over magnesium sulphate. The solution was filtered and the solvent volume reduced at low pressure. The resulting yellow/brown oil was added to dimethyl formamide (20 mL), 3-hydroxyacetophenone (2.8 g, 22.5 mmol) and potassium carbonate (2.9 g, 22.5 mmol). The solution was heated at 100°C overnight. The mixture was cooled and extracted with ether, followed by successive washings by water and saturated sodium chloride. After concentrating under reduced pressure the thick oil was placed in a 3:1:1 mixture of tetrahydrofuran:acetic acid:water (20 mL) and stirred for 24 hours to eliminate the silyl group. This step was followed by chromatography utilizing 20% ethyl acetate in hexanes solution. First product band (major) was consistent with 3-hydroxystyrene (as determined by <sup>1</sup>H NMR) and the second product band gave colourless crystals which upon recrystallization from ethanol/water gave a 2% (100 mg, 0.4 mmol) isolated yield. The crystals give data consistent with the desired product.

#### (4a) 3-[2-(3-Hydroxyphenyl)ethoxy]acetophenone

**<sup>1</sup>H NMR:** δ (CDCl<sub>3</sub>) = 2.57 (s, 3H), 3.03 (t, 2H), 4.19 (t, 2H), 5.20 (s, 1H), 6.77 (m, 3H), 7.08 (m, 1H), 7.16 (m, 1H), 7.33 (m, 1H), 7.46 (m, 2H).

**<sup>13</sup>C NMR:**  $\delta$  (CDCl<sub>3</sub>) = 26.7, 35.5, 68.7, 113.2, 113.6, 120.2, 121.2, 121.4, 129.6, 129.7, 138.4, 139.9, 155.8, 159.0, 198.4.

**IR:** (KBr): 3209 (b), 3113 (w), 2943 (w), 2925 (w), 1668 (s), 1596 (s), 1581 (s), 1495 (w), 1285 (s), 1211 (m), 1156 (m), 1034 (m), 879 (w), 789 (m), 690 (w), 603 (w).

**MS:** (m/e(I)): 256 (20), 121 (100), 103 (120), 91 (15), 77 (18).

**Mass:** Calculated for C<sub>16</sub>H<sub>16</sub>O<sub>3</sub>: 256.1099. Found 256.1094.

**Melting point:** 88.7 - 90.6 °C.

**UV:**  $\lambda_{\text{max}}$  (MeCN) = 218 nm( $\epsilon$  = 29800), sh = 200, 244, 276, 302.

#### **4.4**            **General Method:**

##### **4.4.1**    **Preparation and Purification of Hydroxy Containing Compounds**

Either 1-bromo-2-(4-hydroxyphenyl)ethane or 1-bromo-2-(3-hydroxyphenyl)ethane (2g, 10 mmol) was placed in benzene (20 mL) with pyridine (1.1 equivalents, 0.85 mL). While keeping the contents of the flask under nitrogen trimethylchlorosilane (1.1 equivalents, 1.2 mL) was added dropwise by syringe. The flask was maintained so that the temperature did not rise above 35°C. The mixture was stirred at room temperature for approximately six hours; after which ether (20 mL) was added and the solution was filtered. The filtrate was concentrated under reduced pressure for 1 hour. The protected alkylbromophenol was then added to dry acetone (30 mL) with



potassium carbonate (1.1 equivalents) and the desired hydroxyacetophenones (1.1 equivalents). The solution then was refluxed for 1 to 3 days (as monitored by  $^1\text{H}$  NMR) depending on the compounds being coupled. After the reaction was complete the solution was filtered and the acetone removed under vacuum. The yellow oil obtained was acidified with dilute hydrochloric acid and subsequently was extracted into ether (3 x 30 mL). The ethereal phase was then washed once with water (30 mL) and then saturated brine (30 mL). The organic layer was then dried over magnesium sulphate, filtered and concentrated under vacuum. Purification of compounds was performed by chromatography utilizing ethyl acetate / hexanes solutions (20/80 v/v) or ethyl acetate / methylene chloride (15/85 v/v) for the benzophenone derivatives. Isolated yields are low mostly due to problems encountered during the isolation step. The compounds and their spectral properties are listed below:

(2a) 4-[2-(3-hydroxyphenyl)ethoxy]acetophenone:

**$^1\text{H}$  NMR:**  $\delta$  ( $\text{CDCl}_3$ ) = 2.53 (s, 3H), 3.05 (t, 2H), 4.19 (t, 2H), 5.20 (s, 1H), 6.72 (m, 3H), 6.89 (d, 2H), 7.15 (m, 1H), 7.89 (d, 2H).

**$^{13}\text{C}$  NMR:**  $\delta$  ( $\text{CDCl}_3$ ) = 26.3, 35.4, 68.7, 113.6, 114.2 (2), 115.9, 121.3, 129.7, 130.1, 130.6, 139.6, 155.8, 162.8, 197.1.

**IR:** (KBr): 3333 (b), 3262 (b), 2962 (w), 2926 (w), 1653 (s), 1598 (s), 1583 (s), 1512 (m), 1361 (m), 1271 (s), 1168 (m), 1017 (m), 833 (s), 705 (m), 586 (m).

**MS:** (m/e(I)): 256 (20), 165 (25), 121 (100), 107 (10), 97 (15), 69 (40), 55 (38).

**Mass:** Calculated mass for  $C_{16}H_{16}O_3$ : 256.1099. Found: 256.1119.

**Melting Point:** 96.5 - 97.6°C.

**UV:**  $\lambda_{\max}$  (MeCN) = 266 nm( $\epsilon$  = 15000), sh = 198, 214.

**(3a) 3-[2-(4-hydroxyphenyl)ethoxy]acetophenone:**

**$^1H$  NMR:**  $\delta$  ( $CDCl_3$ ) = 2.56 (s, 3H), 3.02 (t, 2H), 4.15 (t, 2H), 4.76 (s, 1H), 6.76 (d, 2H), 7.08 (m, 1H), 7.13 (d, 2H), 7.33 (m, 1H), 7.48 (m, 2H).

**$^{13}C$  NMR:**  $\delta$  ( $CDCl_3$ ) = 26.7, 34.8, 69.1, 113.1, 115.4, 120.1, 121.1, 129.6, 130.2, 130.3, 138.4, 154.2, 159.1.

**IR:** (KBr): 3244 (s,b), 2942 (w), 2854 (w), 1667 (s), 1613 (m), 1579 (m), 1516 (s), 1449 (s), 1357 (m), 1298 (s), 1220 (m), 1043 (s), 885 (m), 774 (m), 684 (m).

**MS:** (m/e(I)): 256 (15), 165 (5), 121 (100), 107 (30), 103 (10), 91 (13), 77 (15).

**Mass:** Calculated mass for  $C_{16}H_{16}O_3$ : 256.1099. Found: 256.1116.

**Melting Point:** 71.9 - 72.6°C.

**UV:**  $\lambda_{\max}$  (MeCN) = 216 nm( $\epsilon$  = 17800), sh = 196, 244, 280, 302.

(5) 4-[2-(4-hydroxyphenyl)ethoxy]-(3-methoxy)acetophenone:

**<sup>1</sup>H NMR:**  $\delta$  (CDCl<sub>3</sub>) = 2.54 (s, 3H), 3.09 (t, 3H), 3.90 (s, 3H), 4.20 (t, 2H), 4.94 (s, 1H), 6.76 (d, 2H), 6.81 (d, 1H), 7.13 (d, 2H), 7.15 (m, 2H).

**<sup>13</sup>C NMR:**  $\delta$  (DMSO-d<sub>6</sub>) = 26.1, 33.8, 55.4, 69.1, 110.4, 111.7, 114.8 (2), 122.9, 127.7, 129.7 (3), 148.4, 152.1, 155.0, 191.7.

**IR:** (KBr): 3457 (b), 2928 (w), 2853 (w), 1666 (s), 1596 (s), 1509 (s), 1420 (m), 1265 (s), 1220 (m), 1026 (w), 1006 (m), 883 (w).

**MS:** (m/e(I)): 286 (12), 151 (4), 121 (100), 103 (5), 77 (5), 43 (8).

**Mass:** Calculated for C<sub>17</sub>H<sub>18</sub>O<sub>4</sub>: 286.1205. Found: 286.1213.

**Melting Point:** 171.8 - 173.5°C.

**UV:**  $\lambda_{\max}$  (MeCN) = 198 nm( $\epsilon$  = 26000), sh = 224, 270, 298.

(6) 4-[2-(3-hydroxyphenyl)ethoxy]-(3-methoxy)acetophenone:

**<sup>1</sup>H NMR:**  $\delta$  (CDCl<sub>3</sub>) = 2.54 (s, 3H), 3.12 (t, 2H), 3.90 (s, 3H), 4.24 (t, 2H), 5.01 (s, 1H), 6.80 (m, 4H), 7.17 (m, 1H), 7.51 (m, 2H).

**<sup>13</sup>C NMR:**  $\delta$  (DMSO-d<sub>6</sub>) = 26.3, 34.8, 55.6, 68.9, 110.6, 111.9, 113.2, 115.8, 119.6, 123.1, 129.2, 129.9, 139.3, 148.6, 152.3, 157.2, 191.8.

**IR:** (KBr): 3311 (b), 2961 (w), 2936 (w), 1652 (s), 1586 (s), 1514 (m), 1462 (s), 11272 (s), 1223 (s), 1016 (s), 882 (m), 806 (m), 698 (m), 575 (m).

**MS:** (m/e(I)): 286 (45), 166 (10), 151 (15), 121 (100), 103 (10), 91 (7), 77 (8), 43 (10).

**Mass:** Calculated for C<sub>17</sub>H<sub>18</sub>O<sub>4</sub>: 286.1205. Found: 286.1216.

**Melting Point:** 115.4 - 117°C.

**UV:**  $\lambda_{\text{max}}$  (MeCN) = 200 nm ( $\epsilon$  = 27300), sh = 224, 270, 298.

(7) 4-[2-(4-hydroxyphenyl)ethoxy]benzophenone:

**$^1\text{H}$  NMR:**  $\delta$  ( $\text{CDCl}_3$ ) = 3.04 (t, 2H), 4.19 (t, 2H), 4.77 (s, 1H), 6.79 (d, 2H), 6.91 (d, 2H), 7.14 (d, 2H), 7.50 (m, 3H), 7.75 (m, 4H).

**$^{13}\text{C}$  NMR:**  $\delta$  ( $\text{CDCl}_3$ ) = 34.7, 69.1, 114.1 (2), 115.4 (2), 128.2, 129.7, 130.1 (2), 130.2 (2), 131.9, 132.6, 138.3 (2), 162.5, 190.6.

**IR:** (KBr): 3279 (b), 2949 (w), 2918 (w), 1640 (s), 1598 (s), 1515 (s), 1321 (m), 1263 (s), 1152 (s), 1017 (m), 886 (m), 701 (m), 627 (m).

**MS:** (m/e(I)): 318 (12), 121 (100), 105 (9), 77 (7), 58 (15).

**Mass:** Calculated for  $\text{C}_{21}\text{H}_{18}\text{O}_3$ : 318.1256. Found: 318.1247.

**Melting Point:** 93.8 - 95°C.

**UV:**  $\lambda_{\text{max}}$  (MeCN) = 200 nm ( $\epsilon$  = 33400), sh = 222, 248, 282.

(8) 4-[2-(3-hydroxyphenyl)ethoxy]benzophenone:

**$^1\text{H}$  NMR:**  $\delta$  ( $\text{CDCl}_3$ ) = 3.05 (t, 2H), 4.21 (t, 2H), 6.73 (m, 3H), 6.94 (d, 2H), 7.17 (m, 1H), 7.45 (m, 3H), 7.73 (d, 2H), 7.79 (d, 2H).

**$^{13}\text{C}$  NMR:**  $\delta$  ( $\text{CDCl}_3$ ) = 35.4, 68.7, 113.6, 114.1, 115.9, 121.3, 128.2, 129.7, 130.1, 132.0, 132.6, 132.9, 138.2, 139.6, 155.8, 162.5, 190.6.

**IR:** (KBr): 3280 (b), 2948 (w), 1625 (s), 1601 (s), 1575 (s), 1452 (m), 1254 (m), 1151 (m), 1018 (m), 849 (s), 792 (m), 630 (m).

**MS:** (m/e(I)): 318 (20), 198 (35), 121 (100), 105 (15), 77 (13), 58 (18).

**Mass:** Calculated for  $C_{21}H_{18}O_3$ : 318.1256. Found: 318.1247.

**Melting Point:** 82.7 - 84.2 °C.

**UV:**  $\lambda_{\max}$  (MeCN) = 202 nm( $\epsilon$  = 31000), sh = 222, 248, 280.



## **4.5**            **Preparation of Methoxy Analogs**

### **4.5.1**    **General Procedure**

General procedure for preparation of the methoxy analogs involves combining the proper methoxy-phenyl bromide with a given hydroxy-acetophenone to obtain the desired compound. More specifically preparation was accomplished using 0.8 equivalents of hydroxyacetophenone with 1 equivalent of potassium carbonate utilizing acetone (30 mL) as solvent. This mixture was then allowed to gently reflux until reaction was complete (as monitored by  $^1\text{H}$  NMR spectroscopy) usually for 15 hours. The solution was then filtered and concentrated under reduced pressure. The residue was extracted with ether (3 x 30 mL). The ethereal layers were combined, washed with water (1 x 30 mL), dried with magnesium sulphate and the solvent removed under vacuo. Chromatographic separation was achieved using a 2mm thick plate on a chromatotron with a 20% ethyl acetate in hexanes solution. This produced a colorless solid which was further recrystallized using ethanol/water mixture. The crystals obtained gave spectral properties consistent with the following compounds:

#### **(1b) 4-[2-(4-methoxyphenyl)ethoxy]acetophenone:**

The melting point and spectral properties are in excellent agreement with those previously published.<sup>24</sup> The isolated yield was 10% as considerable elimination occurred in the coupling reaction.

(2b) 4-[2-(3-methoxyphenyl)ethoxy]acetophenone:

**<sup>1</sup>H NMR:**  $\delta$  (CDCl<sub>3</sub>) = 2.53 (s, 3H), 3.08 (t, 2H), 3.79 (s, 3H), 4.21 (t, 2H), 6.86 (m, 5H), 7.23 (m, 1H), 7.89 (d, 2H).

**<sup>13</sup>C NMR:**  $\delta$  (CDCl<sub>3</sub>) = 26.3, 35.7, 55.2, 68.8, 111.9, 114.2, 114.9, 121.3, 129.5, 130.4, 130.6, 139.4, 159.8, 162.7, 196.8.

**IR:** (KBr): 2965 (w), 2914 (w), 2839 (w), 1680 (s), 1604 (s), 1473 (m), 1364 (m), 1275 (s), 1170 (m), 1018 (m), 830 (m), 797 (m), 699 (m).

**MS:** (m/e(I)): 270 (15), 135 (100), 121 (8), 105 (12), 91 (10), 77 (10).

**Mass:** Calculated for C<sub>17</sub>H<sub>18</sub>O<sub>3</sub>: 270.1256. Found: 270.1253.

**Melting Point:** 68 - 69°C.

**UV:**  $\lambda_{\text{max}}$ (ACN) = 196 nm( $\epsilon$  = 26000), sh = 216, 266.

(3b) 3-[2-(4-methoxyphenyl)ethoxy]acetophenone:

**<sup>1</sup>H NMR:**  $\delta$  (CDCl<sub>3</sub>) = 2.56 (s, 3H), 3.04 (t, 2H), 3.78 (s, 3H), 4.17 (t, 2H), 6.84 (d, 2H), 7.09 (m, 1H), 7.19 (d, 2H), 7.33 (m, 1H), 7.49 (m, 2H).

**<sup>13</sup>C NMR:**  $\delta$  (CDCl<sub>3</sub>) = 26.7, 34.8, 55.3, 69.1, 113.2, 114.0, 120.0, 121.1, 129.5, 129.9, 130.0, 138.5, 158.3, 159.1, 197.9.

**IR:** (KBr): 2954 (m), 2936 (w), 2838 (w), 1678 (s), 1610 (m), 1580 (s), 1513 (s), 1443(m), 1360 (m), 1244 (s), 1212 (s), 1112 (m), 1027 (s), 818 (m), 784 (m), 683 (m), 600 (m).

**MS:** (m/e(I)): 270 (10), 135 (100), 121 (30), 105 (10), 91 (7).

**Mass:** Calculated for  $C_{17}H_{18}O_3$ : 270.1256. Found: 270.1253.

**Melting Point:** 46.3 - 47.7°C.

**UV:**  $\lambda_{max}$ (ACN) = 196 nm( $\epsilon$  = 20000), sh = 216, 244, 280, 302.

### **3.5.2 Preparation of 3-[2-(3-methoxyphenyl)ethoxy]acetophenone:**

Due to complete formation of methoxy styrene, the previous method for preparation of methoxy derivatives could not be utilized. Instead 3-[2-(3-hydroxyphenyl)ethoxy]acetophenone (500 mg, 1.95 mmol) and potassium carbonate (1 equivalent) was placed in a flame dried flask under nitrogen. To this iodomethane (5 mmol) was added dropwise by syringe. The contents were allowed to stir for two hours by which time the reaction was almost at completion. Stirring was continued for another two hours after which the salts were filtered off and the residue was extracted with ether (3 x 10 mL), the ethereal layers were combined and washed with water (1 x 10 mL), dried over magnesium sulphate and concentrated under reduced pressure. A white solid which was recrystallized with ethanol/water. An isolated yield of 67% was obtained as white needles (350 mg, 1.3 mmol). The spectral properties are consistent with the compound **4b**.

#### **(4b) 3-[2-(3-methoxyphenyl)ethoxy]acetophenone:**

**$^1H$  NMR:**  $\delta$  ( $CDCl_3$ ) = 2.57 (s, 3H), 3.07 (t, 2H), 3.79 (s, 3H), 4.21 (t, 2H), 6.79 (m, 3H), 7.09 (m, 1H), 7.23 (m, 1H), 7.34 (m, 1H), 7.50 (m, 2H).

**<sup>13</sup>C NMR:**  $\delta$  (CDCl<sub>3</sub>) = 26.7, 35.8, 55.2, 68.8, 111.9, 113.2, 114.8, 120.1, 121.3, 129.6, 130.3, 138.5, 159.0, 160.4, 197.9.

**IR:** (KBr): 2964 (w), 2935 (w), 1678 (s), 1604 (m), 1580 (s), 1513 (m), 1360 (m), 1283 (s), 1244 (m), 1037 (m), 1027 (m), 818 (m).

**MS:** (m/e(I)): 270 (22), 135 (100), 121 (20), 105 (30), 91 (40), 77 (29), 65 (20), 43 (40).

**Mass:** Calculated for C<sub>17</sub>H<sub>18</sub>O<sub>3</sub>: 270.1256. Found: 270.1253.

**Melting Point:** 54.3 - 56.0°C

**UV:**  $\lambda_{\text{max}}$ (ACN) = 218 nm( $\epsilon$  = 29800), sh = 200, 244, 276, 302.

## **4.6 Instrumentation and Techniques**

### **4.6.1 Nanosecond Laser Flash Photolysis Experiments**

Nanosecond laser flash photolysis experiments employed the pulses from a Lumonics TE-861M excimer laser filled with Xe/HCl/H<sub>2</sub>/He (308 nm, 15 ns, ca. 40 mJ) or N<sub>2</sub>/He (337 nm, 6 ns, ca. 4 mJ) or F<sub>2</sub>/Kr/He (248 nm, ca. 16 ns). The detection system, which is computer controlled, has been described in detail elsewhere.<sup>(26)</sup> For Arrhenius experiments, the sample compartment was surrounded by a quartz sleeve, through which either heated or cooled nitrogen was passed in order to vary the sample temperature accordingly. Sample temperatures were measured using a Cole-Parmer Type K digital thermocouple thermometer and are accurate to  $\pm 0.1^\circ\text{C}$ . The samples were allowed to equilibrate for 10 minutes prior to recording the experiment.

**Sample Preparation:** Samples in acetonitrile were contained in 3 x 7mm Suprasil quartz cells for the experiments performed using 248 nm laser wavelength. Suprasil quartz cells that were 7 x 7 mm were utilized for samples irradiated at either 308 nm or 337 nm. Samples were prepared by varying the concentration of solute in order to obtain an optical density of ca. 0.7 at the laser wavelength that would be used in the experiment. In all cases the sample was fitted with a septum and purged with dry nitrogen prior to use. Quenchers were added to these solutions as aliquots of standard solutions.

#### **4.6.2 Steady State Photolysis**

Steady state photolyses were performed using a Rayonet reactor (6 x 300 nm lamps) fitted with a merry-go-round. Nitrogen purged solutions were irradiated in 10 mm i.d. quartz tubes for periods of time ranging from 10 to 90 min. The irradiated samples were monitored by gas chromatography both before and after irradiation times.

#### **4.6.3 Phosphorescence Spectra and Lifetime Determination**

Phosphorescence measurements were performed on a Photon Technologies, Inc. LS-100 spectrofluorimeter with a Xenon lamp and utilizing PTI software. Samples were dissolved at 1 mg / 10 ml concentrations in freshly prepared solutions of 4:1 ethanol/methanol. These samples were then put into 0.3 mm o.d. quartz tube, sealed with a rubber septum, and rigorously purged with nitrogen. The purged samples were then placed into a liquid nitrogen dewar which was fitted with a quartz cold finger. The samples, now contained in a glass matrix could then be placed into the spectrometer for analysis.

*Phosphorescence Spectra:* The samples were excited with a wavelength of 285 nm and spectra recorded between 350 - 550 nm in 1nm increments. The time between excitation pulses is divided by 1000 and signal integration was performed from 50/1000 to

200/1000 between excitation pulses. Photomultiplier gain was set at 200, lamp rate was 100 and the number average flash was 20. In all cases three scans were performed and averaged over the entire wavelength range.

*Phosphorescence Lifetimes:* Decay traces were measured using an excitation wavelength 285 nm and a monitoring wavelength of 410 nm. Data collection was performed using 200 channels and generally 5 ms/channel (dependent on the phosphorescent lifetime). Photomultiplier gain was set to automatic and 25 measurements were averaged for each channel.

## APPENDIX

F	Favorable geometry for quenching	18
U	Unfavorable geometry for quenching	18
h	Planck's constant	18
$\nu$	Frequency at which absorption occurs	18
F*	Excited state of F	18
U*	Excited state of U	18
$k_{UF}$	Rate constant for conversion from conformer U to F	18
$k_r$	Rate constant for reaction from favorable excited state (F*)	18
P	Rate constant for reaction of biradical to product	18
$\chi_F$	Equilibrium fractional population of favorable conformers	18
$\chi_u$	Equilibrium fractional population of unfavorable conformers	18
$\Phi$	Quantum yield = $\frac{\text{\# molecules undergoing event of interest}}{\text{\# photons absorbed by system}}$	18
$\phi_{isc}$	Quantum yield for intersystem crossing	53
$\phi_{MN*3}$	Quantum yield for formation of 1-methylnaphthalene triplets	53
$k_q$	Rate constant for quenching	53
$\tau_K$	Ketone triplet lifetime	53
$I_a$	Intensity of laser	53
$OD_{MN*3}$	Optical density due to absorption by 1-methylnaphthalene triplet	53
$l$	Optical pathlength	53
$\epsilon$	Molar absorptivity	53



## **REFERENCES**

- (1) Wagner, P.J. in Organic Photochemistry Vol. 11, Padwa, A., Ed., Marcel Dekker Inc., NY, 1991. p227.
- (2) Atkins, P.W. "Physical Chemistry", 3rd Ed. W.H. Freeman and Company, New York, 1986.
- (3) Wagner, P.J.; Kemppainen, A.E.; Schott, H.N. *J. Am. Chem. Soc.*, 1973, 95, 5604.
- (4) Wagner, P.J.; Kemppainen, A.E. *J. Am. Chem. Soc.*, 1968, 90, 5898.
- (5) Yang, N.C.; Dusenberry, R.L. *J. Am. Chem. Soc.*, 1968, 90, 5999.
- (6) Yang, N.C.; McClure, D.S.; Murov, S.L.; Houser, J.J.; Dusenberry, R. *J. Am. Chem. Soc.*, 1967, 89, 5466.
- (7) Scaiano, J.C.; Das, P.K.; Encinas, M.V. *J. Am. Chem. Soc.*, 1981, 103, 4154.
- (8) Scaiano, J.C. *J. Am. Chem. Soc.*, 1983, 105, 1856.
- (9) Steel, C. *J. Am. Chem. Soc.*, 1978, 100, 5147.
- (10) Leermakers, P.A.; Hammond, G.S. *J. Am. Chem. Soc.*, 1962, 84, 207.
- (11) Wagner, P.J. *J. Am. Chem. Soc.*, 1967, 89, 2503.
- (12) Wagner, P.J.; Siebert, E.J. *J. Am. Chem. Soc.*, 1981, 103, 7329.
- (13) Porter, G.; Suppan, P. *Proc. Chem. Soc.*, 1964, 191.
- (14) Wagner, P.J.; Kemppainen, A.E. *J. Am. Chem. Soc.*, 1973, 95, 5604.

- (15) Scaiano, J.C.; Das, P.K.; Encinas, M.V.; Steenken, S. *J. Am. Chem. Soc.*, **1981**, 103, 4162.16) Scaiano, J.C. "Handbook of Photochemistry and Photophysics", vol I & II. CRC Press, Inc., Boca Raton, Florida. 1989.
- (17) Murov, S.L. "Handbook of Photochemistry", Marcel Dekker, Inc., New York. 1973.
- (18) Turro, N.J., Weiss, D.S. *J. Am. Chem. Soc.*, **1968**, 90, 2185.
- (19) Chandra, A.K. *J. of Photochem.*, **1979**, 11, 347.
- (20) Scheffer, J.R. *Org. Photchem.*, **1987**, 8, 249.
- (21) Lewis, E.S. "Isotopes in Organic Chemistry", (E. Buncl and C.C. Lee, Eds), Elsevier, Amsterdam, Vol 2. **1976**. p134.
- (22) Wagner, P.J. *Acc. Chem. Res.*, **1983**, 16, 461.
- (23) Winnik, M.A. *Chem. Rev.*, **1981**, 81, 491.
- (24) Scaiano, J.C.; McGimpsey, W.G.; Leigh, W.J.; Jakobs, S. *J. Org. Chem.*, **1987**, 52, 4540.
- (25) Leigh, W.J.; Jakobs, S. *Tetrahedron*, **1987**, 43, 1393.
- (26) Sluggett, G.W.; Leigh, W.J. *J. Am. Chem. Soc.*, **1992**, 114, 1195: Leigh, W.J.; Workentin, M.S.; Andrews, A. *J. Photochem. & Photobiol. A:Chem.*, **1991**, 57, 97.
- (27) Turro, N.J. Modern Molecular Photochemistry, 2<sup>nd</sup> Edition. Benjamin-Cummings, NY, **1985**.
- (28) Yang, N.C.; Cohen, J.J.; Shani, A. *J. Am. Chem. Soc.*, **1968**, 90, 3264.

- (29) Scaiano, J.C. et al. *J. Photochem.*, **1983**, 21, 137.
- (30) Lowry, T.H.; Richardson, K.S. Mechanism and Theory in Organic Chemistry, Harpor And Row Publishers, NY, **1976**.
- (31) Isaac, N.S. Reactive Intermediates in Organic Chemistry, John Wiley and Sons Ltd., London, **1974**.
- (32) Leigh, W.J.; Workentin, M.S.; Andrews, A. *J. Photochem. & Photobiol. A:Chem.*, **1991**, 57, 97.
- (33) Scaiano, J.C. *J. Am. Chem. Soc.*, **1980**, 102, 5399.
- (34) Carey, F. A.; Sundberg, R.J. "Advanced Organic Chemistry: Part A", 3<sup>rd</sup> ed. Plenum Press, New York. 1990.